Modeling of bending-torsion couplings in active-bending structures. Application to the design of elastic gridshell.

Lionel du Peloux

École des Ponts

ParisTech

Contents

Contents

Contents

List of Figures

List of Tables

Torsion Part I

1 Geometry of smooth and discret curves

1.1 Introduction

Dans ce chapitre, après un bref rappel sur le cadre mathématique d'étude des courbes paramétrique de l'espace, on présente les notions de courbures et de torsion géométrique associées au repère de Frenet. On montre ensuite le cas plus général d'un repère mobile quelconque attaché à une courbe gamma. On définit enfin la particularité d'un repère mobile adapté à un courbe, et on présente, en sus du repère de Frenet, une approche différente pour accrocher des repères le long d'une courbe (Bishop / RMF / Zéro-twisting frame)

1.2 Paramectric Curves

1.2.1 Definition

Let I be an interval [Bis75] of $\mathbb{R}$ and $F: t \mapsto F(t)$ be a map of $\mathcal{C}(I, \mathbb{R}^3)$. Then $\gamma = (I, F)$ is called a *parametric curve* and :

- The 2-uplet (I, F) is called a *parametrization* of γ

- $\gamma = F(I) = \{F(t), t \in I\}$ is called the *graph* or *trace* of γ

- γ is said to be $\mathcal{C}^k$ if $F \in \mathcal{C}^k(I, \mathbb{R}^3)$

Remark. Note that for a given graph in $\mathbb{R}^3$ they may be different possible parameterizations. From now, γ will simply refer to $F(I)$, its graph.

1.2.2 Regularity

Let $\gamma = (I, F)$ be a parametric [**?**] curve, and $t_0 \in I$ a parameter.

- A point of parameter t_0 is called *regular* if $F'(t_0) \neq 0$.
  The curve γ is called *regular* if γ is $\mathcal{C}^1$ and $F'(t) \neq 0, \forall t \in I$

- A point of parameter t_0 is called *biregular* if $F'(t_0)$ and $F''(t_0)$ are not collinear
  The curve γ is called *biregular* if γ is $\mathcal{C}^2$ and $F'(t) \cdot F''(t) \neq 0, \forall t \in I$

1.2.3 Reparametrization

Let $\gamma = (I, F)$ be a parametric curve of class $\mathcal{C}^k$, $J \in \mathbb{R}^3$ an interval, and $\varphi : I \mapsto J$ a $\mathcal{C}^k$ diffeomorphisme. Lets define $G = F \circ \varphi$. Then :

- $G \in \mathcal{C}^k(J, \mathbb{R}^3)$

- $G(J) = F(I)$

- φ is said to be an admissible *change of parameter* for γ

- (J, G) is said to be another *admissible parametrization* for γ

1.2.4 Natural parametrization

Let γ be a space curve of class $\mathcal{C}^1$. A parametrization (I, F) of γ is called *natural* if $\|F'(t)\| = 1, \forall t \in I$. Thus :

- The curve is necessarily regular

- F is strictly monotonic

1.2.5 Curve length

Let $\gamma = (I, F)$ be a parametric curve of class $\mathcal{C}^1$. The length of γ is define as :

$$L = \int_I \|F'(t)\| dt \tag{1.1}$$

Note that the length of γ is invariant under reparametrization.

1.2.6 Arc-length parametrization

Let $\gamma = (I, F)$ be a regular parametric curve of class $\mathcal{C}^1$. Let $t_0 \in I$ be a given parameter. The following map is said to be the *arc-length of origin t_0* of γ :

$$s : t \mapsto \int_{t_0}^t \|F'(u)\| du \quad , \quad s \in I \times \mathbb{R} \tag{1.2}$$

The arc-length $s : I \mapsto s(I)$ is an admissible change of parameter for γ. Indeed, s is a $\mathcal{C}^1$ diffeomorphisme because it is bijective ($s' > 0$).

Lets define $G = F \circ s^{-1}$ and $J = s(I)$. Thus (J, G) is a natural reparametrization of γ and $\|G'(s)\| = 1, \forall s \in J$.

This parametrization is preferred because the natural parameter s traverses the image of γ at unit speed ($\|G'\| = 1$).

1.3 Frenet's Trihedron

The trihedron of Frenet is a fundamental mathematical tool from the field of differential geometry to study local characterization of planar and non-planar space curves. It is a direct orthonormal basis attached to a point P sliding along a parametric curve (γ). Introduced by Jean-Frédéric Frenet in his thesis upon *curves of double curvature* in 1847, it brings out intrinsic local properties of space curves : the curvature (κ) which evaluates the deviance of γ from being a straight line, and the torsion (τ), which evaluates the deviance of γ from being a plane curve. These quantities are also known as "generalized curvatures". The *fundamental theorem of space curves* states that a curve is fully determined by its curvature and torsion up to a solid (or euclidean) movement in space. This assertion is equivalent to the well-known *Serret-Frenet formulas*, which give the first-order linear differential equations system that govern the evolution of Frenet's trihedron along a space curve. For a given curvature and torsion, and a given initial trihedron, the geometry of the space curve can be constructed by integration these differential equations.

In this section we consider $\gamma = (J, G)$ to be a regular ($\|\gamma'\| = 1$) parametric curve of class $\mathcal{C}^2$, parametrized by its arc-length (denoted s). For the sake of simplicity we will refer to $G(s)$ as $\gamma(s)$.

1.3.1 Tangent vector

The first vector of Frenet's trihedron is called the *unit tangent vector* ($\boldsymbol{t}$). At any given parameter $s \in J$, it is defined as :

$$\boldsymbol{t}(s) = \frac{\gamma'(s)}{\|\gamma'(s)\|} = \gamma'(s) \quad , \quad \|\boldsymbol{t}(s)\| = 1 \tag{1.3}$$

In differential geometry, the tangente to the curve γ at point P_0 is obtained as the limit of the (normalized) vector $\overrightarrow{P_0 P}$, as P approaches P_0 on the path γ. For a regular curve, the left-sided and right-sided limits coïncide as P^- and P^+ approche P_0 respectively from the left and the right sides :

$$\boldsymbol{t}(P_0) = \lim_{P \to P_0} \frac{\overrightarrow{P_0 P}}{\left\|\overrightarrow{P_0 P}\right\|} = \lim_{P^- \to P_0} \frac{\overrightarrow{P_0 P^-}}{\left\|\overrightarrow{P_0 P^-}\right\|} = \lim_{P^+ \to P_0} \frac{\overrightarrow{P_0 P^+}}{\|\overrightarrow{P_0 P^+}\|} \tag{1.4}$$

1.3.2 Normal vector

The second vector of Frenet's trihedron is called the *unit normal vector* ($\boldsymbol{n}$). It is constructed from $\boldsymbol{t}'$ which is orthogonal to $\boldsymbol{t}$. Indeed, $\|\boldsymbol{t}\| = 1 \Rightarrow \boldsymbol{t}' \cdot \boldsymbol{t} = 0 \Leftrightarrow \boldsymbol{t}' \perp \boldsymbol{t}$. Thus, at any given parameter $s \in J$, it is defined as :

$$\boldsymbol{n}(s) = \frac{\boldsymbol{t}'(s)}{\|\boldsymbol{t}'(s)\|} = \frac{\gamma''(s)}{\|\gamma''(s)\|} \quad , \quad \|\boldsymbol{n}(s)\| = 1 \tag{1.5}$$

Remark that the notion of "normal vector" would be ambiguous for non-planar curves as far as there is an infinite number of possible vectors laying in the plane orthogonal to the curve's tangent. In practice, the tangent derivative is a convenient choice as it allows to extend the notion of curvature from planar to non-planar space curves. The tangent unit vector and the normal unit vector $\{\boldsymbol{t}, \boldsymbol{n}\}$ define the so-called "osculating plane".

Likewise the differential definition of the tangent exposed in (1.4), the osculating plane could be seen as the limit of the plane defined by 3 points P_0, P^-, P^+, as P^- and P^+ approches P_0 respectively from its left and right side.

1.3.3 Binormal vector

The third vector of Frenet's trihedron is called the *unit binormal vector* ($\boldsymbol{b}$). It is constructed from $\boldsymbol{t}$ and $\boldsymbol{n}$ to form an orthonormal direct basis of $\mathbb{R}^3$. Thus, at any given parameter $s \in J$, it is defined as :

$$\boldsymbol{b}(s) = \boldsymbol{t}(s) \times \boldsymbol{n}(s) \quad , \quad \|\boldsymbol{b}(s)\| = 1 \tag{1.6}$$

The normal unit vector and the binormal unit vector $\{\boldsymbol{n}, \boldsymbol{b}\}$ define the so-called "normal plane". The normal tangent vector and the binormal unit vector $\{\boldsymbol{t}, \boldsymbol{b}\}$ define the so-called "rectifying plane".

1.4 Curvature

Note that from a geometric point of view, $\frac{1}{\kappa(s)}$ represents the radius of the osculating circle of γ at the point of parameter s.

$\kappa(s) = \|\boldsymbol{t}'(s)\| = \|\gamma''(s)\|$

How do you know a curve is curving? And how much? The answer should depend just on the shape of the curve, not on the speed at which it is drawn. So it connects with arclength s, not with a time- parameter t

1.4.1 Osculating circle

Défini de façon directe, le cercle de courbure est le cercle le plus proche de la courbe en P, c'est l'unique cercle osculateur à la courbe en ce point. Ceci signifie qu'il constitue une très
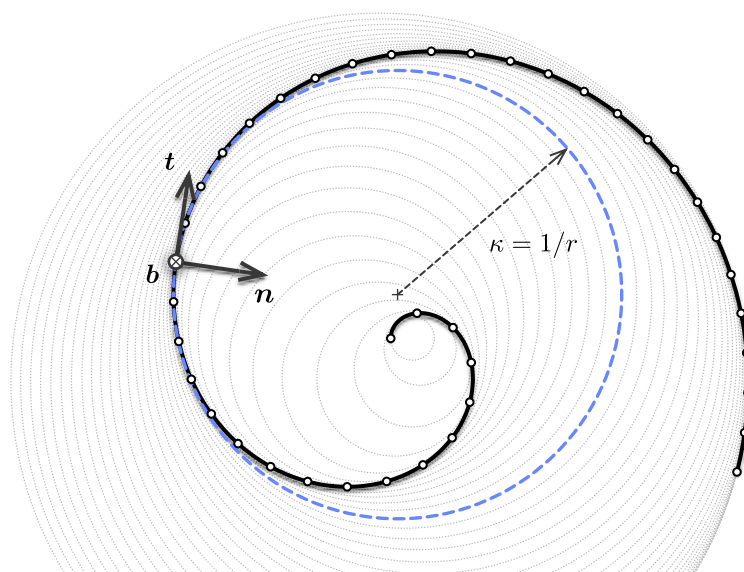
Figure 1.1 – Different osculating circles for a spiral.

bonne approximation de la courbe, meilleure qu'un cercle tangent quelconque. En effet, il donne non seulement une idée de la direction dans laquelle la courbe avance (direction de la tangente), mais aussi de sa tendance à tourner de part ou d'autre de la tangente.

Le centre de courbure est la position limite de l'intersection des deux normales en M(s) et M(s+Ds) et on parle alors de cercle de courbure ou cercle osculateur (du latin osculor, osculatus = caresser).

1.4.2 Curvature binormal vector

Finally, we define the *curvature binormal vector* at any given parameter $s \in J$ as :

$$\boldsymbol{\kappa b}(s) = \boldsymbol{t}(s) \times \boldsymbol{t}'(s) = \kappa(s) \cdot \boldsymbol{b}(s) \quad , \quad \|\boldsymbol{\kappa b}(s)\| = \kappa(s) \tag{1.7}$$

1.5 Torsion

En géométrie différentielle, la torsion d'une courbe tracée dans l'espace mesure la manière dont la courbe se tord pour sortir de son plan osculateur (plan contenant le cercle osculateur). Ainsi, par exemple, une courbe plane a une torsion nulle et une hélice circulaire est de torsion constante. Prises ensemble, la courbure et la torsion d'une courbe de l'espace en définissent la forme comme le fait la courbure pour une courbe plane. La torsion apparait comme coefficient dans les équations différentielles du repère de Frenet.

The *torsion* measures the deviance of γ from being a planar curve and is defined at any

(a) Tangent.

(b) Normal and osculating circle
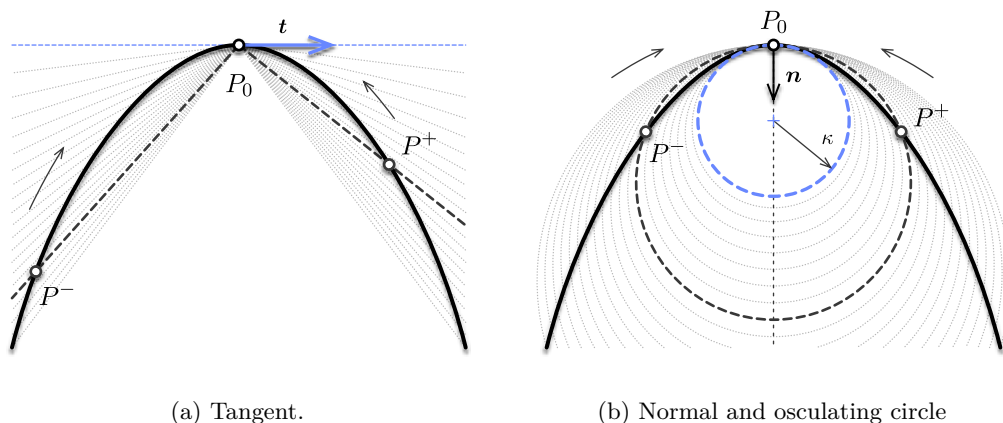
Figure 1.2 – Differential definition of Frenet's trihedron at given point P_0.

given parameter $s \in J$ as :

$$\tau_f(s) = \boldsymbol{n}'(s) \cdot \boldsymbol{b}(s) \tag{1.8}$$

Cette notion est propre aux courbes gauches et mesure comment la courbe se "tord" en changeant de plan. Dans le trièdre de Frenet, elle correspond à l'angle des plans osculateurs P(s) et P(s + Ds) en deux points infiniment proches M(s) et M(s + Ds), donc à l'angle Dû entre les binormales mesurant comment la courbe se tord en passant de P(s) à P(s + Ds). Ainsi, de façon analogue à la courbure, la torsion T en un point sera, par unité d'arc, la limite lorsque Ds tend vers 0 du rapport Dû/Ds :

1.6 Curve Framing

1.6.1 Moving frame

Let $\gamma : s \to \gamma(s)$ be an arc-length parametrized curve. A map F which associates to each point of arc-length s a direct orthonormal trihedron is called a *moving frame* :

$$
\begin{array}{rcl}
F: & [0, L] & \longrightarrow & \mathcal{SO}_3(\mathbb{R}) \\
& s & \longmapsto & F(s) = \{\boldsymbol{e}_3(s), \boldsymbol{e}_1(s), \boldsymbol{e}_2(s)\}
\end{array}
\tag{1.9}
$$

Thus, inherently, a moving frame F attached to γ satisfies for all $s \in [0, L]$:

$$
\begin{cases}
\|\boldsymbol{e}_i(s)\| = 1 \\
\boldsymbol{e}_i(s) \cdot \boldsymbol{e}_j(s) = 0 \quad , \quad i \neq j
\end{cases}
\tag{1.10}
$$

The terme "moving frame" will refer indifferently to the map itself (F), or to a specific evaluation of the map $(F(s))$.
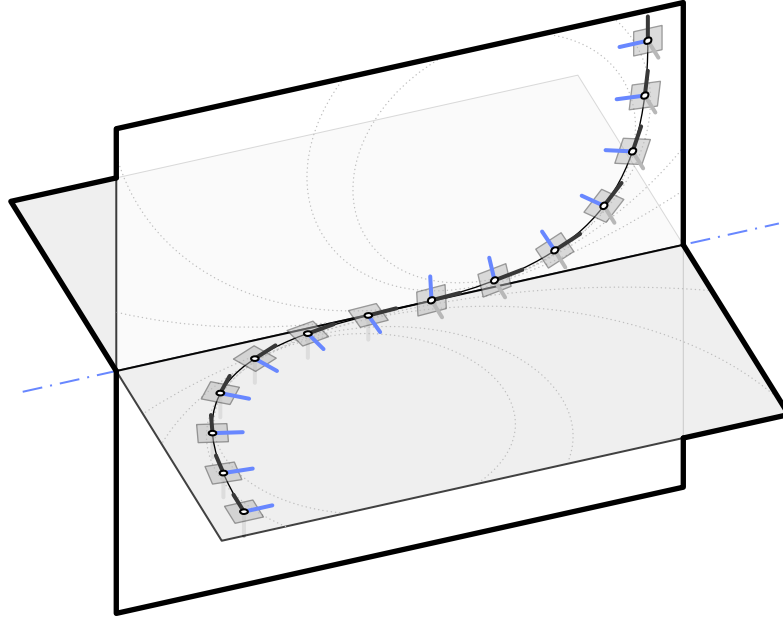
Figure 1.3 – Geometric torsion and rotation of the osculating plane

Governing equations

Computing the derivatives of the previous relationships leads to the following differential equations :

$$
\left\{
\begin{array}{l}
\boldsymbol{e}_i'(s) \cdot \boldsymbol{e}_i(s) = 0 \\
\boldsymbol{e}_i'(s) \cdot \boldsymbol{e}_j(s) = -\boldsymbol{e}_i(s) \cdot \boldsymbol{e}_j'(s) \quad , \quad i \neq j
\end{array}
\right.
\tag{1.11}
$$

Thus, there exists 3 scalar functions $\tau(s)$, $k_1(s)$, $k_2(s)$ such that :

$$
\left\{
\begin{array}{l}
\boldsymbol{e}_3'(s) = k_2(s)\boldsymbol{e}_1(s) - k_1(s)\boldsymbol{e}_2(s) \\
\boldsymbol{e}_1'(s) = -k_2(s)\boldsymbol{e}_3(s) + \tau(s)\boldsymbol{e}_2(s) \\
\boldsymbol{e}_2'(s) = k_1(s)\boldsymbol{e}_3(s) - \tau(s)\boldsymbol{e}_1(s)
\end{array}
\right.
\tag{1.12}
$$

It is common to rewrite this first-order linear differential equations system as a single matrix equation :

$$
\begin{bmatrix} \boldsymbol{e}_3'(s) \\ \boldsymbol{e}_1'(s) \\ \boldsymbol{e}_2'(s) \end{bmatrix} =
\begin{bmatrix} 0 & k_2(s) & -k_1(s) \\ -k_2(s) & 0 & \tau(s) \\ k_1(s) & -\tau(s) & 0 \end{bmatrix}
\begin{bmatrix} \boldsymbol{e}_3(s) \\ \boldsymbol{e}_1(s) \\ \boldsymbol{e}_2(s) \end{bmatrix}
\tag{1.13}
$$

Since the progression of any moving frame along γ is ruled by a first-order differential equation, a unique triplet $\{\tau, k_1, k_2\}$ leads to a set of moving frames equal to each other within a constant of integration. Basically, with a given triplet $\{\tau, k_1, k_2\}$, one would "propagate" a given initial direct orthonormal trihedron (at $s = 0$ for instance) through the
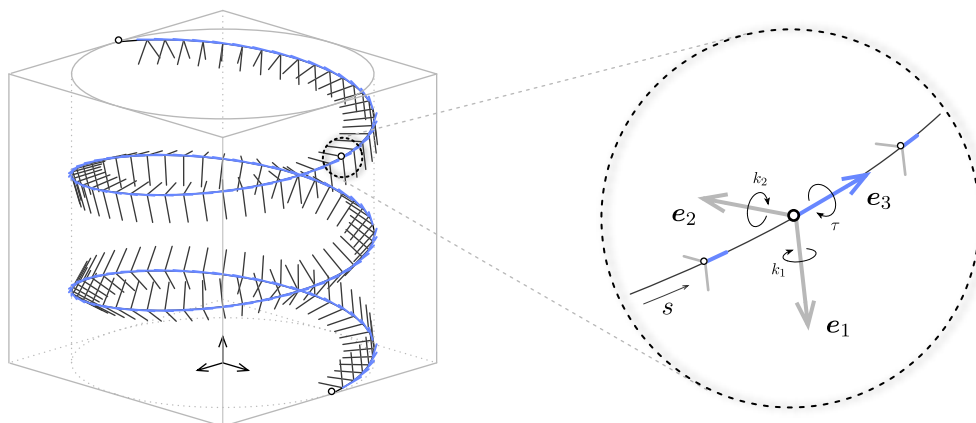
Figure 1.4 – Adapted moving frame $F(s) = \{\boldsymbol{e}_3(s), \boldsymbol{e}_1(s), \boldsymbol{e}_2(s)\}$ where $\boldsymbol{e}_3(s) = \boldsymbol{t}(s)$.

whole curve by integrating the differential system. In general, a moving frame will be fully determined by τ, κ_1, κ_2 plus $\{\boldsymbol{e}_3(s=0), \boldsymbol{e}_1(s=0), \boldsymbol{e}_2(s=0)\}$.

Darboux vector

It is relevant to consider the mobile frame's evolution along γ introducing the so-called *Darboux vector* ($\boldsymbol{\Omega}$), which corresponds to the instantaneous angular velocity of F at each point of arc-length s. Thus, the previous differential system governing the evolution of $F(s)$ along γ becomes :

$$\boldsymbol{e}_i'(s) = \boldsymbol{\Omega}(s) \times \boldsymbol{e}_i(s) \quad avec \quad \boldsymbol{\Omega}(s) = \begin{bmatrix} \tau(s) \\ k_1(s) \\ k_2(s) \end{bmatrix} \tag{1.14}$$

This result is straightforward deduced from (1.13). Note that the cross product "reveals" that the system is skew-symmetric, which could already be seen in (1.13). Geometrically, decomposing the infinitesimal rotation of the moving frame around its directors between arc-length s and $s + ds$ (Figure 1.5) shows that the scalar functions $\tau(s)$, $k_1(s)$, $k_2(s)$ effectively correspond to the angular speed of the frame, respectively around $\boldsymbol{e}_3(s)$, $\boldsymbol{e}_1(s)$, $\boldsymbol{e}_2(s)$:

$$\frac{d\theta_3}{dt}(s) = \tau(s) \quad , \quad \frac{d\theta_1}{dt}(s) = k_1(s) \quad , \quad \frac{d\theta_2}{dt}(s) = k_2(s) \tag{1.15}$$
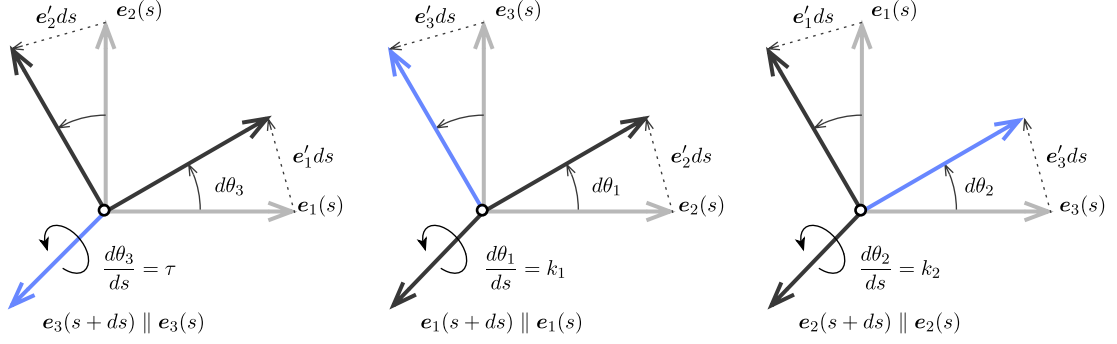
Figure 1.5 – Geometric interpretation of the Darboux vector of a moving frame.

1.6.2 Adapted frame

Let F be a moving frame as defined in the previous section. F is said to be *adapted* to γ if at each point $\gamma(s)$, $e_3(s)$ is tangent to γ :

$$\boldsymbol{d_3}(s) = \boldsymbol{t}(s) = \frac{\gamma'(s)}{\|\gamma(s)\|}, \quad \forall s \in [0, L] \tag{1.16}$$

For an adapted frame, the components k_1 and k_2 of the Darboux vector are related to the curve's curvature. Indeed, recall from 1.2 that $\kappa \equiv \|\gamma''\| = \|\boldsymbol{t}'\|$. Or $\boldsymbol{t} = \boldsymbol{d}_3$ for an adapted frame. Thus, the following relation holds :

$$\kappa = \|\boldsymbol{d}_3'\| = \sqrt{{k_1}^2 + {k_2}^2} \tag{1.17}$$

La courbure est une quantité géométrique intrinsèque, indépendante du choix du repère mobile attaché à la courbe. C'est donc un invariant. Et donc quelque soit le choix du repère mobile adapté $\|\boldsymbol{t}'\| = \sqrt{\kappa_1^2 + \kappa_2^2}$ est un invariant (la courbure).

Faire le lien avec l'énergie de flexion, qui ne dépend donc que de la géométrie de la courbe dans le cas d'une isotropic rod $\mathcal{E}_b = EI\kappa^2$.

1.6.3 Frenet frame

Definition

The Frenet frame is a well-known particular adapted moving frame (section 1.3). At any given regular point $\gamma(s)$ it is define as $\{\boldsymbol{t}(s), \boldsymbol{n}(s), \boldsymbol{b}(s)\}$ where :

$$\boldsymbol{t}(s) = \frac{\gamma'(s)}{\|\gamma'(s)\|} \quad , \quad \boldsymbol{n}(s) = \frac{\boldsymbol{t}'(s)}{\kappa(s)} \quad , \quad \boldsymbol{b}(s) = \boldsymbol{t}(s) \times \boldsymbol{n}(s) \tag{1.18}$$

Governing equations

The Frenet frame satisfies the *Frenet-Serret* formulas, which govern the evolution of the frame along the curve γ :

$$\begin{bmatrix} \boldsymbol{t}^{'}(s) \\ \boldsymbol{n}^{'}(s) \\ \boldsymbol{b}^{'}(s) \end{bmatrix} = \begin{bmatrix} 0 & \kappa(s) & 0 \\ -\kappa(s) & 0 & \tau_f(s) \\ 0 & -\tau_f(s) & 0 \end{bmatrix} \begin{bmatrix} \boldsymbol{t}(s) \\ \boldsymbol{n}(s) \\ \boldsymbol{b}(s) \end{bmatrix} \tag{1.19}$$

One can remember the generic differential equations of an adapted moving frame attached to a curve, where :

$$\boldsymbol{d_3}(s) = \boldsymbol{t}(s) = \frac{\gamma^{'}(s)}{\|\gamma(s)\|} \quad , \quad \kappa_1(s) = 0 \quad , \quad \kappa_2(s) = \kappa(s) \quad , \quad \tau(s) = \tau_f(s) \tag{1.20}$$

Darboux vector

Consequently, the Darboux vector $(\boldsymbol{\Omega_f})$ of the Frenet frame is given by :

$$\boldsymbol{\Omega_f}(s) = \begin{bmatrix} \tau_f(s) \\ 0 \\ \kappa(s) \end{bmatrix} \tag{1.21}$$

Specific points

undefined when curvature vanishes : montrer des examples

not related to mechanical torsion

une perturbation de la courbe dans le sens le sens de la courbure engendre une variation de longueur de la courbe proportionnelle à l'inverse de la courbure (au premier ordre) + schéma

une perturbation de la courbe dans le sens de la binormale (en tout point) préserve la longueur de la courbe au 1er ordre : c'est un déplacement qui conserve l'hypothèse d'inextensibilité au premier ordre

Examiner la question de la fermeture sur une boucle fermée. Schéma.

1.6.4 Bishop frame

Definition

Different ways to frame a curve. The usual one is Frenet. But, it could not be as relevant as we want in our field of interest.

The Bishop frame is defined as a a well-known particular adapted moving frame (section 1.3). At any given regular point $\gamma(s)$ it is define as $\{\boldsymbol{t}(s), \boldsymbol{n}(s), \boldsymbol{b}(s)\}$ where :

$$\boldsymbol{t}(s) = \frac{\gamma^{'}(s)}{\|\gamma'(s)\|} \quad , \quad \boldsymbol{n}(s) = \frac{\boldsymbol{t}'(s)}{\boldsymbol{\kappa}(s)} \quad , \quad \boldsymbol{b}(s) = \boldsymbol{t}(s) \times \boldsymbol{n}(s) \tag{1.22}$$

Governing equations

The Bishop frame evolution is governed by the following differential equations :

$$\begin{bmatrix} \boldsymbol{t}^{'}(s) \\ \boldsymbol{u}^{'}(s) \\ \boldsymbol{v}^{'}(s) \end{bmatrix} = \begin{bmatrix} 0 & \kappa_2(s) & -\kappa_1(s) \\ -\kappa_2(s) & 0 & 0 \\ \kappa_1(s) & 0 & 0 \end{bmatrix} \begin{bmatrix} \boldsymbol{t}(s) \\ \boldsymbol{u}(s) \\ \boldsymbol{v}(s) \end{bmatrix} \tag{1.23}$$

One can remember the generic differential equations of an adapted moving frame attached to a curve, where :

$$\boldsymbol{d_3}(s) = \boldsymbol{t}(s) = \frac{\gamma^{'}(s)}{\|\gamma(s)\|} \quad , \quad \kappa_1(s) = 0 \quad , \quad \kappa_2(s) = \kappa(s) \quad , \quad \tau(s) = \tau_f(s) \tag{1.24}$$

Darboux vector

Consequently, the Darboux vector $(\boldsymbol{\Omega_b})$ of the Bishop frame is given by :

$$\boldsymbol{\Omega_b}(s) = \begin{bmatrix} 0 \\ \kappa_1(s) \\ \kappa_2(s) \end{bmatrix} \tag{1.25}$$

Specific points

well defined when curvature vanishes

related to mechanical torsion

expliquer la relation entre bishop et frenet : bishop est obtenu par rotation d'un angle $\alpha = \int \tau_f$ par rapport à frenet.

expliquer la notion de parallèle comme l'a formulé Laurent Hauswirth : la projection de u' et v' dans le plan normal à la tangente t est nulle, cad que d'un plan à un autre la projection de u et v est conservée + faire schéma.

Laurent Hauswirth : la complexité d'un problème est en général proportionnelle à la codimension de l'objet étudié et donc, de ce fait les courbes ($codim = 3 - 1 = 2$) sont des objets plus compliqués que les surfaces ($codim = 3 - 2 = 1$) ds $\mathbb{R}^3$.

Expliquer le défaut de fermeture sur une boucle fermée. Calcul du writhe. Quelle différence

avec Frenet ?

1.6.5 Comparison between Frenet and Bishop frames

Example A : circular helix

$$\begin{cases} \rho = a \\ z = b\theta \end{cases} \tag{1.26}$$

Example B : conical helix (spiral)

$$\begin{cases} \rho = ae^{k\theta} \\ z = \rho \cot \alpha \end{cases} \tag{1.27}$$

soit pour une spirale dont on connait

(a) Frenet frame   (b) Bishop frame
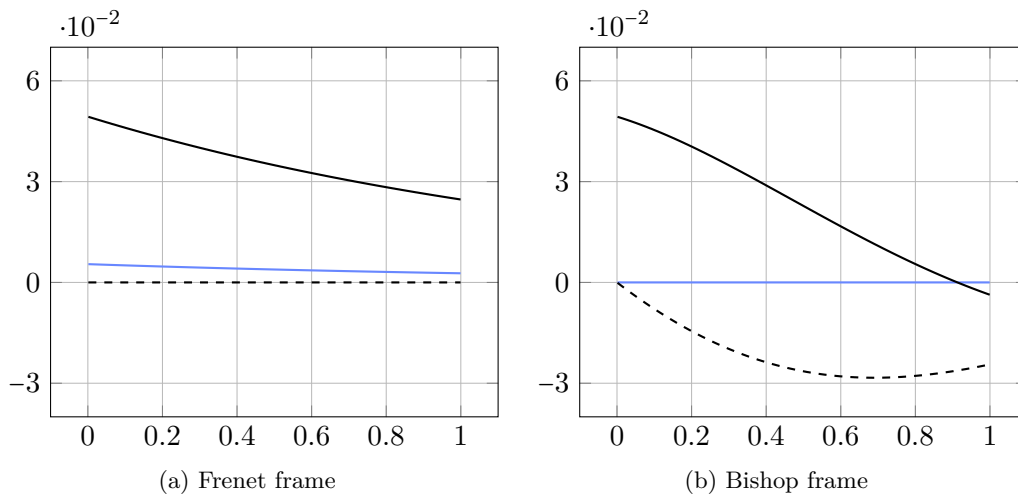
Figure 1.6 – Comparison between Frenet and Bishop frame velocity for a spirale curve.

1.7 Discrete Curvature

1.7.1 Definition

[Hof08]

The edge osculating circle. The vertex osculating circle. La localité est meilleur dans le cas du vertex-based discret osculating circle. Pour des anlges élevés, le edge-based discret osculating circle est plus pertinent. La courbure tend vers l'infini quand les 2 edges deviennent colineaires.

La définition du plan osculateur est univoque dans le cas discret : c'est localement le plan défini par 2 edges consécutifs.
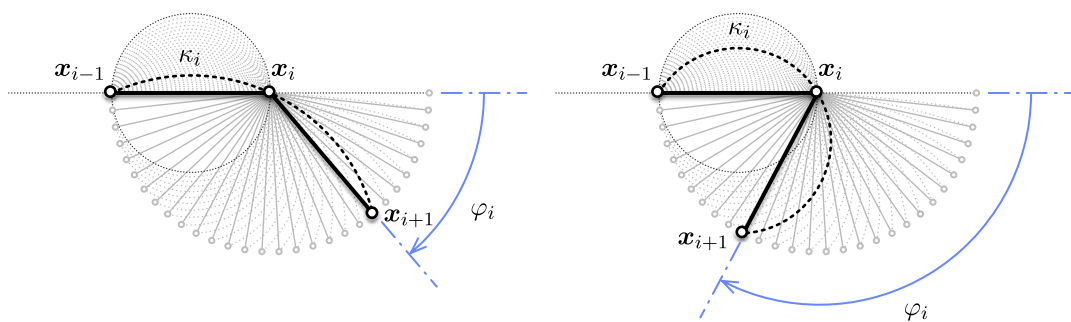
Figure 1.7 – Variation of the vertex-based discrete curvature.
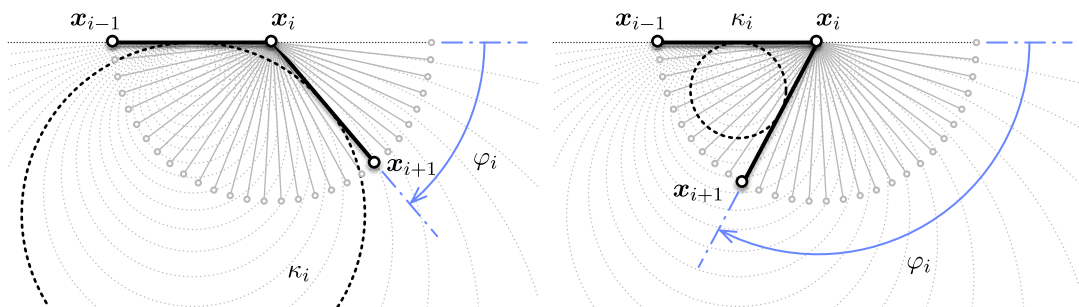
Figure 1.8 – Variation of the edge-based discrete curvature.

Ce n'est pas le cas de la courbure qui perd son côté intrinsèque.

courbure discrète dans le cas général

Vertex-based osculating circle

$$\kappa_1 = \frac{2\,sin(\varphi_i)}{\|\boldsymbol{e}_{i-1} + \boldsymbol{e}_i\|}, \tag{1.28}$$

Edge-based osculating circle

$$\kappa_2 = \frac{4\,tan(\varphi_i/2)}{\|\boldsymbol{e}_{i-1}\| + \|\boldsymbol{e}_i\|} \tag{1.29}$$

(a) vertex-based osculating circle   (b) edge-based osculating circle
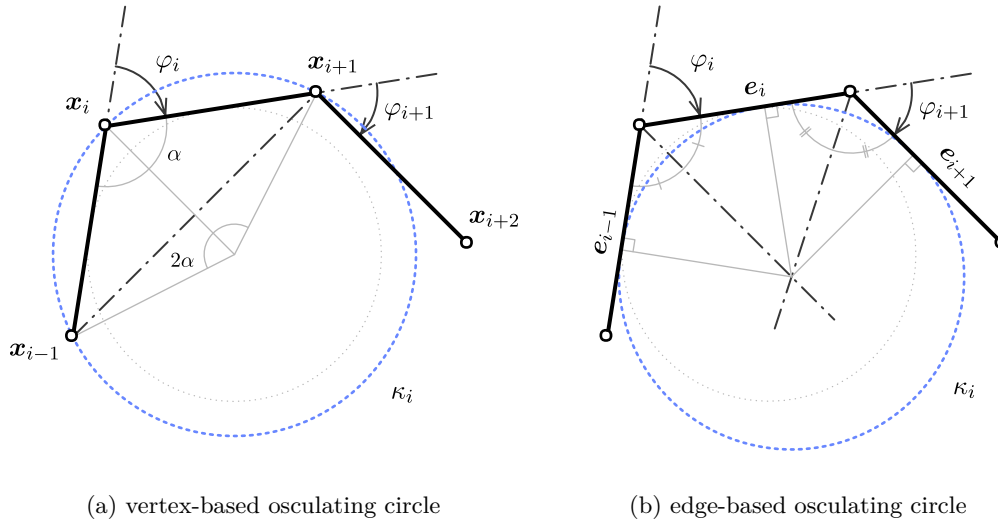
Figure 1.9 – Definition of the osculating circle for discrete curves.

$$|\boldsymbol{e}_i| = cst$$
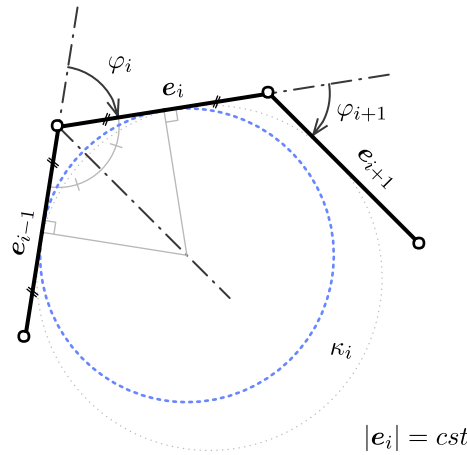
Figure 1.10 – Another definition of the osculating circle for arc-length parametrized curves.

1.7.2 Variability of discrete curvature regarding α

Qu'on réécrit en posant $\|\boldsymbol{e}_{i-1}\| = \alpha\|\boldsymbol{e}_i\|$, $\alpha \geq 0$:

$$\kappa_1 = \frac{2\,sin(\varphi_i)}{\|\boldsymbol{e}_i\|(1+\alpha^2+2\alpha\,cos(\varphi_i))^{1/2}}, \quad \kappa_2 = \frac{4\,tan(\varphi_i/2)}{\|\boldsymbol{e}_i\|(1+\alpha)} \tag{1.30}$$

$$\frac{\kappa_1}{\kappa_2}(\alpha) = \frac{\kappa_1}{\kappa_2}(1/\alpha) = \frac{1+\alpha}{(1+\alpha^2+2\alpha\,cos(\varphi_i))^{1/2}}\,cos^2(\varphi_i/2) \tag{1.31}$$
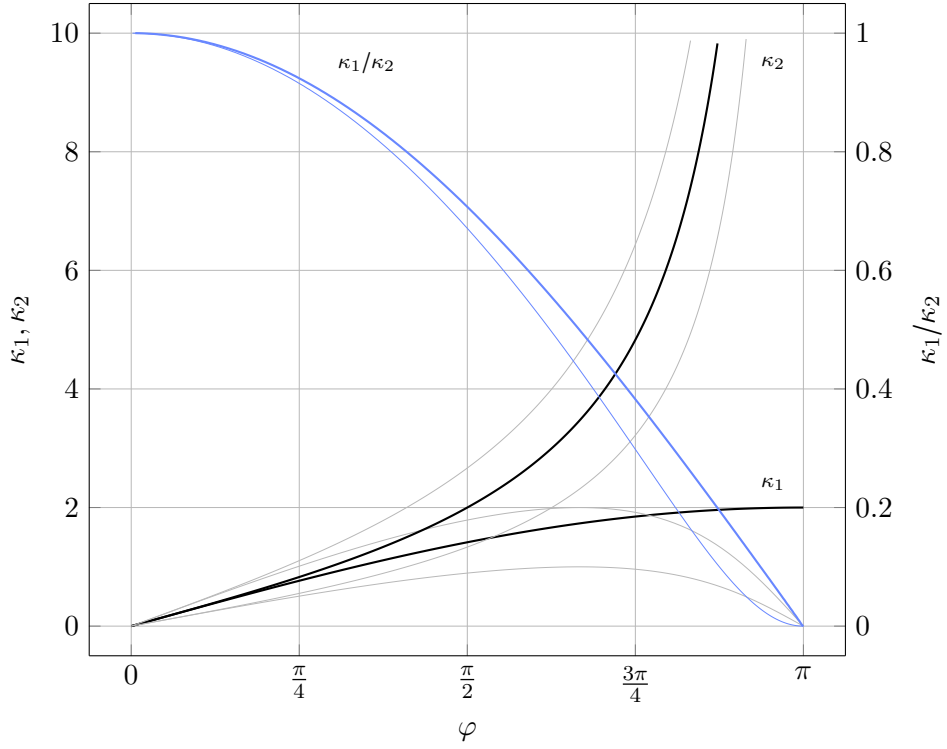
Figure 1.11 – Discrete curvature comparison for $\alpha \in [0.5, 2]$

1.7.3 Convergence benchmark κ_1 vs. κ_2

Straight line

Circle

Smooth curve settings:

$$\mathcal{E} = \int_0^l \kappa^2 ds = \kappa\pi, \quad l = \pi r, \quad \kappa = \frac{1}{r} \tag{1.32}$$

Discrete curve :

$$\varphi_N = \frac{\pi}{N}, \quad |e| = 2r\sin\frac{\varphi}{2}, \quad l_N = N|e| = 2Nr\sin\frac{\varphi}{2} = l\frac{\sin\frac{\varphi}{2}}{\frac{\varphi}{2}} \tag{1.33}$$

Discrete bending energies :

$$\mathcal{E}_1 = \mathcal{E}\frac{\sin\frac{\varphi}{2}}{\frac{\varphi}{2}}, \quad \mathcal{E}_2 = \mathcal{E}\frac{\sin\frac{\varphi}{2}}{\frac{\varphi}{2}\cos^2\frac{\varphi}{2}}, \tag{1.34}$$

Remarque that ratios are independent of scale change (independent of R)
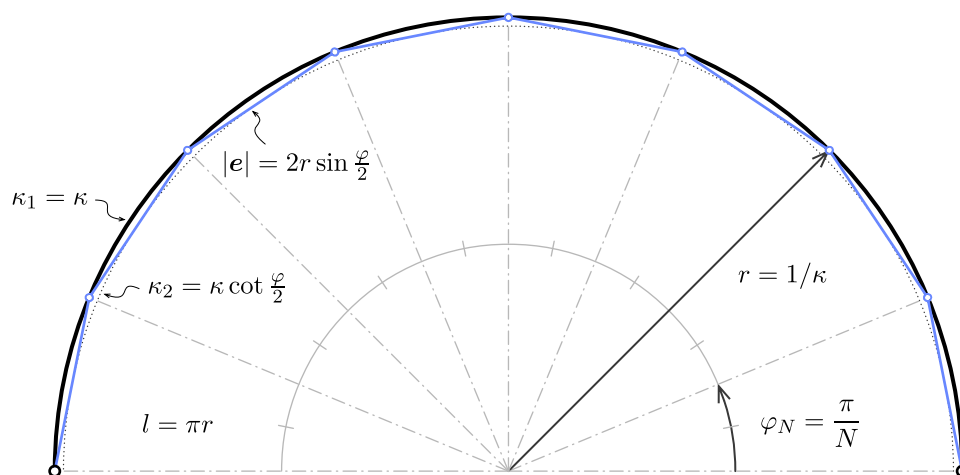
Figure 1.12 – Another definition of the osculating circle for arc-length parametrized curves.

qsmldkqsmldk s qsd qsd sqd qs dqs=dlk qs=ldk sq
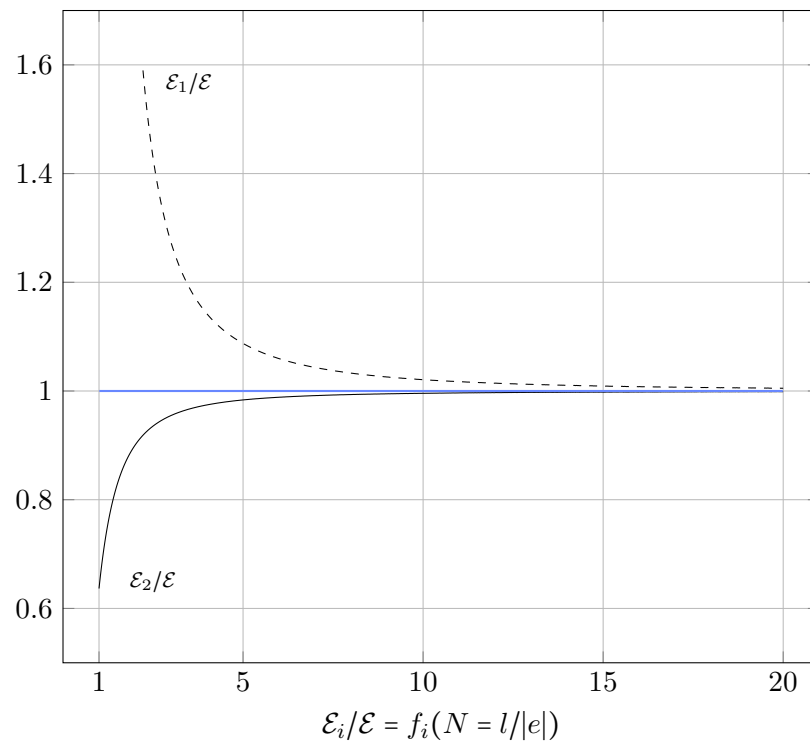
Figure 1.13 – Discrete curvature comparison for $\alpha \in [0.5, 2]$

Elastica
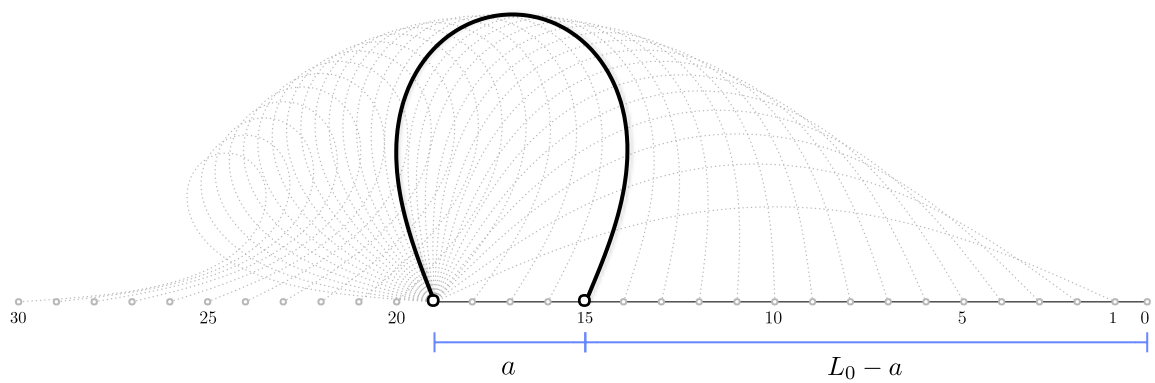
Figure 1.14 – Another definition of the osculating circle for arc-length parametrized curves.
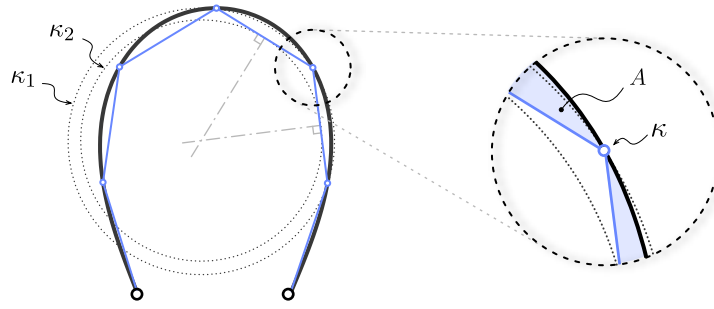
Figure 1.15 – Another definition of the osculating circle for arc-length parametrized curves.

(a) $\mathcal{E}_1/\mathcal{E} = f(N = l/|e|)$

(b) $\mathcal{E}_2/\mathcal{E} = f(N = l/|e|)$
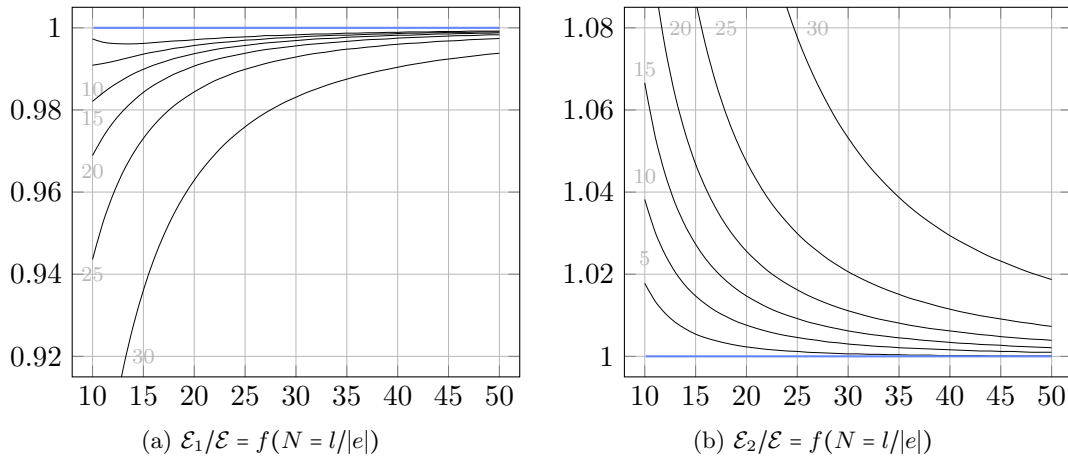
Figure 1.16 – Bending energy representativity

Bibliography

[Bis75] Richard L. Bishop. There is more than one way to frame a curve. *Mathematical Association of America*, 1975.

[Hof08] Tim Hoffmann. Discrete Differential Geometry of Curves and Surfaces, 2008.

2 Elastic rod : variational approch

2.1 Introduction

2.1.1 Goals and contribution

In this section a novel element with 4 degrees of freedom accounting for torsion and bending behaviours is presented. The beam is considered in Kirchhoff's theory framework, so that it is supposed to be inextensible and its sections are supposed to remain orthogonal to the centreline during deformation. The reduction from the classic 6-DoF model to this 4-DoF model is achieved by an appropriate curve-angle representation based on a relevant curve framing. Energies are then formulated and leads to internal forces and moments acting on the beam. The static equilibrium is deduced from a damped fictitious dynamic with an adapted dynamic relaxation algorithm.

2.1.2 Related work

Basile [BAV+10] Basile [BWR+08] Basile [**?**] Sina [Nab14] [Ful78], [dV05], [Vau00], [Ber09]

Dynamic relaxation : [Lew03] En particulier,voir pour un comparatif avec une méthode implicite.

2.1.3 Overview

1. quaternion pour piloter les input / ouput ?

2. calcul de la hessienne au moins pour les θ comme Audoly. Ne serait-ce pas possible pour les x ? Avec ma technique du transport parallèle il me semble pourvoir avoir accès au DL à l'ordre 2 ...

3. Formulation pour les efforts ponctuels / moments extérieurs en vue d'une résolution

par minimisation. Voir F. Bertails

4. prise en compte des contraintes => méméthide des multiplicateurs de lagrange

2.2 Kirchhoff rod

The geometric configuration of the rod is described by its centerline $\boldsymbol{x}(s)$ and its cross sections. The centerline is parameterized by its arc-length. Cross sections orientations are followed along the centerline by their material frame $\{\boldsymbol{d}_3(s), \boldsymbol{d}_1(s), \boldsymbol{d}_2(s)\}$ which is an adapted orthonormal moving frame aligned to section's principal axes of inertia. Here, "adapted" means $\boldsymbol{d}_3(s) = \boldsymbol{x}'(s) = \boldsymbol{t}(s)$ is aligned to the centerline's tangent. In the literature, this description is also known as a *Cosserat Curve* [ST07].

2.2.1 Inextensibility

Note the previous description is only valid for inextensible rods in order to follow material points by their arc-length indifferently in their rest or deformed configuration. As explained in [AAP10], this hypothesis is usually relevant for slender beams. Indeed, in practice, if a slender member faces substantial axial strain the bending behaviour would become negligible due to the important difference between axial and bending stiffness. The length of the rod will be denoted L and the arc-length s will vary (with no loss of generality) in $[0, L]$.

2.2.2 Euler-Bernouilli

Strains are supposed to remain small so that material frame remains orthogonal to the centerline in the deformed configuration. Thus, differentiating the conditions of orthonormality leads to the following differential equations governing the evolution of $\{\boldsymbol{d}_3(s), \boldsymbol{d}_1(s), \boldsymbol{d}_2(s)\}$ along the centerline :

$$\begin{bmatrix} \mathbf{d_3'}(s) \\ \mathbf{d_1'}(s) \\ \mathbf{d_2'}(s) \end{bmatrix} = \begin{bmatrix} 0 & \kappa_2(s) & -\kappa_1(s) \\ -\kappa_2(s) & 0 & \tau(s) \\ \kappa_1(s) & -\tau(s) & 0 \end{bmatrix} \begin{bmatrix} \mathbf{d_3}(s) \\ \mathbf{d_1}(s) \\ \mathbf{d_2}(s) \end{bmatrix} \tag{2.1}$$

La théorie des poutres est une application de la théorie de l'élasticité isotrope. Pour mener les calculs de résistance des matériaux, on considère les hypothèses suivantes :

(1) hypothèse de Bernoulli : au cours de la déformation, les sections droites restent perpendiculaires à la courbe moyenne ;

(2) les sections droites restent planes selon Navier-Bernoulli (pas de gauchissement).

L'hypothèse de Bernoulli permet de négliger le cisaillement dans le cas de la flexion : le risque de rupture est alors due à l'extension des fibres situées à l'extérieur de la flexion, et

la flèche est due au moment fléchissant. Cette hypothèse n'est pas valable pour les poutres courtes car ces dernières sont hors des limites de validité du modèle de poutre, à savoir que la dimension des sections doit être petite devant la longueur de la courbe moyenne. Le cisaillement est pris en compte dans le modèle de Timoshenko et Mindlin.

2.2.3 Darboux vector

Those equations can be formulated with the *Darboux vector* of the chosen material frame, which represents the rotational velocity of the frame along $\boldsymbol{x}(s)$:

$$\boldsymbol{d}_i'(s) = \boldsymbol{\Omega}_m(s) \times \boldsymbol{d}_i(s) \quad , \quad \boldsymbol{\Omega}_m(s) = \begin{bmatrix} \tau(s) \\ \kappa_1(s) \\ \kappa_2(s) \end{bmatrix} \tag{2.2}$$

Where $\kappa_1(s)$, $\kappa_2(s)$ and $\tau(s)$ represent respectively the rate of rotation of the material frame around the axis $\boldsymbol{d}_1(s)$, $\boldsymbol{d}_2(s)$ and $\boldsymbol{d}_3(s)$.

2.2.4 Curvatures and twist

The material curvatures are denoted $\kappa_1(s)$ and $\kappa_2(s)$ and represent the rod's flexion in the principal planes respectively normal to $\boldsymbol{d}_1(s)$ and $\boldsymbol{d}_2(s)$ .The material twist is denoted $\tau(s)$ and represents the section's rate of rotation around $\boldsymbol{d}_3(s)$. Those scalar functions measure directly the strain as defined in Kirchhoff's theory (Figure 4). Recall that the Frenet frame $\{\boldsymbol{t}(s), \boldsymbol{n}(s), \boldsymbol{b}(s)\}$ defines the osculating plane and the total curvature (κ) of a spatial curve :

$$\boldsymbol{t}'(s) = \kappa(s)\boldsymbol{n}(s) \quad , \quad \kappa(s) = \|\boldsymbol{t}'(s)\| \quad , \quad \boldsymbol{b}(s) = \boldsymbol{t}(s) \times \boldsymbol{n}(s) = \frac{\boldsymbol{t}(s) \times \boldsymbol{t}'(s)}{\kappa(s)} \tag{2.3}$$

To describe the osculating plane in which lies the bending part of the deformation, let's introduce the *curvature binormal* $\kappa\boldsymbol{b}(s) = \boldsymbol{t}(s) \times \boldsymbol{t}'(s)$, the vector of direction $\boldsymbol{b}(s)$ and norm $\kappa(s)$. At each point of arc-length s the osculating plane is normal to $\kappa\boldsymbol{b}(s)$.

2.2.5 Elastic energy

Kirrchhoff's theory assigns an elastic energy to beams according to their strain [AAP10]. In this theory, a beam is supposed to be inextensible. Thus the elastic energy $(\mathcal{E}_p)$ only accounts for torsion and bending behaviors and is given by :

$$\mathcal{E}_p = \tfrac{1}{2} \int_0^L EI_1(\kappa_1 - \overline{\kappa_1})^2 + EI_2(\kappa_2 - \overline{\kappa_2})^2 ds + \tfrac{1}{2} \int_0^L \beta(\tau - \bar{\tau})^2 ds \tag{2.4}$$

Here, $\overline{\kappa_1}$, $\overline{\kappa_2}$ and $\bar{\tau}$ denote the natural curvature and twist of the rod in the rest position (no stress).

2.3 Curve-angle representation

The previous paragraph has shown how the elastic potential energy of a rod can be computed following both its centerline and its cross sections orientations, which represents a model with 6-DoF : 3 for centerline positions and 3 for cross section orientations.

Following [BWR$^+$08], let's introduce a reduced coordinate formulation of the rod that account for only 4-DoF. This reduction of DoF relies on the concept of zero-twisting frame which gives a reference frame with zero twist along a given centerline. Thus, cross section orientations $\{d_3(s), d_1(s), d_2(s)\}$ can be tracked only by the measure of an angle θ from this reference frame denoted $\{d_3(s), u(s), v(s)\}$ (Figure 5).

Note that an alternative solution could be to parameterize the global rotations of local material frame and to compute the rotation needed to align two successive frames along the curve's tangent.

Ici, expliquer la succession des dépendances : les vecteurs matériaux dépendent du repère de bishop par la seule variable theta. Le repère de bishop quand à lui est entièrement déterminé (au choix d'une constante de départ près) par la donnée de la centerline x.

Faire un schéma explicatif.

quid du transport parallèle en temps et non en espace ?

2.3.1 Zero-twisting frame

Zero-twisting frame, also known as Bishop frame, was introduced by Bishop in 1964. Bishop remarked that there was more than one way to frame a curve [Bis75]. Indeed, for a given curve, any orthonormal moving frame would satisfy the following differential equations, where $k_1(s)$, $k_2(s)$ and $\tau(s)$ are scalar functions that define completely the moving frame :

$$\begin{bmatrix} \mathbf{e_3'}(s) \\ \mathbf{e_1'}(s) \\ \mathbf{e_2'}(s) \end{bmatrix} = \begin{bmatrix} 0 & k_2(s) & -k_1(s) \\ -k_2(s) & 0 & \tau(s) \\ k_1(s) & -\tau(s) & 0 \end{bmatrix} \begin{bmatrix} \mathbf{e_3}(s) \\ \mathbf{e_1}(s) \\ \mathbf{e_2}(s) \end{bmatrix} \tag{2.5}$$

For instance, a Frenet frame $\{t(s), n(s), b(s)\}$ is a frame which satisfies $k_1(s) = 0$. Note that this frame suffers from major disadvantages : it is undefined where the curvature vanishes and it flips at inflexion points. A Bishop frame $\{t(s), u(s), v(s)\}$ is a frame which satisfies $\tau(s) = 0$. By construction, this frame has no angular velocity (i.e. no twist) around the curve's tangent ($u \cdot v' = u' \cdot v = 0$). Its evolution along the curve is described by the corresponding Darboux vector : $\mathbf{\Omega}_b(s) = \kappa b = t \times t'$. Remark that $\mathbf{\Omega}_b(s)$ only depends on the centerline and is well defined even when the curvature vanishes.

Thus, by the help of $\mathbf{\Omega}_b(s)$, it's possible to transport a given vector e along the centerline with no twist : $e' = \kappa b \times e$. This is called *parallel transport*.

2.4 Strains

2.4.1 Axial strain

There is no axial strain to be considered as far as the rod is supposed to be unstretchable.

Remark that the inextensibility hypothesis implies that any admissible perturbation $(\lambda \boldsymbol{h}_x)$ of the rod's centerline $(\boldsymbol{x})$ is locally orthogonal to the centerline itself. Indeed, at each arc-length s an inextensible rod must satisfies :

$$\|\boldsymbol{x}'\| = \|(\boldsymbol{x} + \lambda \boldsymbol{h}_x)'\| = 1 \Rightarrow \boldsymbol{d}_3 \cdot \boldsymbol{h}_x' = -\tfrac{\lambda^2}{2}\|\boldsymbol{h}_x'\|^2 = o(\lambda) \simeq 0 \tag{2.6}$$

In other words, this means that the same arc-length parametrization can be used to locate beam sections along the centerline along the deformation path. This would not be the case if the centerline would shorten or stretch out during its deformation. It is worth to mention here that this property $(\boldsymbol{d}_3 \cdot \boldsymbol{h}_x' = 0)$ will be used several times in the following sections.

2.4.2 Bending strain

Let's compute the bending strains κ_1 and κ_2 regarding the geometric configuration of the rod. Remark that :

$$\kappa \boldsymbol{b} \cdot \boldsymbol{d}_1 = (\boldsymbol{d}_3 \times \boldsymbol{d}_3') \cdot \boldsymbol{d}_1 = (\boldsymbol{d}_1 \times \boldsymbol{d}_3) \cdot \boldsymbol{d}_3' = -\boldsymbol{d}_2 \cdot \boldsymbol{d}_3' = \kappa_1 \tag{2.7a}$$

$$\kappa \boldsymbol{b} \cdot \boldsymbol{d}_2 = (\boldsymbol{d}_3 \times \boldsymbol{d}_3') \cdot \boldsymbol{d}_2 = (\boldsymbol{d}_2 \times \boldsymbol{d}_3) \cdot \boldsymbol{d}_3' = \boldsymbol{d}_1 \cdot \boldsymbol{d}_3' = \kappa_2 \tag{2.7b}$$

That is to say $\kappa \boldsymbol{b}$ is orthogonal to $\boldsymbol{d}_3$:

$$\kappa \boldsymbol{b} = \kappa_1 \boldsymbol{d}_1 + \kappa_2 \boldsymbol{d}_2 \tag{2.8}$$

Thus, the vector of material curvatures $(\boldsymbol{\omega})$ expressed on material frame axes $\{\boldsymbol{d}_1(s), \boldsymbol{d}_2(s)\}$ is defined as :

$$\boldsymbol{\omega} = \begin{bmatrix} \kappa_1 \\ \kappa_2 \end{bmatrix} = \begin{bmatrix} \kappa \boldsymbol{b} \cdot \boldsymbol{d}_1 \\ \kappa \boldsymbol{b} \cdot \boldsymbol{d}_2 \end{bmatrix} = \begin{bmatrix} -\boldsymbol{x}'' \cdot \boldsymbol{d}_2 \\ \boldsymbol{x}'' \cdot \boldsymbol{d}_1 \end{bmatrix} \tag{2.9}$$

2.4.3 Torsional strain

Let's compute the twist or torsional strain τ regarding the geometric configuration of the rod. Decomposing the material frame on the bishop frame gives :

$$\begin{bmatrix} \boldsymbol{d}_1 \\ \boldsymbol{d}_2 \end{bmatrix} = \begin{bmatrix} \cos\theta & \sin\theta \\ -\sin\theta & \cos\theta \end{bmatrix} \begin{bmatrix} \boldsymbol{u} \\ \boldsymbol{v} \end{bmatrix} \tag{2.10}$$

Thus, the twist can be identified directly as the variation of θ along the curve :

$$\tau = \boldsymbol{d}_1' \cdot \boldsymbol{d}_2 = (\theta' \boldsymbol{d}_2 + \kappa \boldsymbol{b} \times \boldsymbol{d}_1) \cdot \boldsymbol{d}_2 = \theta' + \boldsymbol{d}_3 \cdot \kappa \boldsymbol{b} = \theta' \tag{2.11}$$

Note that the Frenet frame does not lead to a correct evaluation of the twist.

2.5   Elastic energy

Introducing $\boldsymbol{\omega}$ and θ, the elastic energy can be rewritten as follow :

$$\mathcal{E}_p = \mathcal{E}_b + \mathcal{E}_t = \frac{1}{2} \int_0^L (\boldsymbol{\omega} - \overline{\boldsymbol{\omega}})^T B (\boldsymbol{\omega} - \overline{\boldsymbol{\omega}}) ds + \frac{1}{2} \int_0^L \beta (\theta' - \overline{\theta'})^2 ds \tag{2.12}$$

Where B is the bending stiffness matrix along the principal axes of inertia and β is the torsional stiffness :

$$B = \begin{bmatrix} EI_1 & 0 \\ 0 & EI_2 \end{bmatrix} \quad , \quad \beta = GJ \tag{2.13}$$

Recall that the rod is supposed to be inextensible in Kirchhoff's theory. Thus, there is no stretching energy associated with an axial strain. However, this constraint may be enforced via a penalty energy, which in practice is somehow very similar as considering an axial stiffness into the beam's

Remark that the twisting energy ($\mathcal{E}_t$) only depends on θ and is independent regarding $\boldsymbol{x}$ while the bending energy ($\mathcal{E}_b$) depends on both θ and $\boldsymbol{x}$ variables (remind that κ_1 and κ_2 are the projections of $\kappa\boldsymbol{b}$ over $\boldsymbol{d}_1$ over $\boldsymbol{d}_2$). Thus, a coupling between bending and twisting appears as the minimum of the whole elastic energy is not necessarily reached for concomitant minimums of bending and twisting energies.

From this energy formulation, an interesting an well-known result on elastic rods could be highlighted : "torsion is uniform in an isotropic rod that is straight in its rest configuration" [ABW99].

Indeed, let's take an isotropic rod ($EI_1 = EI_2 = EI$) that is straight in its rest configuration ($\overline{\kappa_1} = \overline{\kappa_2} = 0$). Then, the bending energy becomes : $\mathcal{E}_b = EI_1\kappa_1^2 + EI_2\kappa_2^2 = EI\kappa^2$, and consequently doesn't depends on θ anymore. The curvature of the rod only depends on the geometry of its centerline ($\kappa = \|\kappa\boldsymbol{b}\| = \|\boldsymbol{x}' \times \boldsymbol{x}''\|$). Thus, there is no more coupling between bending and twisting and the global minimum of elastic energy is reached while minimizing separately bending an twisting energies. That is to say the geometry of the rod ($\boldsymbol{x}$) is the one that minimized $\mathcal{E}_b$. The minimum of $\mathcal{E}_t$ is zero and is achieved for a uniform twist along the centerline, only prescribed by the boundary conditions.

2.6   Quasistatic assumption

Following [BWR$^+$08], it is relevant to assume that the propagation of twist waves is instantaneous compared to the one of bending waves. Thus, internal forces $\boldsymbol{f}^{int}$ and moment of torsion $\boldsymbol{m}^{int}$ acts on two different timescales in the rod dynamic. Thus on the timescale of action of the force $\boldsymbol{f}^{int}$ on the center line, driving the bending waves, the twist

waves propagate instantaneously, so that $\forall s \in [0, L]$, $\delta\mathcal{E}_p/\delta\theta = 0$ for the computation of $\boldsymbol{f}^{int}$. This assumption may not be enforced, as in [Nab14], but leads to simpler and faster computations.

2.7 Energy gradient with respect to θ : moment of torsion

Internal moment of torsion and forces acting on the rod are classically obtained by differentiating the potential energy of the system with respect to θ and $\boldsymbol{x}$. Here, the calculus is a bit tricky as far as the differentiation takes place in function spaces. After a brief reminder on functional derivative, the main results of the calculations of the energy derivatives are given.

2.7.1 Derivative of material directors with respect to θ

Recalling that θ and $\boldsymbol{x}$ are independant variables and that Bishop frame $\{\boldsymbol{u}, \boldsymbol{v}\}$ only depends on $\boldsymbol{x}$, the decomposition of material frame directors $\{\boldsymbol{d}_1, \boldsymbol{d}_2\}$ on Bishop frame leads directly to the following expression for the derivative of the material directors :

$$\boldsymbol{D}_\theta \boldsymbol{d}_1(s) \cdot h_\theta = \frac{d}{d\lambda}\boldsymbol{d}_1[\theta + \lambda h_\theta]\bigg|_{\lambda=0} = (-\sin\theta\,\boldsymbol{u} + \cos\theta\,\boldsymbol{v}) \cdot h_\theta = \boldsymbol{d}_2 \cdot h_\theta \tag{2.14a}$$

$$\boldsymbol{D}_\theta \boldsymbol{d}_2(s) \cdot h_\theta = \frac{d}{d\lambda}\boldsymbol{d}_2[\theta + \lambda h_\theta]\bigg|_{\lambda=0} = (-\cos\theta\,\boldsymbol{u} - \sin\theta\,\boldsymbol{v}) \cdot h_\theta = -\boldsymbol{d}_1 \cdot h_\theta \tag{2.14b}$$

2.7.2 Derivative of the material curvatures vector with respect to θ

Regarding the definition of the material curvatures vector and the derivative of material directors with respect to θ, it follows immediately that :

$$\boldsymbol{D}_\theta \boldsymbol{\omega}(s) \cdot h_\theta = \frac{d}{d\lambda}\boldsymbol{\omega}[\theta + \lambda h_\theta]\bigg|_{\lambda=0} = \begin{bmatrix} \kappa\boldsymbol{b} \cdot \boldsymbol{d}_2 \\ -\kappa\boldsymbol{b} \cdot \boldsymbol{d}_1 \end{bmatrix} \cdot h_\theta = -\boldsymbol{J}\boldsymbol{\omega} \cdot h_\theta \tag{2.15}$$

Where $\boldsymbol{J}$ is the matrix that acts on two dimensional vectors by counter-clockwise rotation of angle $\frac{\pi}{2}$:

$$\boldsymbol{J} = \begin{bmatrix} 0 & -1 \\ 1 & 0 \end{bmatrix} \tag{2.16}$$

2.7.3 Computation of the moment of torsion

The moment of torsion is given by the functional derivative of the potential elastic energy with respect to θ which can be decomposed according to the chaine rule :

$$\langle -m(s)\,;h_\theta\rangle = \boldsymbol{D}_\theta\mathcal{E}_p(s) \cdot h_\theta = \boldsymbol{D}_\theta\mathcal{E}_b(s) \cdot h_\theta + \boldsymbol{D}_\theta\mathcal{E}_t(s) \cdot h_\theta$$
$$= \boldsymbol{D}_\theta\mathcal{E}_b[\boldsymbol{\omega}[\theta]](s) \cdot h_\theta + \boldsymbol{D}_\theta\mathcal{E}_t[\theta](s) \cdot h_\theta \tag{2.17}$$

Derivative of the torsion energy with respect to θ

Decomposing the previous calculus gives:

$$
\begin{aligned}
\boldsymbol{D}_\theta \mathcal{E}_t[\theta](s) \cdot h_\theta &= \frac{d}{d\lambda}\mathcal{E}_t[\theta + \lambda h_\theta]\Big|_{\lambda=0} \\
&= \frac{d}{d\lambda}\left(\tfrac{1}{2}\int_0^L \beta\left((\theta + \lambda h_\theta)' - \overline{\theta'}\right)^2 \, dt\right)\Big|_{\lambda=0} \\
&= \int_0^L \beta(\theta' - \overline{\theta'})\cdot h_\theta' \, dt \\
&= \left[\beta(\theta' - \overline{\theta'})\cdot h_\theta\right]_0^L - \int_0^L \left(\beta(\theta' - \overline{\theta'})\right)' \cdot h_\theta \, dt \\
&= \int_0^L \left(\beta(\theta' - \overline{\theta'})(\delta_L - \delta_0) - \left(\beta(\theta' - \overline{\theta'})\right)'\right)\cdot h_\theta \, dt
\end{aligned}
\tag{2.18}
$$

Derivative of the bending energy with respect to θ

The derivative of $\mathcal{E}_b$ is obtained with the chaine rule :

$$
\begin{aligned}
\boldsymbol{D}_\omega \mathcal{E}_b[\boldsymbol{\omega}](s) \cdot \boldsymbol{h}_\omega &= \frac{d}{d\lambda}\mathcal{E}_b[\boldsymbol{\omega} + \lambda \boldsymbol{h}_\omega]\Big|_{\lambda=0} \\
&= \frac{d}{d\lambda}\left(\tfrac{1}{2}\int_0^L \left((\boldsymbol{\omega} + \lambda \boldsymbol{h}_\omega) - \overline{\boldsymbol{\omega}}\right)^T \boldsymbol{B}\left((\boldsymbol{\omega} + \lambda \boldsymbol{h}_\omega) - \overline{\boldsymbol{\omega}}\right) \, dt\right)\Big|_{\lambda=0} \\
&= \int_0^L (\boldsymbol{\omega} - \overline{\boldsymbol{\omega}})^T \boldsymbol{B}\cdot \boldsymbol{h}_\omega \, dt
\end{aligned}
\tag{2.19}
$$

Finally, reminding eq 4.14 :

$$
\begin{aligned}
\boldsymbol{D}_\theta \mathcal{E}_b[\boldsymbol{\omega}[\theta]](s) \cdot h_\theta &= \boldsymbol{D}_\omega \mathcal{E}_b[\boldsymbol{\omega}](s) \cdot \left(\boldsymbol{D}_\theta \boldsymbol{\omega}[\theta](s) \cdot h_\theta\right) \\
&= -\int_0^L (\boldsymbol{\omega} - \overline{\boldsymbol{\omega}})^T \boldsymbol{B}\boldsymbol{J}\boldsymbol{\omega} \cdot h_\theta \, dt
\end{aligned}
\tag{2.20}
$$

Moment of torsion

Thus, the

$$
\begin{aligned}
\langle -m(s)\,;h_\theta\rangle &= \boldsymbol{D}_\theta \mathcal{E}_b[\boldsymbol{\omega}[\theta]](s) \cdot h_\theta + \boldsymbol{D}_\theta \mathcal{E}_t[\theta](s) \cdot h_\theta \\
&= \int_0^L \left(\left(\beta(\theta' - \overline{\theta'})(\delta_L - \delta_0) - \left(\beta(\theta' - \overline{\theta'})\right)'\right) - (\boldsymbol{\omega} - \overline{\boldsymbol{\omega}})^T \boldsymbol{B}\boldsymbol{J}\boldsymbol{\omega}\right)\cdot h_\theta \, dt
\end{aligned}
\tag{2.21}
$$

Finally, we can conclude on the expression of the internal moment of torsion :

$$
m(s) = -\left(\beta(\theta' - \overline{\theta'})(\delta_L - \delta_0) - \left(\beta(\theta' - \overline{\theta'})\right)'\right) + (\boldsymbol{\omega} - \overline{\boldsymbol{\omega}})^T \boldsymbol{B}\boldsymbol{J}\boldsymbol{\omega}
\tag{2.22}
$$

Quasistatic hypothesis

$$
\left(\beta(\theta' - \overline{\theta'})\right)' + (\boldsymbol{\omega} - \overline{\boldsymbol{\omega}})^T \boldsymbol{B}\boldsymbol{J}\boldsymbol{\omega} = 0
\tag{2.23}
$$

2.8 Energy gradient with respect to x : internal forces

Internal torsional moments and forces acting on the rod are classically obtained by differentiating the potential energy of the system with respect to θ and $\boldsymbol{x}$. Here, the calculus is a bit tricky as far as the differentiation takes place in function spaces. After a brief reminder on functional derivative, the main results of the calculations of the energy derivatives are given.

paragraphe entièrment à revoir. Expliquer le cheminement. x fixe bishop et theta fixe d1,d2 par rapport à bishop. x est indépendant de theta. Seul des CL peuvent créer des couplages entre x et theta

Donc les vrais degrés de liberté du problème sont en fait les vecteurs matériels et les positions x. Se reporter à une modélisation du pb dans SO3 comme Spillmann par exemple.

Le calcul des gradients se résume donc à calculer les gradients des vecteurs matériels par rapport à des perturbations infinitésimales en x et theta. Pour theta, c'est facile. Pour kb, c'est facile. Reste la variation par rapport à x, qui est en fait la variation de bishop qu'on explique avec le writhe (défaut de fermeture de bishop sur une boucle fermée) et le transport parallèle. Le calcul se fait aisément en écrivant la double rotation et en effectuant le DL au premier ordre.

Le reste est quasiment immédiat. Reste la question des CL et des termes aux bords.

Il faut aussi se positionner par rapport à l'article de Basile. Regarder la question applied displacement vs settlement pour imposer une CL.

2.8.1 Derivative of material directors with respect to $\boldsymbol{x}$

ici expliquer le fonctionnement de la figure

A variation of the centerline $\boldsymbol{x}$ by $\boldsymbol{\epsilon} = \lambda \boldsymbol{h}_x$ would cause a variation in the Bishop frame because parallel transport depends on the centerline itself. As far as $\boldsymbol{x}$ and θ are independent variables, this leads necessarily to a variation of the material frame. Let us denote :

- $F = \{\boldsymbol{t}, \boldsymbol{u}, \boldsymbol{v}\}$: the Bishop frame in the reference configuration ;

- $F_\epsilon = \{\boldsymbol{t}_\epsilon, \boldsymbol{u}_\epsilon, \boldsymbol{v}_\epsilon\}$: the Bishop frame in the deformed configuration ;

- $\tilde{F}_\epsilon = \{\boldsymbol{t}, \tilde{\boldsymbol{u}}_\epsilon, \tilde{\boldsymbol{v}}_\epsilon\}$: the frame obtained by parallel transporting F_ϵ back on F.

What we want to achive is to write at arc-length s the Bishop frame in the deformed configuration $\{\boldsymbol{t}_\epsilon, \boldsymbol{u}_\epsilon, \boldsymbol{v}_\epsilon\}$ on the Bishop frame in the reference configuration $\{\boldsymbol{t}, \boldsymbol{u}, \boldsymbol{v}\}$ for a small perturbation ϵ of the centerline. This transformation can be decomposed in two rotations :
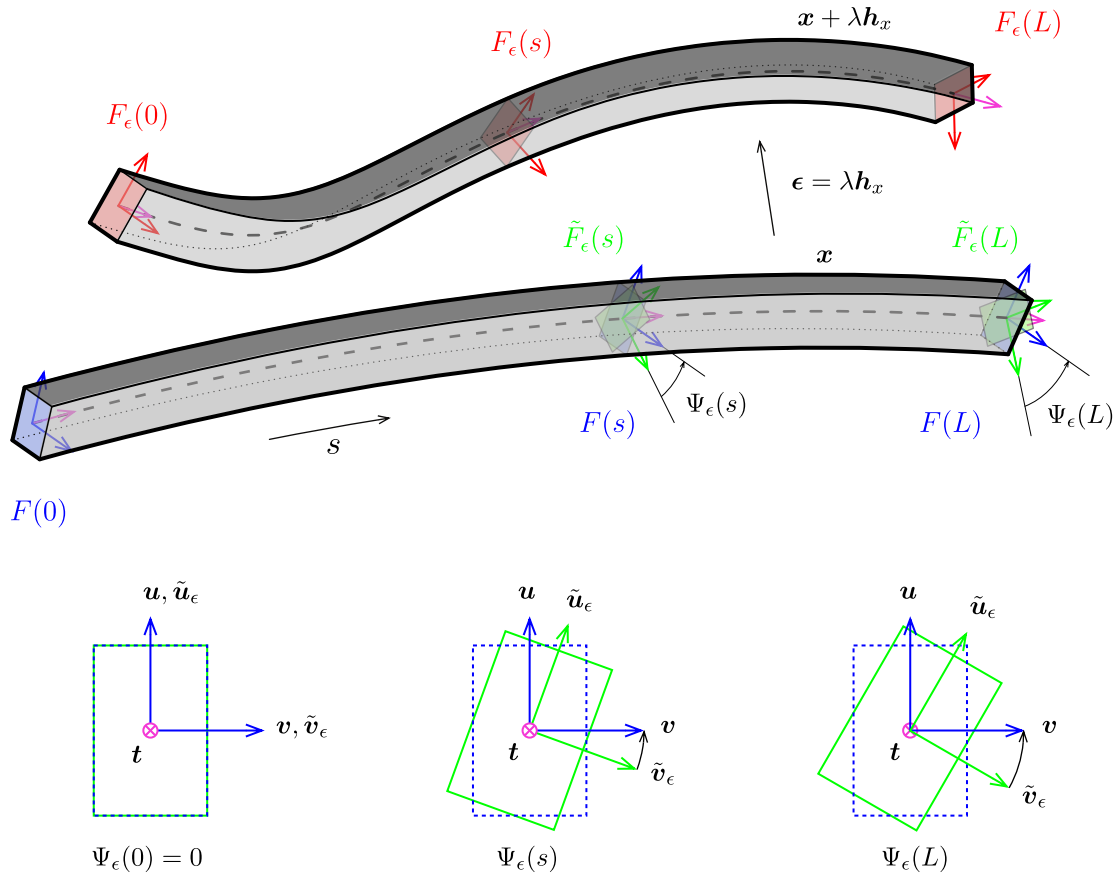
Figure 2.1 – Repères de Frenet attachés à γ.

- $F_\epsilon \to \tilde{F}_\epsilon$: parallel transporting F_ϵ from $\boldsymbol{t}_\epsilon$ to $\boldsymbol{t}$. This is equivalent to a rotation around $\boldsymbol{t}_\epsilon \times \boldsymbol{t}$ by an angle α_ϵ.

- $\tilde{F}_\epsilon \to F$: aligning $\tilde{F}_\epsilon$ over F. This is equivalent to a rotation around $\boldsymbol{t}$ of an angle Ψ_ϵ.

Firstly, let's decompose $\{\boldsymbol{t}_\epsilon, \boldsymbol{u}_\epsilon, \boldsymbol{v}_\epsilon\}$ on the basis $\{\boldsymbol{t}, \tilde{\boldsymbol{u}}_\epsilon, \tilde{\boldsymbol{v}}_\epsilon\}$. Note that $\tilde{F}_\epsilon$ is expressed by rotating $\tilde{F}_\epsilon$ by an angle $\Psi_\epsilon[\boldsymbol{x}](s)$ around $\boldsymbol{t}$ because $\tilde{F}_\epsilon$ is obtained by parallel transporting F_ϵ from $\boldsymbol{t}_\epsilon$ to $\boldsymbol{t}$.

Calculation of Ψ_ϵ

This variation is closely related to the writhe of closed curves. As explained in [Ful78] when parallel transporting an adapted frame around a closed curve it might not realigned with itself after one complete loop. This "lack of alignement" is directly measured by the change of writhe which can be computed with Fuller's Formula [Ful78].

Note that the derivative of θ with respect to $\boldsymbol{x}$ can be evaluated by the change of writhe in the curve as suggested in [dV05]. This approach is completly equivalent.
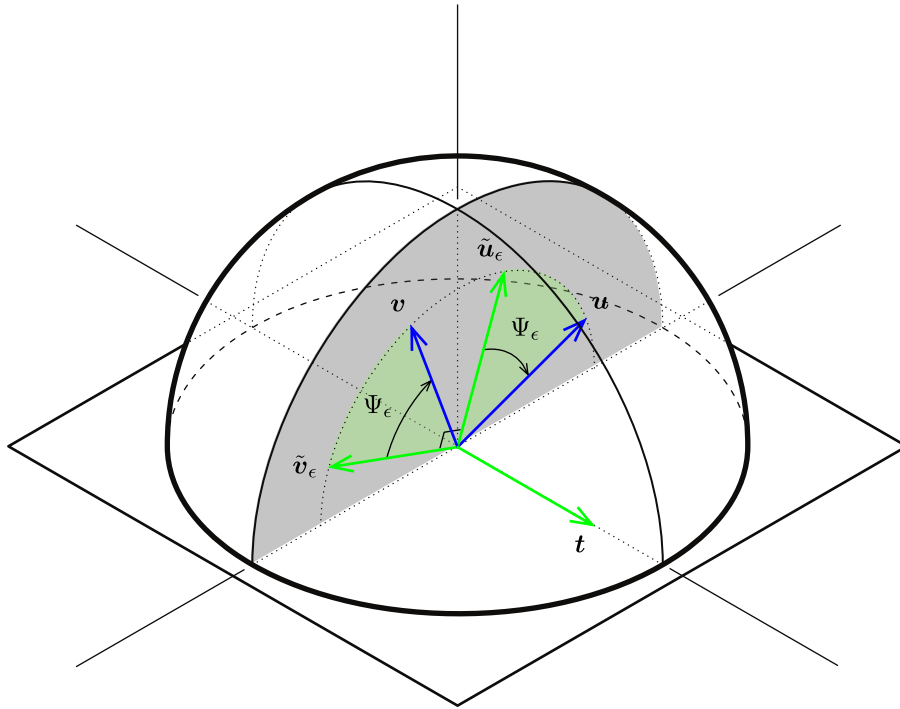
Figure 2.2 – F is obtained by rotating $\tilde{F}_\epsilon$ around $\boldsymbol{t}$ of an angle Ψ_ϵ.
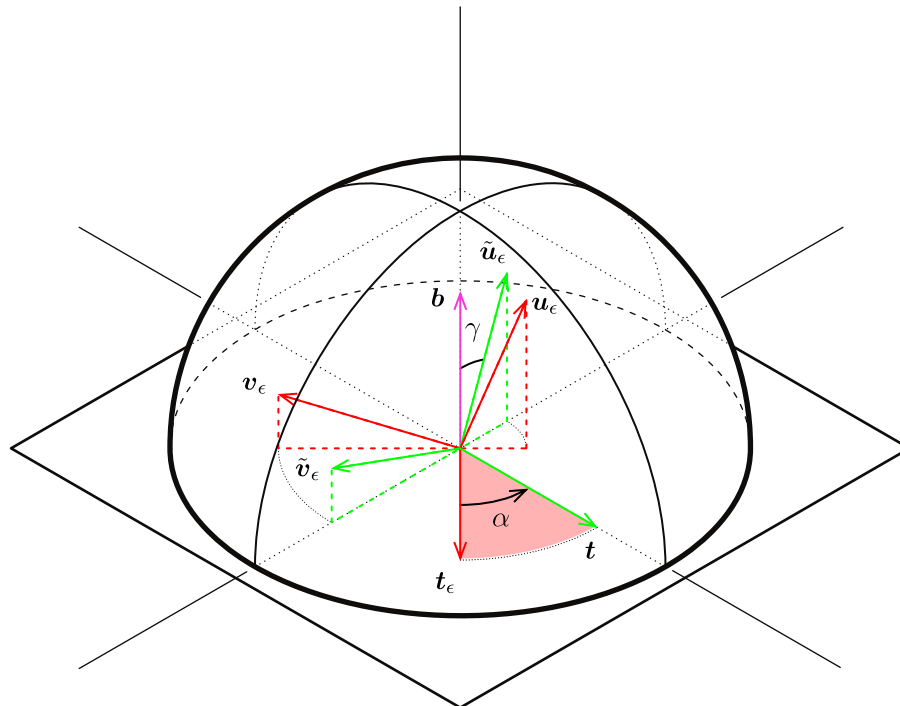
Figure 2.3 – $\tilde{F}_\epsilon$ is obtained by parallel transporting F_ϵ from $\boldsymbol{t}_\epsilon$ to $\boldsymbol{t}$. This operation could be seen as a rotation around $\boldsymbol{t}_\epsilon \times \boldsymbol{t}$ of an angle α_ϵ.

One can also see this lack of alignement in terms of rotation. Parallel transport being a propagation of frame from $s = 0$, the cumulated rotation of Bishop frame from the deformed configuration around the initial configuration at arc-length s is the cumulated angle of rotation of $\boldsymbol{u}[\boldsymbol{x} + \lambda \boldsymbol{h}_x]$ around $\boldsymbol{d}_3[\boldsymbol{x}]$. Recalling the rotation rate of $\boldsymbol{u}[\boldsymbol{x} + \lambda \boldsymbol{h}_x]$ is $\kappa \boldsymbol{b}[\boldsymbol{x} + \lambda \boldsymbol{h}_x]$ by definition of zero-twisting frame, one can write :

$$\Psi_\epsilon[\boldsymbol{x}](s) = - \int_0^s \kappa \boldsymbol{b}[\boldsymbol{x} + \lambda \boldsymbol{h}_x] \cdot \boldsymbol{d}_3[\boldsymbol{x}] \, dt \tag{2.24}$$

The calculation of $\kappa \boldsymbol{b}[\boldsymbol{x} + \lambda \boldsymbol{h}_x]$ is straight forward from the curvature binormal definition :

$$\begin{aligned}
\kappa \boldsymbol{b}[\boldsymbol{x} + \lambda \boldsymbol{h}_x] &= (\boldsymbol{x} + \lambda \boldsymbol{h}_x)' \times (\boldsymbol{x} + \lambda \boldsymbol{h}_x)'' \\
&= \kappa \boldsymbol{b}[\boldsymbol{x}] + \lambda(\boldsymbol{x}' \times \boldsymbol{h}_x'' + \boldsymbol{h}_x' \times \boldsymbol{x}'') + \lambda^2(\boldsymbol{h}_x' \times \boldsymbol{h}_x'') \\
&= \kappa \boldsymbol{b}[\boldsymbol{x}] + \lambda(\boldsymbol{x}' \times \boldsymbol{h}_x'' + \boldsymbol{h}_x' \times \boldsymbol{x}'') + o(\lambda)
\end{aligned} \tag{2.25}$$

Thus, reminding that $\boldsymbol{d}_3[\boldsymbol{x}] = \boldsymbol{x}'$ and $\kappa \boldsymbol{b}[\boldsymbol{x}] \cdot \boldsymbol{d}_3[\boldsymbol{x}] = 0$, and using the invariance of circular product by cyclic permutation, one can express :

$$\begin{aligned}
\Psi_\epsilon[\boldsymbol{x}](s) &= - \int_0^s \kappa \boldsymbol{b}[\boldsymbol{x} + \lambda \boldsymbol{h}_x] \cdot \boldsymbol{d}_3[\boldsymbol{x}] \, dt \\
&= -\lambda \int_0^s (\boldsymbol{x}' \times \boldsymbol{h}_x'' + \boldsymbol{h}_x' \times \boldsymbol{x}'') \cdot \boldsymbol{x}' \, dt + o(\lambda) \\
&= -\lambda \int_0^s \kappa \boldsymbol{b}[\boldsymbol{x}] \cdot \boldsymbol{h}_x' \, dt + o(\lambda)
\end{aligned} \tag{2.26}$$

By integration by parts, dropping the implicit reference to $\boldsymbol{x}$ in the notation, and denoting by δ_s and H_s the Dirac function and the Heaviside step function centered at s, $\Psi_\epsilon(s)$ could be rewritten as :

$$\begin{aligned}
\Psi_\epsilon(s) &= -\lambda \int_0^s \kappa \boldsymbol{b} \cdot \boldsymbol{h}_x' \, dt + o(\lambda) \\
&= -\lambda \left(\left[\kappa \boldsymbol{b} \cdot \boldsymbol{h}_x \right]_0^s - \int_0^s \kappa \boldsymbol{b}' \cdot \boldsymbol{h}_x \, dt \right) + o(\lambda) \\
&= -\lambda \left(\int_0^s \left((\delta_s - \delta_0) \kappa \boldsymbol{b} - \kappa \boldsymbol{b}' \right) \cdot \boldsymbol{h}_x \, dt \right) + o(\lambda) \\
&= -\lambda \left(\int_0^L \left((\delta_s - \delta_0) \kappa \boldsymbol{b} - (1 - H_s) \kappa \boldsymbol{b}' \right) \cdot \boldsymbol{h}_x \, dt \right) + o(\lambda)
\end{aligned} \tag{2.27}$$

Note that, as expected, $\Psi_\epsilon(s)$ is in first order of λ and thus gets negligible when λ tends to zero, that is to say when the perturbation of $\boldsymbol{x}$ is infinitesimal :

$$\lim_{\lambda \to 0} \Psi_\epsilon(s) = 0 \tag{2.28}$$

$H_s : t \mapsto \begin{cases} 0, & t < s \\ 1, & t \geqslant s \end{cases}$ est la fonction de Heaviside.

$\delta_s : t \mapsto \delta(t - s)$ est la distribution de dirac centrée en s.

Calculation of α_ϵ

Recall that $\tilde{F}_\epsilon$ is obtained by parallel tranpsorting F_ϵ from $\boldsymbol{t}_\epsilon$ to $\boldsymbol{t}$. $\tilde{F}_\epsilon$ results from the rotation of F_ϵ around $\boldsymbol{b} = \boldsymbol{t}_\epsilon \times \boldsymbol{t}$ by an angle α_ϵ.

Recall from (2.6) that because the rod is supposed to be unstretchable, $\boldsymbol{t}_\epsilon$ stays collinear to $\boldsymbol{t}$ for an infinitesimal perturbation of the centerline :

$$\|\boldsymbol{t}\| = \|\boldsymbol{t}_\epsilon\| = 1 \Rightarrow (\boldsymbol{x} + \boldsymbol{\epsilon})' \cdot (\boldsymbol{x} + \boldsymbol{\epsilon})' = 1 \Leftrightarrow \boldsymbol{x}' \cdot \boldsymbol{\epsilon}' = -\tfrac{\lambda^2}{2} \|\boldsymbol{h}'_x\|^2 \tag{2.29}$$

Which leeds to :

$$\cos\alpha_\epsilon(s) = \boldsymbol{t} \cdot \boldsymbol{t}_\epsilon = \boldsymbol{x}' \cdot (\boldsymbol{x} + \boldsymbol{\epsilon})' = 1 + \boldsymbol{x}' \cdot \boldsymbol{\epsilon}' = 1 - \tfrac{\lambda^2}{2} \|\boldsymbol{h}'_x\|^2 \tag{2.30}$$

Thus, at second order in λ :

$$\cos\alpha_\epsilon = 1 - \tfrac{\lambda^2}{2} \|\boldsymbol{h}'_x\|^2 \tag{2.31a}$$

$$\sin\alpha_\epsilon = \sqrt{1 - \cos^2\alpha_\epsilon} = \lambda\|\boldsymbol{h}'_x\| + o(\lambda^2) \tag{2.31b}$$

$$\sin^2\alpha_\epsilon/2 = \tfrac{\lambda^2}{4} \|\boldsymbol{h}'_x\|^2 \tag{2.31c}$$

Finally, it's possible to conclude that $\alpha_\epsilon(s)$ is in first order of λ and thus gets negligible when λ tends to zero :

$$\lim_{\lambda\to 0} \alpha_\epsilon(s) = 0 \tag{2.32}$$

Aligning $\tilde{F}_\epsilon$ towards F_ϵ

Recall that aligning $\tilde{F}_\epsilon$ over F is nothing but a rotation around $\boldsymbol{t}$ by an angle Ψ_ϵ. This leads to :

$$\tilde{\boldsymbol{u}}_\epsilon = \cos\Psi_\epsilon \, \boldsymbol{u} + \sin\Psi_\epsilon \, \boldsymbol{v} \tag{2.33a}$$

$$\tilde{\boldsymbol{v}}_\epsilon = -\sin\Psi_\epsilon \, \boldsymbol{u} + \cos\Psi_\epsilon \, \boldsymbol{v} \tag{2.33b}$$

Aligning F_ϵ towards $\boldsymbol{t}$

Recall that $\tilde{F}_\epsilon$ is obtained by parallel tranpsorting F_ϵ from $\boldsymbol{t}_\epsilon$ to $\boldsymbol{t}$. This operation could be seen as a rotation around $\boldsymbol{t}_\epsilon \times \boldsymbol{t}$ of an angle α_ϵ. Where :

$$\boldsymbol{b} = \boldsymbol{t}_\epsilon \times \boldsymbol{t} = \cos\gamma \, \tilde{\boldsymbol{u}}_\epsilon + \sin\gamma \, \tilde{\boldsymbol{v}}_\epsilon = \cos\gamma \, \boldsymbol{u}_\epsilon + \sin\gamma \, \boldsymbol{v}_\epsilon \tag{2.34}$$

Expressing F_ϵ on the basis $\tilde{F}_\epsilon$ gives for $\boldsymbol{u}_\epsilon$ and $\boldsymbol{v}_\epsilon$:

$$\boldsymbol{u}_\epsilon = \sin\gamma\,\boldsymbol{b} + \cos\gamma\left(\sin\alpha_\epsilon\,\tilde{\boldsymbol{t}} + \cos\alpha_\epsilon\left(\cos\gamma\,\tilde{\boldsymbol{u}}_\epsilon - \sin\gamma\,\tilde{\boldsymbol{v}}_\epsilon\right)\right) \tag{2.35a}$$

$$\boldsymbol{v}_\epsilon = \cos\gamma\,\boldsymbol{b} + \sin\gamma\left(-\sin\alpha_\epsilon\,\tilde{\boldsymbol{t}} + \cos\alpha_\epsilon\left(\sin\gamma\,\tilde{\boldsymbol{u}}_\epsilon - \cos\gamma\,\tilde{\boldsymbol{v}}_\epsilon\right)\right) \tag{2.35b}$$

Which can be rearranged in :

$$\boldsymbol{u}_\epsilon = \cos\gamma\sin\alpha_\epsilon\,\boldsymbol{t} + \left(\cos\alpha_\epsilon\cos^2\gamma + \cos^2\gamma\right)\tilde{\boldsymbol{u}}_\epsilon + \sin\gamma\cos\gamma\left(1 - \cos\alpha_\epsilon\right)\tilde{\boldsymbol{v}}_\epsilon \tag{2.36a}$$

$$\boldsymbol{v}_\epsilon = -\sin\gamma\sin\alpha_\epsilon\,\boldsymbol{t} + \cos\gamma\sin\gamma\left(1 - \cos\alpha_\epsilon\right)\tilde{\boldsymbol{u}}_\epsilon + \left(\cos^2\gamma + \cos\alpha_\epsilon\sin^2\gamma\right)\tilde{\boldsymbol{v}}_\epsilon \tag{2.36b}$$

Variation of Bishop frame with respect to $\boldsymbol{x}$

Finally, one can express F_ϵ on the basis F as the composition of two rotations :

$$\boldsymbol{u}_\epsilon = \begin{bmatrix} 1 & 0 & 0 \\ 0 & \cos\Psi_\epsilon & -\sin\Psi_\epsilon \\ 0 & \sin\Psi_\epsilon & \cos\Psi_\epsilon \end{bmatrix}\begin{bmatrix} \cos\gamma\sin\alpha_\epsilon \\ 1 - 2\cos^2\gamma\sin^2\alpha_\epsilon/2 \\ 2\sin\gamma\cos\gamma\sin^2\alpha_\epsilon/2 \end{bmatrix} = \begin{bmatrix} \alpha_\epsilon\cos\gamma \\ 1 \\ \Psi_\epsilon \end{bmatrix} + o(\lambda) \tag{2.37a}$$

$$\boldsymbol{v}_\epsilon = \begin{bmatrix} 1 & 0 & 0 \\ 0 & \cos\Psi_\epsilon & -\sin\Psi_\epsilon \\ 0 & \sin\Psi_\epsilon & \cos\Psi_\epsilon \end{bmatrix}\begin{bmatrix} -\sin\gamma\sin\alpha_\epsilon \\ 2\sin\gamma\cos\gamma\sin^2\alpha_\epsilon/2 \\ 1 - 2\sin\gamma^2\sin^2\alpha_\epsilon/2 \end{bmatrix} = \begin{bmatrix} -\alpha_\epsilon\sin\gamma \\ -\Psi_\epsilon \\ 1 \end{bmatrix} + o(\lambda) \tag{2.37b}$$

Here, the expressions have been developed in first order of λ as far as α_ϵ and Ψ_ϵ it's been proofed in eq [] that those quantities tends two zero when the perturbation of the centerline is infinitesimal.

Finally, one can express the variation of material directors with respect to an infinitesimal variation of rod's centerline :

$$\boldsymbol{u}_\epsilon = \alpha_\epsilon\cos\gamma\,\boldsymbol{t} + \boldsymbol{u} + \Psi_\epsilon\boldsymbol{v} + o(\lambda) \tag{2.38a}$$

$$\boldsymbol{v}_\epsilon = -\alpha_\epsilon\sin\gamma\,\boldsymbol{t} + \boldsymbol{v} - \Psi_\epsilon\boldsymbol{u} + o(\lambda) \tag{2.38b}$$

Variation of material frame with respect to $\boldsymbol{x}$

Recalling the expression of the material frame expressed in the reference Bishop frame, it's now easy to deduce the variation of material frame with respect to a variation of the rod's centerline :

$$\boldsymbol{d}_1[\boldsymbol{x} + \lambda\boldsymbol{h}_x] = \cos\theta\,\boldsymbol{u}_\epsilon + \sin\theta\,\boldsymbol{v}_\epsilon \tag{2.39a}$$

$$\boldsymbol{d}_2[\boldsymbol{x} + \lambda\boldsymbol{h}_x] = -\sin\theta\,\boldsymbol{u}_\epsilon + \cos\theta\,\boldsymbol{v}_\epsilon \tag{2.39b}$$

Which leads according to the previous equation to :

$$\boldsymbol{d}_1[\boldsymbol{x} + \lambda\boldsymbol{h}_x] = \boldsymbol{d}_1[\boldsymbol{x}] + \Psi_\epsilon\boldsymbol{d}_2[\boldsymbol{x}] + \alpha_\epsilon\cos\left(\theta - \gamma\right)\boldsymbol{t}[\boldsymbol{x}] + o(\lambda) \tag{2.40a}$$

$$\boldsymbol{d}_2[\boldsymbol{x} + \lambda\boldsymbol{h}_x] = \boldsymbol{d}_2[\boldsymbol{x}] - \Psi_\epsilon\boldsymbol{d}_1[\boldsymbol{x}] - \alpha_\epsilon\sin\left(\theta + \gamma\right)\boldsymbol{t}[\boldsymbol{x}] + o(\lambda) \tag{2.40b}$$

2.8.2 Derivative of the material curvatures vector with respect to $\boldsymbol{x}$

It's know straightforward from the previous section to express the variation of the material curvatures with respect to a variation $\boldsymbol{\epsilon} = \lambda \boldsymbol{h}_x$ of $\boldsymbol{x}$ while θ remains unchanged.

$$(\boldsymbol{x} + \lambda \boldsymbol{h}_x)'' \cdot \boldsymbol{d}_1[\boldsymbol{x} + \lambda \boldsymbol{h}_x] = (\boldsymbol{x}'' + \lambda \boldsymbol{h}_x'') \cdot \Big(\boldsymbol{d}_1 + \Psi_\epsilon \boldsymbol{d}_2 + \alpha_\epsilon \cos(\theta - \gamma)\, \boldsymbol{t} + o(\lambda)\Big) \quad (2.41\text{a})$$

$$(\boldsymbol{x} + \lambda \boldsymbol{h}_x)'' \cdot \boldsymbol{d}_2[\boldsymbol{x} + \lambda \boldsymbol{h}_x] = (\boldsymbol{x}'' + \lambda \boldsymbol{h}_x'') \cdot \Big(\boldsymbol{d}_2 - \Psi_\epsilon \boldsymbol{d}_1 - \alpha_\epsilon \sin(\theta + \gamma)\, \boldsymbol{t} + o(\lambda)\Big) \quad (2.41\text{b})$$

Thus, recalling that $\boldsymbol{x}'' \cdot \boldsymbol{d}_3 = 0$ and that α_ϵ and Ψ_ϵ are first order quantities in λ :

$$(\boldsymbol{x} + \lambda \boldsymbol{h}_x)'' \cdot \boldsymbol{d}_1[\boldsymbol{x} + \lambda \boldsymbol{h}_x] = \boldsymbol{x}'' \cdot \boldsymbol{d}_1 + \Psi_\epsilon \boldsymbol{x}'' \cdot \boldsymbol{d}_2 + \lambda \boldsymbol{h}_x'' \cdot \boldsymbol{d}_1 + o(\lambda) \quad (2.42\text{a})$$

$$(\boldsymbol{x} + \lambda \boldsymbol{h}_x)'' \cdot \boldsymbol{d}_2[\boldsymbol{x} + \lambda \boldsymbol{h}_x] = \boldsymbol{x}'' \cdot \boldsymbol{d}_2 - \Psi_\epsilon \boldsymbol{x}'' \cdot \boldsymbol{d}_1 + \lambda \boldsymbol{h}_x'' \cdot \boldsymbol{d}_2 + o(\lambda) \quad (2.42\text{b})$$

Which finally leads to :

$$\boldsymbol{\omega}[\boldsymbol{x} + \lambda \boldsymbol{h}_x] = \boldsymbol{\omega}[\boldsymbol{x}] - \Psi_\epsilon \boldsymbol{J}\boldsymbol{\omega}[\boldsymbol{x}] + \lambda \begin{bmatrix} -\boldsymbol{h}_x'' \cdot \boldsymbol{d}_2 \\ \boldsymbol{h}_x'' \cdot \boldsymbol{d}_1 \end{bmatrix} + o(\lambda) \quad (2.43)$$

Reminding the expression of Ψ_ϵ computed in paragraphe[], one can express the derivative of the material curvatures vector with respect to $\boldsymbol{x}$:

$$\boldsymbol{D}_x\boldsymbol{\omega}(s) \cdot \boldsymbol{h}_x = \left(\int_0^L \big((\delta_s - \delta_0)\,\kappa\boldsymbol{b} - (1 - H_s)\kappa\boldsymbol{b}'\big) \cdot \boldsymbol{h}_x\, dt \right) \boldsymbol{J}\boldsymbol{\omega} + \begin{bmatrix} -\boldsymbol{d}_2^T \\ \boldsymbol{d}_1^T \end{bmatrix} \cdot \boldsymbol{h}_x'' \quad (2.44)$$

2.8.3 Computation of the forces acting on the centerline

The forces acting on the centerline are given by the functional derivative of the potential elastic energy with respect to x which can be decomposed according to the chain rule :

$$\langle -f(s)\,;\boldsymbol{h}_x \rangle = \boldsymbol{D}_x\mathcal{E}_p(s) \cdot \boldsymbol{h}_x = \boldsymbol{D}_x\mathcal{E}_b(s) \cdot \boldsymbol{h}_x + \boldsymbol{D}_x\mathcal{E}_t(s) \cdot \boldsymbol{h}_x$$
$$= \boldsymbol{D}_x\mathcal{E}_b[\boldsymbol{\omega}[\boldsymbol{x}]](s) \cdot \boldsymbol{h}_x + \boldsymbol{D}_x\mathcal{E}_t[\boldsymbol{x}](s) \cdot \boldsymbol{h}_x \quad (2.45)$$

Derivative of the torsion energy with respect to x

Recall that the torsion energy only depends on θ which is independent of x. Thus, $\mathcal{E}_t$ is independent of x :

$$\boldsymbol{D}_x\mathcal{E}_t[\boldsymbol{x}](s) \cdot \boldsymbol{h}_x = \frac{d}{d\lambda}\mathcal{E}_t[\boldsymbol{x} + \lambda \boldsymbol{h}_x]\Big|_{\lambda=0} = 0 \quad (2.46)$$

Derivative of the bending energy with respect to x

The derivative of $\mathcal{E}_b$ is obtained with the chain rule :

$$\boldsymbol{D}_\omega\mathcal{E}_b[\boldsymbol{\omega}](s) \cdot \boldsymbol{h}_\omega = \frac{d}{d\lambda}\mathcal{E}_b[\boldsymbol{\omega} + \lambda \boldsymbol{h}_\omega]\Big|_{\lambda=0} = \int_0^L (\boldsymbol{\omega} - \overline{\boldsymbol{\omega}})^T \boldsymbol{B} \cdot \boldsymbol{h}_\omega\, dt \quad (2.47)$$

Finally, reminding eq 4.14 :

$$\boldsymbol{D}_x\mathcal{E}_b[\boldsymbol{\omega}[\boldsymbol{x}]](s)\cdot\boldsymbol{h}_x = \boldsymbol{D}_\omega\mathcal{E}_b[\boldsymbol{\omega}](s)\cdot(\boldsymbol{D}_x\boldsymbol{\omega}[\boldsymbol{x}](s)\cdot\boldsymbol{h}_x) = \mathcal{A} + \mathcal{B} + \mathcal{C} \tag{2.48}$$

Where :

$$\mathcal{A} = \int_0^L (\boldsymbol{\omega} - \overline{\boldsymbol{\omega}})^T \boldsymbol{B} \begin{bmatrix} -\boldsymbol{d_2}^T \\ \boldsymbol{d_1}^T \end{bmatrix} \cdot \boldsymbol{h}_x'' \, dt \tag{2.49a}$$

$$\mathcal{B} = \int_{t=0}^L (\boldsymbol{\omega} - \overline{\boldsymbol{\omega}})^T \boldsymbol{B}\boldsymbol{J}\boldsymbol{\omega} \left(\int_{u=0}^L (\delta_t - \delta_0)\,\kappa\boldsymbol{b}\cdot\boldsymbol{h}_x \, du \right) dt \tag{2.49b}$$

$$\mathcal{C} = \int_{t=0}^L -(\boldsymbol{\omega} - \overline{\boldsymbol{\omega}})^T \boldsymbol{B}\boldsymbol{J}\boldsymbol{\omega} \left(\int_{u=0}^L (1 - H_t)\,\kappa\boldsymbol{b}'\cdot\boldsymbol{h}_x \, du \right) dt \tag{2.49c}$$

Calculus of $\mathcal{A}$:

$$\mathcal{A} = \int_0^L (\boldsymbol{\omega} - \overline{\boldsymbol{\omega}})^T \boldsymbol{B} \begin{bmatrix} -\boldsymbol{d_2}^T \\ \boldsymbol{d_1}^T \end{bmatrix} \cdot \boldsymbol{h}_x'' \, dt \tag{2.50}$$

Recalling the bending moment is given by :

$$\boldsymbol{M} = (\kappa_1 - \overline{\kappa_1})EI_1\boldsymbol{d_1} + (\kappa_2 - \overline{\kappa_2})EI_2\boldsymbol{d_2} = M_1\boldsymbol{d_1} + M_2\boldsymbol{d_2} \tag{2.51}$$

One can remark that :

$$(\boldsymbol{\omega} - \overline{\boldsymbol{\omega}})^T \boldsymbol{B} \begin{bmatrix} -\boldsymbol{d_2}^T \\ \boldsymbol{d_1}^T \end{bmatrix} = M_2\boldsymbol{d_1}^T - M_1\boldsymbol{d_2}^T = -(\boldsymbol{d_3} \times \boldsymbol{M})^T \tag{2.52}$$

Rq : on mixe abusivement 2 formes d'écritures, matricielle et vectorielle, à cause du produit scalaire que l'on écrit tantôt sous sa forme vectorielle et parfois matricielle (à l'aide de la transposée).

Thus, $\mathcal{A}$ could be rewritten in it's vectoriel form :

$$\begin{aligned} \mathcal{A} &= -\int_0^L (\boldsymbol{d_3} \times \boldsymbol{M})\cdot\boldsymbol{h}_x'' \, dt \\ &= -\left[(\boldsymbol{d_3} \times \boldsymbol{M})\cdot\boldsymbol{h}_x' \right]_0^L + \int_0^L (\boldsymbol{d_3} \times \boldsymbol{M})'\cdot\boldsymbol{h}_x' \, dt \\ &= -\left[(\boldsymbol{d_3} \times \boldsymbol{M})\cdot\boldsymbol{h}_x' \right]_0^L + \int_0^L \left((\boldsymbol{d_3} \times \boldsymbol{M}')\cdot\boldsymbol{h}_x' + (\boldsymbol{h}_x' \times \boldsymbol{d_3})\cdot\boldsymbol{M} \right) dt \end{aligned} \tag{2.53}$$

Recall that from (2.6) that $\boldsymbol{h}_x'\cdot\boldsymbol{d_3} = 0$ and from (2.1) that $\boldsymbol{d_3}'\cdot\boldsymbol{d_3} = 0$. Hence, $\boldsymbol{h}_x' \times \boldsymbol{d_3}'$ is colinear to $\boldsymbol{d_3}$. Or by definition $\boldsymbol{M}$ is orthogonal to $\boldsymbol{d_3}$. Thus, $(\boldsymbol{h}_x' \times \boldsymbol{d_3}')\cdot\boldsymbol{M} = 0$. Finally, after a second integration by parts :

$$\begin{aligned} \mathcal{A} &= -\left[(\boldsymbol{d_3} \times \boldsymbol{M})\cdot\boldsymbol{h}_x' \right]_0^L + \int_0^L (\boldsymbol{d_3} \times \boldsymbol{M}')\cdot\boldsymbol{h}_x' \, dt \\ &= \left[(\boldsymbol{d_3} \times \boldsymbol{M}')\cdot\boldsymbol{h}_x'' - (\boldsymbol{d_3} \times \boldsymbol{M})\cdot\boldsymbol{h}_x' \right]_0^L - \int_0^L (\boldsymbol{d_3} \times \boldsymbol{M}')'\cdot\boldsymbol{h}_x \, dt \end{aligned} \tag{2.54}$$

Calculus of $\mathcal{B}$:

$$\mathcal{B} = \int_{t=0}^{L} (\boldsymbol{\omega} - \overline{\boldsymbol{\omega}})^T \boldsymbol{B} \boldsymbol{J} \boldsymbol{\omega} \left(\int_{u=0}^{L} (\delta_t - \delta_0) \kappa \boldsymbol{b} \cdot \boldsymbol{h}_x \, du \right) dt$$
$$= -(\kappa \boldsymbol{b} \cdot \boldsymbol{h}_x)(0) \int_{t=0}^{L} (\boldsymbol{\omega} - \overline{\boldsymbol{\omega}})^T \boldsymbol{B} \boldsymbol{J} \boldsymbol{\omega} \, dt + \int_{t=0}^{L} (\boldsymbol{\omega} - \overline{\boldsymbol{\omega}})^T \boldsymbol{B} \boldsymbol{J} \boldsymbol{\omega} \kappa \boldsymbol{b} \cdot \boldsymbol{h}_x \, dt \qquad (2.55)$$

Calculus of $\mathcal{C}$:

$$\mathcal{C} = \int_{t=0}^{L} -(\boldsymbol{\omega} - \overline{\boldsymbol{\omega}})^T \boldsymbol{B} \boldsymbol{J} \boldsymbol{\omega} \left(\int_{u=0}^{L} (1 - H_t) \kappa \boldsymbol{b}' \cdot \boldsymbol{h}_x \, du \right) dt$$
$$= \int_{u=0}^{L} \int_{t=u}^{L} -\left((\boldsymbol{\omega} - \overline{\boldsymbol{\omega}})^T \boldsymbol{B} \boldsymbol{J} \boldsymbol{\omega} \right)(t) \left(\kappa \boldsymbol{b}' \cdot \boldsymbol{h}_x \right)(u) \, dt \, du \qquad (2.56)$$
$$= \int_{u=0}^{L} -\left(\int_{t=u}^{L} (\boldsymbol{\omega} - \overline{\boldsymbol{\omega}})^T \boldsymbol{B} \boldsymbol{J} \boldsymbol{\omega} \, dt \right) \left(\kappa \boldsymbol{b}' \cdot \boldsymbol{h}_x \right) du$$

By several integration by parts, using Fubini's theorem once and supposing that the terms vanishes at $s = 0$ and $s = L$:

$$\mathcal{B} + \mathcal{C} = \int_{t=0}^{L} \left((\boldsymbol{\omega} - \overline{\boldsymbol{\omega}})^T \boldsymbol{B} \boldsymbol{J} \boldsymbol{\omega} \kappa \boldsymbol{b} - \left(\int_{u=t}^{L} (\boldsymbol{\omega} - \overline{\boldsymbol{\omega}})^T \boldsymbol{B} \boldsymbol{J} \boldsymbol{\omega} \, du \right) \kappa \boldsymbol{b}' \right) \cdot \boldsymbol{h}_x \, dt$$
$$= \int_{t=0}^{L} \left(-\left(\int_{u=t}^{L} (\boldsymbol{\omega} - \overline{\boldsymbol{\omega}})^T \boldsymbol{B} \boldsymbol{J} \boldsymbol{\omega} \, du \right)' \kappa \boldsymbol{b} - \left(\int_{u=t}^{L} (\boldsymbol{\omega} - \overline{\boldsymbol{\omega}})^T \boldsymbol{B} \boldsymbol{J} \boldsymbol{\omega} \, du \right) \kappa \boldsymbol{b}' \right) \cdot \boldsymbol{h}_x \, dt \quad (2.57)$$
$$= \int_{t=0}^{L} \left(-\left(\int_{u=t}^{L} (\boldsymbol{\omega} - \overline{\boldsymbol{\omega}})^T \boldsymbol{B} \boldsymbol{J} \boldsymbol{\omega} \, du \right) \kappa \boldsymbol{b} \right)' \cdot \boldsymbol{h}_x \, dt$$

Which can be rewritted using the quasi-static hypothesis :

$$\mathcal{B} + \mathcal{C} = \int_{t=0}^{L} \left(-\left(\int_{u=t}^{L} (\boldsymbol{\omega} - \overline{\boldsymbol{\omega}})^T \boldsymbol{B} \boldsymbol{J} \boldsymbol{\omega} \, du \right) \kappa \boldsymbol{b} \right)' \cdot \boldsymbol{h}_x \, dt$$
$$= \int_{t=0}^{L} \left(-\left(\int_{u=t}^{L} \beta(\theta' - \overline{\theta'})(\delta_L - \delta_0) - (\beta(\theta' - \overline{\theta'}))' \, du \right) \kappa \boldsymbol{b} \right)' \cdot \boldsymbol{h}_x \, dt$$
$$= \int_{t=0}^{L} \left(-\left(\beta(\theta' - \overline{\theta'})(L) - [\beta(\theta' - \overline{\theta'})]_t^L \right) \kappa \boldsymbol{b} \right)' \cdot \boldsymbol{h}_x \, dt \qquad (2.58)$$
$$= \int_{t=0}^{L} -\left(\beta(\theta' - \overline{\theta'}) \kappa \boldsymbol{b} \right)' \cdot \boldsymbol{h}_x \, dt$$

Finally :

$$\boldsymbol{D}_x \mathcal{E}_b[\boldsymbol{\omega}[\boldsymbol{x}]](s) \cdot \boldsymbol{h}_x = \int_0^L \left(-(\boldsymbol{d}_3 \times \boldsymbol{M}')' - (\beta(\theta' - \overline{\theta'}) \kappa \boldsymbol{b})' \right) \cdot \boldsymbol{h}_x \, dt \qquad (2.59)$$

Internal forces

Thus, the internal forces are related to the variation of internal elastic energy as :

$$\langle -\boldsymbol{f}(s) ; \boldsymbol{h}_x \rangle = \boldsymbol{D}_x \mathcal{E}_p(s) \cdot \boldsymbol{h}_x = -\int_0^L \left((\boldsymbol{d}_3 \times \boldsymbol{M}')' + (\beta(\theta' - \overline{\theta'}) \kappa \boldsymbol{b})' \right) \cdot \boldsymbol{h}_x \, dt \qquad (2.60)$$

Finally, we can conclude on the expression of the internal forces :

$$\boldsymbol{f}(s) = \left(\boldsymbol{d}_3 \times \boldsymbol{M}'\right)' + \left(\beta(\theta' - \overline{\theta}')\kappa\boldsymbol{b}\right)' \tag{2.61}$$

Remarquer ici que l'expression est purement locale. Elle ne dépend pas du sens de parcours de la poutre, contrairement au raisonnement suivi. Cette différence est notable avec la démarche de B. Audoly. Faire le bilan des bénéfices de l'hypothèse quasi-statique : - expressions rigoureusement vraies à l'équilibre statique - simplification ds le calcul des efforts - rapidité dans le calcul avec des expressions plus simples - il n'est pas forcément intéressant en terme d'algorithmie d'imposer l'hypothèse quasistatique au cours du calcul. Il faudrait faire un bench pour savoir.

On retombe sur les équations de Kirchhoff à un terme manquant pret. Qui exprime la contribution de la variation moment de flexion à cause de la torsion $\tau\boldsymbol{M}$'. Peut-être que ce terme est finalement d'un ordre supérieur, si l'on suppose une variation lente de la torsion ? Comment comprendre la disparition de ce terme qui semble nécessaire à l'équilibre statique d'un élément de poutre si l'on en croit les équations de Kirchhoff ?

2.9   Conclusion

On retrouve les équations de kirchhoff dynamique où l'on a négligé les forces inertielles de rotation d'un élément de poutre autour de $\boldsymbol{d}_1$ et $\boldsymbol{d}_2$ pour ne garder que la dynamique de rotation de la section autour de la fibre neutre $\boldsymbol{d}_3$.

The shear force acting on the right side of a section is nothing but $\boldsymbol{T} = \int \boldsymbol{f}$:

$$\boldsymbol{T}(s) = \boldsymbol{d}_3 \times \boldsymbol{M}' + Q\kappa\boldsymbol{b} \tag{2.62}$$

The linear momentum acting on the centerline is given by :

$$m(s) = Q' - \kappa\boldsymbol{b} \cdot (\boldsymbol{d}_3 \times \boldsymbol{M}) \tag{2.63}$$

The main hypothesis are :

- Bernoulli : $\boldsymbol{d}_i \cdot \boldsymbol{d}_j = \delta_{ij}$

- Inextensibility : $\|\boldsymbol{d}_3'\| = 1$

- Quasistatic : at each timestep regarding bending motion $m(s) = 0$

Bibliography

[AAP10]   Basile Audoly, M Amar, and Yves Pomeau. *Elasticity and geometry.* 2010.

[ABW99]   Sigrid Adriaenssens, Michael Barnes, and Christopher Williams. A new analytic and numerical basis for the form-finding and analysis of spline and gridshell

structures. In B Kumar and B H V Topping, editors, *Computing Developments in Civil and Structural Engineering*, pages 83–91. Civil-Comp Press, Edinburgh, 1999.

[BAV⁺10] Miklós Bergou, Basile Audoly, Etienne Vouga, Max Wardetzky, and Eitan Grinspun. Discrete viscous threads. *ACM Transactions on . . .* , pages 1–10, 2010.

[Ber09] Mitchell Berger. Topological Quantities: Calculating Winding, Writhing, Linking, and Higher order Invariants. *Lecture Notes in Mathematics*, 1973:75–97, 2009.

[Bis75] Richard L. Bishop. There is more than one way to frame a curve. *Mathematical Association of America*, 1975.

[BWR⁺08] Miklós Bergou, Max Wardetzky, Stephen Robinson, Basile Audoly, and Eitan Grinspun. Discrete elastic rods. *ACM SIGGRAPH*, pages 1–12, 2008.

[dV05] Renko de Vries. Evaluating changes of writhe in computer simulations of supercoiled DNA. *The Journal of Chemical Physics*, 122(6), 2005.

[Ful78] F Brock Fuller. Decomposition of the linking number of a closed ribbon : A problem from molecular biology. 75(8):3557–3561, 1978.

[Lew03] Wanda Lewis. *Tension structures: form and behaviour*. Telford, Thomas, 2003.

[Nab14] Sina Nabei. *Mechanical form-finding of timber fabric structures*. PhD thesis, EPFL, 2014.

[ST07] Jonas Spillmann and Matthias Teschner. CORDE : Cosserat Rod Elements for the Dynamic Simulation of One-Dimensional Elastic Objects. *Eurographics/ ACM SIGGRAPH Symposium on Computer Animation*, pages 1–10, 2007.

[Vau00] Rue Vauquelin. Writhing Geometry at Finite Temperature : Random Walks and Geometric phases for Stiff Polymers. (1), 2000.

3 Elastic rod : equilibrium approach

3.1 Introduction

Ici on explique que l'approche par les équations d'équilibre est beaucoup plus directe que l'approche énergétique.

3.1.1 Goals and contribution

Dans ce chapitre, après un bref rappel sur le cadre mathématique d'étude des courbes paramétrique de l'espace, on présente les notions de courbures et de torsion géométrique associées au repère de fraient. On montre ensuite le cas plus général d'un repère mobile quelconque attaché à une courbe gamma. On définit enfin la particularité d'un repère mobile adapté à un courbe, et on présente, en sus du repère de Frenet, une approche différente pour accrocher des repères le long d'une courbe (Bishop / RMF / Zéro-twisting frame)

Ici il faudrait préciser la terminologie des auteurs / équations / hypothèses : Euler-Bernoulli, Navier-Bernoulli, Kirchhoff, Love, Clebesh, Cosserat, Vlassov

3.1.2 Related work

On peu s'instruire dans la publi de Dill [Dil92]. Regarder en particulier le premier chapitre de l'HDR de Neukirch [Neu09]. Regarder également la chronologie des modèles proposée dans la thèse de Theetten [The07]. Pourquoi pas proposer une frise chronologique + un tableau de synthèse des hyptohèses.

[Dil92] [Neu09] [ABW99] [Hoo06] [LL09] [Spi08]

[Neu09] : p69 - [Dil92] : p16

3.1.3   Overview

Résumé du chapitre

3.2   Dynamic Kirchhoff equations

3.2.1   Balance of the linear momentum

On fait un bilan sur une tranche d'épaisseur ds, de centre de gravité G positionné en $\boldsymbol{x}_G$:

$$\boldsymbol{F}(s+ds) - \boldsymbol{F}(s) + \boldsymbol{f}(s)ds = \left(\frac{\partial \boldsymbol{F}}{\partial s}(s) + \boldsymbol{f}(s)\right)ds = (\rho S ds)\ddot{\boldsymbol{x}}_G \tag{3.1}$$

Which leads to the first equation of Kirchhoff law :

$$\frac{\partial \boldsymbol{F}}{\partial s} + \boldsymbol{f} = \rho S \ddot{\boldsymbol{x}}_G \tag{3.2}$$

3.2.2   Balance of the angular momentum

On fait un bilan sur une tranche d'épaisseur ds, de centre de gravité G positionné en $\boldsymbol{x}_G$. On applique le théorème du moment cinétique dans un référentiel inertiel :

$$\begin{aligned}
\frac{d}{dt}(dI_G) &= \boldsymbol{M}(s+ds) - \boldsymbol{M}(s) + \boldsymbol{m}(s)ds + (\tfrac{1}{2}ds\boldsymbol{x}') \times \boldsymbol{F}(s+ds) + (-\tfrac{1}{2}ds\boldsymbol{x}') \times -\boldsymbol{F}(s) \\
&= \left(\frac{\partial \boldsymbol{M}}{\partial s}(s) + \boldsymbol{m}(s) + \boldsymbol{x}' \times \boldsymbol{F}(s)\right)ds
\end{aligned} \tag{3.3}$$

L'évolution temporelle des vecteurs matériels est cette fois décrite par un vecteur de Darboux temporel noté $\boldsymbol{\Lambda}$ tel que :

$$\dot{\boldsymbol{d}}_i(s) = \boldsymbol{\Lambda}(t) \times \boldsymbol{d}_i(s) \quad , \quad \boldsymbol{\Lambda}(t) = \begin{bmatrix} \Lambda_3(t) \\ \Lambda_1(t) \\ \Lambda_2(t) \end{bmatrix} \tag{3.4}$$

Les lois de composition / dérivation de la mécanique nous permettent décrire :

$$\frac{d}{dt}(dI_G) = dI_G\dot{\boldsymbol{\Lambda}} + \boldsymbol{\Lambda} \times dI_G \tag{3.5}$$

Qu'est ce qu'on met dans dI_G ? Et bien tout simplement l'opérateur d'inertie de la section, qui s'exprime à l'aide des moments quadratiques des directions principales de la façon suivante, dans la base des directions principales d'inertie au premier ordre en ds :

$$dI_G = \begin{bmatrix} dI_{G3} & 0 & 0 \\ 0 & dI_{G1} & 0 \\ 0 & 0 & dI_{G2} \end{bmatrix} \simeq \rho ds \begin{bmatrix} I_1 + I_2 & 0 & 0 \\ 0 & I_1 & 0 \\ 0 & 0 & I_2 \end{bmatrix} \tag{3.6}$$

Where :

$$dI_{G3} = \int_V \rho(x_1^2 + x_2^2)\, dV \simeq \rho ds \int_V (x_1^2 + x_2^2)\, dx_1 dx_2 \simeq \rho ds(I_1 + I_2) \tag{3.7a}$$

$$dI_{G1} = \int_V \rho(x_2^2 + x_3^2)\, dV \simeq \rho ds \int_V x_2^2\, dx_1 dx_2 \simeq \rho ds I_1 \tag{3.7b}$$

$$dI_{G2} = \int_V \rho(x_1^2 + x_3^2)\, dV \simeq \rho ds \int_V x_1^2\, dx_1 dx_2 \simeq \rho ds I_2 \tag{3.7c}$$

Et l'on peut alors écrire la seconde loi de Kirchhoff sous la forme suivante :

$$\frac{\partial \boldsymbol{M}}{\partial s}(s) + \boldsymbol{m}(s) + \boldsymbol{x}' \times \boldsymbol{F}(s) = \rho \begin{bmatrix} (I_1 + I_2)\dot{\Lambda}_3 + (I_2 - I_1)\Lambda_1\Lambda_2 \\ I_1(\dot{\Lambda}_1 + \Lambda_2\Lambda_3) \\ I_2(\dot{\Lambda}_2 - \Lambda_3\Lambda_1) \end{bmatrix} \tag{3.8}$$

On montre ensuite :

$$\begin{cases} \dot{\boldsymbol{d}}_3 = \boldsymbol{\Lambda} \times \boldsymbol{d}_3 = \Lambda_2\boldsymbol{d_1} - \Lambda_1\boldsymbol{d_2} \\ \dot{\boldsymbol{d}}_1 = \boldsymbol{\Lambda} \times \boldsymbol{d}_1 = -\Lambda_2\boldsymbol{d_3} + \Lambda_3\boldsymbol{d_2} \\ \dot{\boldsymbol{d}}_2 = \boldsymbol{\Lambda} \times \boldsymbol{d}_2 = \Lambda_1\boldsymbol{d_3} - \Lambda_3\boldsymbol{d_1} \end{cases} \Rightarrow \begin{cases} \ddot{\boldsymbol{d}}_3 = \dot{\Lambda}_2\boldsymbol{d_1} - \dot{\Lambda}_1\boldsymbol{d_2} + \boldsymbol{\Lambda} \times \dot{\boldsymbol{d}}_3 \\ \ddot{\boldsymbol{d}}_1 = -\dot{\Lambda}_2\boldsymbol{d_3} + \dot{\Lambda}_3\boldsymbol{d_2} + \boldsymbol{\Lambda} \times \dot{\boldsymbol{d}}_1 \\ \ddot{\boldsymbol{d}}_2 = \dot{\Lambda}_1\boldsymbol{d_3} - \dot{\Lambda}_3\boldsymbol{d_1} + \boldsymbol{\Lambda} \times \dot{\boldsymbol{d}}_2 \end{cases} \tag{3.9}$$

On en déduit en remarquant que $(\boldsymbol{\Lambda} \times \dot{\boldsymbol{d}}_i) \times \boldsymbol{d}_i = \Lambda_i(\boldsymbol{\Lambda} \times \dot{\boldsymbol{d}}_i)$ que :

$$\begin{cases} \ddot{\boldsymbol{d}}_3 \times \boldsymbol{d}_3 = (\dot{\Lambda}_2\boldsymbol{d_1} - \dot{\Lambda}_1\boldsymbol{d_2} + \boldsymbol{\Lambda} \times \dot{\boldsymbol{d}}_3) \times \boldsymbol{d}_3 = (-\dot{\Lambda}_1 + \Lambda_2\Lambda_3)\boldsymbol{d_1} - (\dot{\Lambda}_2 + \Lambda_1\Lambda_3)\boldsymbol{d_2} \\ \ddot{\boldsymbol{d}}_1 \times \boldsymbol{d}_1 = -\dot{\Lambda}_2\boldsymbol{d_3} + \dot{\Lambda}_3\boldsymbol{d_2} + \boldsymbol{\Lambda} \times \dot{\boldsymbol{d}}_1 \times \boldsymbol{d}_1 = -(\dot{\Lambda}_3 + \Lambda_1\Lambda_2)\boldsymbol{d_3} + (-\dot{\Lambda}_2 + \Lambda_1\Lambda_3)\boldsymbol{d_2} \\ \ddot{\boldsymbol{d}}_2 \times \boldsymbol{d}_2 = \dot{\Lambda}_1\boldsymbol{d_3} - \dot{\Lambda}_3\boldsymbol{d_1} + \boldsymbol{\Lambda} \times \dot{\boldsymbol{d}}_2 \times \boldsymbol{d}_2 = (-\dot{\Lambda}_3 + \Lambda_1\Lambda_2)\boldsymbol{d_3} - (\dot{\Lambda}_1 + \Lambda_2\Lambda_3)\boldsymbol{d_1} \end{cases} \tag{3.10}$$

On peut alors conclure sur l'expression de l'equation de kirchoff :

$$\frac{\partial \boldsymbol{M}}{\partial s}(s) + \boldsymbol{m}(s) + \boldsymbol{d}'_3 \times \boldsymbol{F}(s) = I_1\boldsymbol{d}_1 \times \ddot{\boldsymbol{d}}_1 + I_2\boldsymbol{d}_2 \times \ddot{\boldsymbol{d}}_2 \tag{3.11}$$

3.3 Equations of motion

3.3.1 Constitutive equations

Attention, pas d'effort normal par loi constitutive en principe car on est dans un modèle inextensible. L'effort normal est calculé par la loi d'équilibre avec les moments et/ou efforts tranchants. Ici, on postulera tout de même une telle loi constitutive pour la résolution numérique. Ce qui nous amène à considérer une tige quasiment inextensible.

point à creuser. en gros je suis entrain de dire que dans le modèle classique à 3DOF type Douthe ou Barnes, il n'est pas nécessaire d'introduire la raideur axiale (mais alors où intervient la section ?). L'effort normal est déduit des équations d'équilibre.

En fait cela ne semble pas possible. Il faaut alors revenir à l'équation constitutive qui donne l'effort normal, mais alors quid de l'hypothèse quasistatique ?

Dans le fond, l'hyptohèse d'inextensibilité c'est dire que les déformations axiales sont négligeable devant les autres modes de déformation (flexion et/ou torsion). Mais pour caractériser l'effort normal lui même, il faut bien considérer une élongation.

Ou alors, peut-être qu'il faut comprendre que l'effort normal est déduit uniquement des conditions aux limites et/ou éventuellement des efforts extérieurs appliqués à la centerline.

Pour comprendre le traitement de l'inextensibilité, regarder [Ant05] p50. Qu'apporte l'hypothèse d'inextensibilité. Est-elle raisonnable. Tps de calcul par rapport au cas extensible.

$$\boldsymbol{N} = ES(\|\boldsymbol{d}_3'\| - \|\overline{\boldsymbol{d}_3}'\|)\boldsymbol{d}_3 \tag{3.12a}$$

$$\boldsymbol{M_1} = EI_1(\kappa_1 - \overline{\kappa_1})\boldsymbol{d}_1 \tag{3.12b}$$

$$\boldsymbol{M_2} = EI_2(\kappa_2 - \overline{\kappa_2})\boldsymbol{d}_2 \tag{3.12c}$$

$$\boldsymbol{Q} = [GJ(\theta' - \bar{\theta}') - EC_w(\theta''' - \bar{\theta}''')]\boldsymbol{d}_3 \tag{3.12d}$$

3.3.2 Internal forces and moments

Efforts internes de coupure :

$$\boldsymbol{F}_{int} = N\boldsymbol{d}_3 + T_1\boldsymbol{d}_1 + T_2\boldsymbol{d}_2 \tag{3.13a}$$

$$\boldsymbol{M}_{int} = Q\boldsymbol{d}_3 + M_1\boldsymbol{d}_1 + M_2\boldsymbol{d}_2 \tag{3.13b}$$

Efforts externes appliqués linéiques :

$$\boldsymbol{f}_{ext} = f_3\boldsymbol{d}_3 + f_1\boldsymbol{d}_1 + f_2\boldsymbol{d}_2 \tag{3.14a}$$

$$\boldsymbol{m}_{ext} = m_3\boldsymbol{d}_3 + m_1\boldsymbol{d}_1 + m_2\boldsymbol{d}_2 \tag{3.14b}$$

3.3.3 Rod dynamic

First Kirchhoff law projecting on the material frame basis :

$$N' + \kappa_1 T_2 - \kappa_2 T_1 + f_3 = \rho S \ddot{x}_3 \tag{3.15a}$$

$$T_1' + \kappa_2 N - \tau T_2 + f_1 = \rho S \ddot{x}_1 \tag{3.15b}$$

$$T_2' - \kappa_1 N + \tau T_1 + f_2 = \rho S \ddot{x}_2 \tag{3.15c}$$

Second Kirchhoff law projecting on the material frame basis :

$$Q' + \kappa_1 M_2 - \kappa_2 M_1 + m_3 = (I_1 + I_2)\dot{\Lambda}_3 + (I_2 - I_1)\Lambda_1\Lambda_2 \tag{3.16a}$$

$$M_1' + \kappa_2 Q - \tau M_2 - T_2 + m_1 = I_1(\dot{\Lambda}_1 + \Lambda_2\Lambda_3) \tag{3.16b}$$

$$M_2' - \kappa_1 Q + \tau M_1 + T_1 + m_2 = I_2(\dot{\Lambda}_2 - \Lambda_3\Lambda_1) \tag{3.16c}$$

3.4 Geometric interpretation

Ici, on peut mettre l'interprétation géométrique (cf pdf LDP notes). Cela consiste essentiellement à 2/3 schémas bien pensés à produire + à écrire les projections au 1er ordre.

3.5 Main hypothesis

On néglige les forces d'inertie liées à la rotation de l'élément (devant quoi ?? traitement quasi-statique par rapport à la rotation). Cette hypothèse est faite explicitement chez Florence Bertail :

[CBd13] "neglecting inertial momentum due to the vanishing cross- section lead to the following dynamic equations for a Kirchhoff rod"

Cette hypothèse est faite mais passée sous silence chez Douthe, Adriaenssen, D'Amico lorsqu'ils déduisent l'effort tranchant du moment de flexion.

Principe :

- les équations constitutives permettent le calcul de M_1, M_2, Q à partir de la géométrie $\{\boldsymbol{x}, \theta\}$.

- La seconde loi de kirchhoff projetée sur les axes matériels 1 et 2 de la section me donnent accès aux efforts tranchants T_1 et T_2.

- La seconde loi de kirchhoff projetée sur les axes matériel 3 (tangente à la centerline) de la section me donnent l"hypothèse quasi-statique de Audoly.

3.6 Conclusion

Remind that the beam is subject to a distributed external force $\boldsymbol{f}_{ext}$ and a distributed external moment $\boldsymbol{m}_{ext}$.

We neglect rotational inertial effects on $\boldsymbol{d}_1$ et $\boldsymbol{d}_2$ in (3.16b) and (3.16c) which leads to the following shear force :

$$\boldsymbol{T}(s) = \boldsymbol{d}_3 \times (\boldsymbol{M}' + \boldsymbol{m}_{ext}) + Q\kappa\boldsymbol{b} - \tau\boldsymbol{M} \tag{3.17}$$

We may neglect as well the last term $(\tau\boldsymbol{M})$ and get back to the shear force obtained by the variational approach.The total internal force acting on the beam is hence given by :

$$\boldsymbol{F}(s) = \boldsymbol{N}(s) + \boldsymbol{T}(s) \tag{3.18}$$

Sections are subject to the following rotational moment around the centerline :

$$\boldsymbol{\Gamma}(s) = Q' + \boldsymbol{d}_3 \cdot (\kappa \boldsymbol{b} \times \boldsymbol{M} + \boldsymbol{m}_{ext}) \tag{3.19}$$

Bibliography

[ABW99] Sigrid Adriaenssens, Michael Barnes, and Christopher Williams. A new analytic and numerical basis for the form-finding and analysis of spline and gridshell structures. In B Kumar and B H V Topping, editors, *Computing Developments in Civil and Structural Engineering*, pages 83–91. Civil-Comp Press, Edinburgh, 1999.

[Ant05] Stuart Antman. *Nonlinear problems of elasticity*. Applied mathematical sciences. Springer, New York, 2005.

[CBd13] Romain Casati and Florence Bertails-descoubes. Super space clothoids. In *SIGGRAPH*, 2013.

[Dil92] Ellis Harold Dill. Kirchhoff's theory of rods. *Archive for History of Exact Sciences*, 1992.

[Hoo06] P C J Hoogenboom. 7 Vlasov torsion theory. (October):1–12, 2006.

[LL09] Holger Lang and Joachim Linn. Lagrangian field theory in space-time for geometrically exact Cosserat rods. 150:21, 2009.

[Neu09] S. Neukirch. *Enroulement , contact et vibrations de tiges élastiques*. PhD thesis, 2009.

[Spi08] Jonas Spillmann. *CORDE : Cosserat rod elements for the animation of interacting elastic rods*. PhD thesis, 2008.

[The07] Adrien Theetten. *Splines dynamiques géométriquement exactes : simulation haute performance et interaction*. PhD thesis, Université des Sciences et Technologies de Lille, 2007.

4 Numerical model

4.1 Introduction

4.1.1 Goals and contribution

Dans ce chapitre on s'attache à la résolution de l'équilibre statique par relaxation dynamique. Peut-être qu'il faudra faire un chapitre "Marsupilami" plus détaillé qui regroupe les différents éléments formulés et les connexions / liaisons On formule l'élément en torsion à partir des équations de Kirchhoff et non du modèle énergétique (un terme est manquant). On effectue une validation numérique. Penser à tracer la contribution de chaque terme pour vérifier les approximations effectuées.

4.1.2 Related work

[Day65] [Ott65] [Pap81] [MAIK14] [Ala12] [RPKAZ11]

Idée pour l'article avec sigrid [Ala12]

4.1.3 Overview

4.2 Dynamic relaxation

4.3 Overview

Ici, repartir de l'explication donnée par Alister Days en 65. Proposer une illustration avec un pendule. Pourquoi pas le système masse-ressort proposé par Days, à savoir une masse au bout d'une poutre encastrée.

4.4 Overview

4.5 Discret curve-angle representation

4.5.1 Discrete centerline

On discrétise la centerline de la façon suivante :

$$s_i = \sum_0^i |\boldsymbol{e}_{i-1}| \quad , \quad i = 0..n \tag{4.1a}$$

$$\boldsymbol{x}_i \quad , \quad i = 0..n \tag{4.1b}$$

$$\boldsymbol{e}_i = \boldsymbol{x}_{i+1} - \boldsymbol{x}_i \quad , \quad i = 0..n-1 \tag{4.1c}$$

4.5.2 Discrete bishop frame

Discrete parallel transport at edges

Discrete parallel at vertices

On définit ici le transport parrallele discret entre edges et entre vertices. A chaque vertex, on associe un repère de bishop et un repère matériel

$$\theta_i \quad , \quad i = 0..n \tag{4.2a}$$

$$\{\boldsymbol{u}_i, \boldsymbol{v}_i\} \quad , \quad i = 0..n \tag{4.2b}$$

$$\{\boldsymbol{d}_i^1, \boldsymbol{d}_i^2\} \quad , \quad i = 0..n \tag{4.2c}$$

4.5.3 Discrete material frame

4.6 Interpolation rules

On fait des hypothèses sur la forme des efforts pour pouvoir effectuer une interpolation entre les noeuds. Thus, we define edge quantities and vertex quantities.

4.6.1 Geometric and material properties

We suppose that the sections are defined at verticies and that section properties remain uniform over $]s_{i-1/2}, s_{i+1/2}[$. Thus, the material and geometric properties (P) of the beam $(E_i, G_i, S_i, I_i^1, I_i^2, J_i, m_i)$ are supposed to be piecewise constant functions of s on [0,L] :

$$P(s) = P_i \quad , \quad s \in [s_{i-1/2}, s_{i+1/2}] \tag{4.3}$$

Note that this functions may be discontinous at edges midspan ($s_{i+1/2}$).

4.6.2 Axial force and strain

Axial force

N is supposed to be piecewise constant between verticies on $[0, L]$:

$$\boldsymbol{N}(s) = N_i \boldsymbol{t}_i \quad , \quad s \in]s_i, s_{i+1}[\tag{4.4}$$

Note that this functions may be discontinous at edges midspan $(s_{i+1/2})$.

Axial strain

Nous avons défini les propriétés géométriques et matérielles aux noeuds et nous avons fait l'hypothèse qu'elles restaient uniformes sur l'intervalle $]s_{i-1/2}, s_{i+1/2}[$. Par ailleurs, nous avons supposé l'effort normal ($\boldsymbol{N}$) uniforme sur l'interval $]s_i, s_{i+1}[$. De fait, la déformation axiale (ϵ) est une fonction constante par morceaux sur les intervalles $]s_i, s_{i+1/2}[$.

Connaissant l'élongation totale du segment $\boldsymbol{e}_i$, et puisque nous avons supposé l'effort normal uniforme sur le segment, il est possible de calculer les déformations axiales ϵ_i^+ et ϵ_{i+1}^- respectivement pour les intervalles $]s_i, s_{i+1/2}[$ et $]s_{i+1/2}, s_{i+1}[$:

$$N_i = [ES]_i \epsilon_i^+ = [ES]_{i+1} \epsilon_{i+1}^- = \alpha_i \epsilon_i \tag{4.5}$$

Avec α_i la raideur axiale équivalente sur le segment $\boldsymbol{e}_i$ qui permet de calculer l'effort normal sur le segment en fonction de l'élongation totale du segment $\boldsymbol{e}_i$ bien que, comme énoncé précédemment, la déformation axiale puisse être différente entre $]s_i, s_{i+1/2}[$ et $]s_{i+1/2}, s_{i+1}[$ si l'on a un changement de raideur axiale ES entre les noeuds $\boldsymbol{x}_i$ et $\boldsymbol{x}_{i+1}$.

Les élongations des demis segments et du segment entier sont données par les équations suivantes, où l'on a considéré l_i^+ et l_{i+1}^- les longueurs respectives des demi segments $]s_i, s_{i+1/2}[$ et $]s_{i+1/2}, s_{i+1}[$:

$$\epsilon_i^+ = \frac{l_i^+ - \overline{l}_i/2}{\overline{l}_i/2} \quad , \quad \epsilon_{i+1}^- = \frac{l_i^- - \overline{l}_i/2}{\overline{l}_i/2} \quad , \quad \epsilon_i = \frac{l_i}{\overline{l}_i} = \frac{\epsilon_i^+}{2} + \frac{\epsilon_{i+1}^-}{2} \tag{4.6}$$

Ces équations de continuité permettent de déduire la raideur axiale équivalente α_i à considérer sur le segement $\boldsymbol{e}_i$ pour obtenir l'effort normal à partir de la déformation globale du segment sur $s \in]s_i, s_{i+1}[$:

$$N(s) = N_i = \alpha_i \epsilon_i \quad , \quad \alpha_i = \frac{2[ES]_i[ES]_{i+1}}{[ES]_i + [ES]_{i+1}} \quad , \quad \epsilon_i = \frac{|l_i| - |\overline{l}_i|}{|\overline{l}_i|} \tag{4.7}$$

On obtient également les déformations axiales sur chacun des intervalles :

$$\epsilon(s) = \epsilon_i^+ = \frac{\alpha_i}{[ES]_i}\epsilon_i \quad , \quad s \in]s_i, s_{i+1/2}[\tag{4.8a}$$

$$\epsilon(s) = \epsilon_{i+1}^- = \frac{\alpha_i}{[ES]_{i+1}}\epsilon_i \quad , \quad s \in]s_{i+1/2}, s_{i+1}[\tag{4.8b}$$

On remarque que pour une poutre aux propriétés uniformes, les déformations sont continues (il n'y a plus de saut) et $\alpha_i = [ES]_i = [ES]_{i+1}$.

4.6.3 Moment of torsion and rate of twist

Moment of torsion

$\boldsymbol{Q}$ is supposed to be piecewise constant between verticies on $[0, L]$:

$$\boldsymbol{Q}(s) = Q_i \boldsymbol{t}_i, \quad s \in]s_i, s_{i+1}[\tag{4.9}$$

Note that this function may be discontinous at edges midspan $(s_{i+1/2})$.

Rate of twist

Nous avons défini les propriétés géométriques et matérielles aux noeuds et nous avons fait l'hypothèse qu'elles restaient uniformes sur l'intervalle $]s_{i-1/2}, s_{i+1/2}[$. Par ailleurs, nous avons supposé le moment de torsion $(\boldsymbol{Q})$ uniforme sur l'interval $]s_i, s_{i+1}[$. De fait, the rate of twist $(\tau = \theta')$ est une fonction constante par morceaux sur les intervalles $]s_i, s_{i+1/2}[$.

Considérons une poutre droite sans twist au repos. Connaissant le twist dans l'état déformé, c'est à dire la variation de θ, sur le segment $\boldsymbol{e}_i$, et puisque nous avons supposé le moment de torsion uniforme sur le segment, il est possible de calculer les rate of twist τ_i^+ et τ_{i+1}^- respectivement pour les intervalles $]s_i, s_{i+1/2}[$ et $]s_{i+1/2}, s_{i+1}[$:

$$Q_i = [GJ]_i \tau_i^+ = [GJ]_{i+1} \tau_{i+1}^- = \beta_i \tau_i \tag{4.10}$$

Avec β_i la raideur en torsion équivalente sur le segment $\boldsymbol{e}_i$ qui permet de calculer le moment de torsion sur le segment en fonction de l'élongation totale du segment $\boldsymbol{e}_i$ bien que, comme énoncé précédemment, le rate of twist puisse être différente entre $]s_i, s_{i+1/2}[$ et $]s_{i+1/2}, s_{i+1}[$ si l'on a un changement de raideur en torsion GJ entre les noeuds $\boldsymbol{x}_i$ et $\boldsymbol{x}_{i+1}$.

Les twists des demis segments et du segment entier sont données par les équations suivantes, où l'on a considéré θ_i^{mid} l'angle de rotation de la section en $s_{i+1/2}$:

$$\tau_i^+ = \frac{\theta_i^{mid} - \theta_i}{l_i/2} \quad , \quad \tau_{i+1}^- = \frac{\theta_{i+1} - \theta_i^{mid}}{l_i/2} \quad , \quad \tau_i = \frac{\theta_{i+1} - \theta_i}{l_i} = \frac{\tau_i^+}{2} + \frac{\tau_{i+1}^-}{2} \tag{4.11}$$

Ces équations de continuité permettent de déduire la raideur en torsion équivalente β_i à considérer sur le segment $\boldsymbol{e}_i$ pour obtenir le moment de torsion à partir du twist global le long du segment sur $s \in]s_i, s_{i+1}[$:

$$Q(s) = Q_i = \beta_i(\tau_i - \overline{\tau}_i) \quad , \quad \beta_i = \frac{2[GJ]_i[GJ]_{i+1}}{[GJ]_i + [GJ]_{i+1}} \quad , \quad \tau_i = \frac{\theta_{i+1} - \theta_i}{l_i} \tag{4.12}$$

On obtient également les rate of twist sur chacun des intervalles dans la configuration au

repos ($\bar{\tau}$) comme déformée (τ) :

$$\tau(s) = \tau_i^+ = \frac{\beta_i}{[GJ]_i}\tau_i \quad , \quad s \in]s_i, s_{i+1/2}[\tag{4.13a}$$

$$\tau(s) = \tau_{i+1}^- = \frac{\beta_i}{[GJ]_{i+1}}\tau_i \quad , \quad s \in]s_{i+1/2}, s_{i+1}[\tag{4.13b}$$

On remarque que pour une poutre aux propriétés uniformes, les déformations sont continues (il n'y a plus de saut) et $\beta_i = [GJ]_i = [GJ]_{i+1}$.

4.6.4 Bending moment and curvature

Bending moment

$\boldsymbol{M}$ is supposed to be continuous and piecewise linear on $[0, L]$. This assumption is quite reasonable because the bending moment is effectively continous for a beam subject to punctual forces and moments. Thus, $\boldsymbol{M}$ is interpolated from the moment computed at vertices :

$$\boldsymbol{M}(s) = \boldsymbol{M}_{i+1/2} + (s - \tfrac{l_i}{2})\boldsymbol{M}'_{i+1/2} \quad , \quad s \in [s_i, s_{i+1}] \tag{4.14}$$

With

$$\boldsymbol{M}_{i+1/2} = \frac{\boldsymbol{M}_i + \boldsymbol{M}_{i+1}}{2} \tag{4.15a}$$

$$\boldsymbol{M}'_{i+1/2} = \frac{\boldsymbol{M}_{i+1} - \boldsymbol{M}_i}{l_i} \tag{4.15b}$$

Curvature

Il y a une sorte de dualité entre le moment et la courbure. Parfois c'est la mesure de la courbure qui donne accès au moment de flexion. Parfois la courbure c'est la connaissance du moment de flexion qui donne la courbure. Si le moment est continu et linéaire par morceaux, la courbure elle est seulement linéaire par morceau. En effet, il peut y a voir un saut de courbure entre deux éléments de EI distinct.

On interpole la courbure à partir des courbures discrètes aux noeuds et des EI (également définis aux noeuds) de part et d'autre des noeuds. On revient à la continuité du moment. Puis on déduit la courbure du moment.

Donc au repos, on considère que $\boldsymbol{B}\kappa\boldsymbol{b}$ est continu et linéaire par morceaux, qui donne l'interpolation de la courbure suivante :

$$\boldsymbol{B}\kappa\boldsymbol{b}(s) = \frac{\boldsymbol{B}_i\kappa\boldsymbol{b}_i + \boldsymbol{B}_{i+1}\kappa\boldsymbol{b}_{i+1}}{2} + (s - \tfrac{l_i}{2})\frac{\boldsymbol{B}_{i+1}\kappa\boldsymbol{b}_{i+1} - \boldsymbol{B}_i\kappa\boldsymbol{b}_i}{l_i} \quad , \quad s \in [s_i, s_{i+1}] \tag{4.16}$$

On défnit alors les courbures binormales à gauche ($\kappa\boldsymbol{b}_{i+1/2}^-$) et à droite ($\kappa\boldsymbol{b}_{i+1/2}^+$) du point

$\boldsymbol{x}_{i+1/2}$ tel que :

$$\kappa\boldsymbol{b}^{-}_{i+1/2} = \frac{\kappa\boldsymbol{b}_i + \boldsymbol{A}_i\kappa\boldsymbol{b}_{i+1}}{2} \tag{4.17a}$$

$$\kappa\boldsymbol{b}^{+}_{i+1/2} = \frac{\boldsymbol{A}_i^{-1}\kappa\boldsymbol{b}_i + \kappa\boldsymbol{b}_{i+1}}{2} \tag{4.17b}$$

Où l'on a posé $\boldsymbol{A}_i = \boldsymbol{B}_i^{-1}\boldsymbol{B}_{i+1}$, la matrice qui représente le saut des propriétés matérielles de flexion entre les noeuds i et $i+1$. Comme attendu, $\boldsymbol{A}_i$ vaut l'identité lorsque $\boldsymbol{B}_i = \boldsymbol{B}_{i+1}$.

De même, on défnit la dérivée de la courbure binormale à gauche ($\kappa\boldsymbol{b'}^{-}_{i+1/2}$) et à droite ($\kappa\boldsymbol{b'}^{+}_{i+1/2}$) du point $\boldsymbol{x}_{i+1/2}$ tel que :

$$\kappa\boldsymbol{b'}^{-}_{i+1/2} = \frac{\boldsymbol{A}_i\kappa\boldsymbol{b}_{i+1} - \kappa\boldsymbol{b}_i}{l_i} \tag{4.18a}$$

$$\kappa\boldsymbol{b'}^{+}_{i+1/2} = \frac{\kappa\boldsymbol{b}_{i+1} - \boldsymbol{A}_i^{-1}\kappa\boldsymbol{b}_i}{l_i} \tag{4.18b}$$

Ainsi, on peut donner les lois d'interpolation des courbures en tout point de la centerline, dans n'importe quelle configuration (repos ou déformée) :

$$\kappa\boldsymbol{b}(s) = \kappa\boldsymbol{b}^{-}_{i+1/2} + (s - \tfrac{l_i}{2})\kappa\boldsymbol{b'}^{-}_{i+1/2} \quad s \in [s_i, s_{i+1/2}[\tag{4.19a}$$

$$\kappa\boldsymbol{b}(s) = \kappa\boldsymbol{b}^{+}_{i+1/2} + (s - \tfrac{l_i}{2})\kappa\boldsymbol{b'}^{+}_{i+1/2} \quad s \in]s_{i+1/2}, s_{i+1}] \tag{4.19b}$$

Dans le cas où les propriétés de la poutre sont conservées ($\boldsymbol{A}_i = \boldsymbol{I}$), on écrira :

$$\kappa\boldsymbol{b}(s) = \kappa\boldsymbol{b}_{i+1/2} + (s - \tfrac{l_i}{2})\kappa\boldsymbol{b'}_{i+1/2} \quad , \quad s \in [s_i, s_{i+1}] \tag{4.20}$$

With

$$\kappa\boldsymbol{b}_{i+1/2} = \kappa\boldsymbol{b}^{-}_{i+1/2} = \kappa\boldsymbol{b}^{+}_{i+1/2} = \frac{\kappa\boldsymbol{b}_i + \kappa\boldsymbol{b}_{i+1}}{2} \tag{4.21a}$$

$$\kappa\boldsymbol{b'}_{i+1/2} = \kappa\boldsymbol{b'}^{-}_{i+1/2} = \kappa\boldsymbol{b'}^{+}_{i+1/2} = \frac{\kappa\boldsymbol{b}_{i+1} - \kappa\boldsymbol{b}_i}{l_i} \tag{4.21b}$$

En pratique, si la correction apportée n'est pas pertinente, on négligera le saut de courbure dans les calculs discrets.

4.6.5 Discretization

Constitutive Equations

$$\tau = \theta' \tag{4.22a}$$

$$Q = ES\epsilon \tag{4.22b}$$

$$Q = GJ(\tau - \bar{\tau}) \tag{4.22c}$$

$$M1 = EI_1(\kappa_1 - \overline{\kappa_1}) \tag{4.22d}$$

$$M1 = EI_2(\kappa_2 - \overline{\kappa_2}) \tag{4.22e}$$

$$\boldsymbol{M} = M_1\boldsymbol{d}_1 + M_2\boldsymbol{d}_2 \tag{4.22f}$$

$$\boldsymbol{Q} = Q\boldsymbol{d}_3 \tag{4.22g}$$

Notes :

$$\boldsymbol{d}_3 \cdot (\boldsymbol{M} \times \boldsymbol{d}_3) = \kappa_1 M_1 + \kappa_2 M_1 \tag{4.23a}$$

$$\boldsymbol{d}_3 \cdot (\kappa\boldsymbol{b} \times \boldsymbol{M}) = \kappa_1 M_2 - \kappa_2 M_1 \tag{4.23b}$$

$$(\boldsymbol{\omega} - \overline{\boldsymbol{\omega}})^T \boldsymbol{BJ\omega} = -\kappa\boldsymbol{b} \cdot (\boldsymbol{d}_3 \times \boldsymbol{M}) = \kappa_1 \boldsymbol{M}_2 - \kappa_2 \boldsymbol{M}_1 \tag{4.23c}$$

Axial Force

$$\boldsymbol{N} = (ES\epsilon)\boldsymbol{d}_3 \tag{4.24}$$

Shear Force

$$\boldsymbol{T} = \boldsymbol{d}_3 \times \boldsymbol{M}' + Q\kappa\boldsymbol{b} - \tau\boldsymbol{M} \tag{4.25}$$

Rotational Moment

$$\boldsymbol{\Gamma}(s) = (Q' + \kappa_1 M_2 - \kappa_2 M_1)\boldsymbol{d}_3 = Q'\boldsymbol{d}_3 + \kappa\boldsymbol{b} \times \boldsymbol{M} \tag{4.26}$$

Quasistatic hypothesis

$$Q' + \kappa_1 M_2 - \kappa_2 M_1 \simeq 0 \tag{4.27}$$

Inextensibility hypothesis

$$\|\boldsymbol{x}'\| = \|(\boldsymbol{x} + \boldsymbol{\epsilon})'\| = 1 \tag{4.28a}$$

$$\|\boldsymbol{e}_i\| = \|\overline{\boldsymbol{e}_i}\| \tag{4.28b}$$

En fait il faut faire quelques hypothèses sur la nature des efforts pour pourvoir les interpoler convenablement le long de la courbe. On va faire qqch qui ressemble à la super-clothoide de Bertails, et qui semble une hypothèse naturelle pour une poutre continue sur plusieurs appuis soumise à des forces et moments ponctuels :

- le moment est continu et linéaire par morceaux. Il est évalué ponctuellement aux noeuds et interpolé linéairement entre les noeuds.

- la courbure est donc continue par morceaux et linéaire par morceaux. Elle est obtenue à partir du moment et de $\boldsymbol{B}$

- N et Q sont constants par morceaux

$$\boldsymbol{N}(s) = \boldsymbol{N}_i \quad , \quad s \in]0, |\boldsymbol{e}_i|[\tag{4.29a}$$

$$\boldsymbol{M}(s) = \boldsymbol{M}_i + s\boldsymbol{M}_i' \quad s \in [0, |\boldsymbol{e}_i|] \quad , \quad \boldsymbol{M}_i' = \frac{\boldsymbol{M}_{i+1} - \boldsymbol{M}_i}{|\boldsymbol{e}_i|} \tag{4.29b}$$

$$\boldsymbol{Q}(s) = \boldsymbol{Q}_i \quad , \quad s \in]0, |\boldsymbol{e}_i|[\tag{4.29c}$$

Faire un tableau vertex / edge quantities :

- les propriétés mécaniques sont définies aux noeuds

- les repères matériels sont définis aux noeuds

- les courbures sont définies aux noeuds

- les moments sont définis aux noeuds et sont interpolés linéairement entre les noeuds

- l'effort normal et le moment de torsion sont supposés uniformes sur les segments (ils sont donc définis aux segments)

- α et β sont des propriétés équivalentess définies sur les segments (égales à celles de noeuds s'il n'y a pas de saut de propriété).

4.6.6 Force

Axial Force

Axial Force exercée par la poutre sur le point courant $\boldsymbol{x}_i$:

$$\boldsymbol{F}_i^{\parallel} = [\boldsymbol{N}]_{i-1/2}^{i+1/2} = \boldsymbol{N}_{i+1} - \boldsymbol{N}_i \tag{4.30}$$

Axial Force exercée par la poutre sur le premier point $\boldsymbol{x}_0$:

$$\boldsymbol{F}_i^{\parallel} = [\boldsymbol{N}]_0 = \boldsymbol{N}_0 \tag{4.31}$$

Axial Force exercée par la poutre sur le dernier point $\boldsymbol{x}_n$:

$$\boldsymbol{F}_i^{\parallel} = -\left[\boldsymbol{N}\right]_0 = -\boldsymbol{N}_n \tag{4.32}$$

Shear Force

Shear Force exercée par la poutre sur le point courant $\boldsymbol{x}_i$:

$$
\begin{aligned}
\boldsymbol{F}_i^{\perp} &= \left[\boldsymbol{d}_3 \times \boldsymbol{M}' + Q\kappa\boldsymbol{b}\right]_{i-1/2}^{i+1/2} \\
&= \frac{\boldsymbol{e}_i}{|\boldsymbol{e}_i|} \times \frac{\boldsymbol{M}_{i+1} - \boldsymbol{M}_i}{|\boldsymbol{e}_i|} - \frac{\boldsymbol{e}_{i-1}}{|\boldsymbol{e}_{i-1}|} \times \frac{\boldsymbol{M}_i - \boldsymbol{M}_{i-1}}{|\boldsymbol{e}_{i-1}|} + Q_i\kappa\boldsymbol{b}_{i+1/2}^{-} - Q_{i-1}\kappa\boldsymbol{b}_{i-1/2}^{+} \\
&= \left(\boldsymbol{F}_i^1 + \boldsymbol{F}_i^2 + \boldsymbol{H}_i^{-}\right) - \left(\boldsymbol{F}_{i-1}^1 + \boldsymbol{F}_{i-1}^2 + \boldsymbol{H}_{i-1}^{+}\right)
\end{aligned} \tag{4.33}
$$

Ici, on a un problème de définition de $\kappa\boldsymbol{b}$ en milieu de segment. En effet, bien que le moment soit continu, la courbure ne l'est pas nécessairement. Lorsqu'il y a un saut de EI il y a nécessairement un saut de $\kappa\boldsymbol{b}$. On pourrait plutôt interpoler le moment à mi-travée et remonter à la courbure - soit à gauche, soit à droite - en fonction des propriétés géométriques locales :

$$\boldsymbol{M}_{i+1/2} = \frac{\boldsymbol{M}_i + \boldsymbol{M}_{i+1}}{2} \tag{4.34a}$$

$$\kappa\boldsymbol{b}_{i+1/2}^{-} = \boldsymbol{B}_i^{-1}\boldsymbol{M}_{i+1/2} + \overline{\kappa\boldsymbol{b}}_{i+1/2}^{-} \tag{4.34b}$$

$$\kappa\boldsymbol{b}_{i+1/2}^{+} = \boldsymbol{B}_{i+1}^{-1}\boldsymbol{M}_{i+1/2} + \overline{\kappa\boldsymbol{b}}_{i+1/2}^{+} \tag{4.34c}$$

$$\boldsymbol{H}_i^{-} = Q_i\kappa\boldsymbol{b}_{i+1/2}^{-} = Q_i\left(\boldsymbol{B}_i^{-1}\boldsymbol{M}_{i+1/2} + \overline{\kappa\boldsymbol{b}}_{i+1/2}^{-}\right) \tag{4.34d}$$

$$\boldsymbol{H}_i^{+} = Q_i\kappa\boldsymbol{b}_{i+1/2}^{+} = Q_i\left(\boldsymbol{B}_{i+1}^{-1}\boldsymbol{M}_{i+1/2} + \overline{\kappa\boldsymbol{b}}_{i+1/2}^{-}\right) \tag{4.34e}$$

L'autre approche consiste à ignorer la discontinuité et à simplement prendre la moyenne :

$$\kappa\boldsymbol{b}_{i+1/2} = \kappa\boldsymbol{b}_{i+1/2}^{-} = \kappa\boldsymbol{b}_{i+1/2}^{+} = \frac{\kappa\boldsymbol{b}_i + \kappa\boldsymbol{b}_{i+1}}{2} \tag{4.35a}$$

$$\boldsymbol{H}_i^{-} = Q_i\kappa\boldsymbol{b}_{i+1/2}^{-} \tag{4.35b}$$

$$\boldsymbol{H}_i^{+} = Q_i\kappa\boldsymbol{b}_{i+1/2}^{+} \tag{4.35c}$$

$$\boldsymbol{H}_i^{-} = \boldsymbol{H}_i^{+} = \frac{\kappa\boldsymbol{b}_i + \kappa\boldsymbol{b}_{i+1}}{2} \tag{4.35d}$$

Cette idée reste intéressante et élégante. Elle n'a de sens que pour une poutre à propriétés variables (sinon on a la continuité de la courbure également).

Shear Force exercée par la poutre sur le premier point $\boldsymbol{x}_0$:

$$
\begin{aligned}
\boldsymbol{F}_0^{\perp} &= \left[\boldsymbol{d}_3 \times \boldsymbol{M}' + Q\kappa\boldsymbol{b}\right]_0 \\
&= \frac{\boldsymbol{e}_0}{|\boldsymbol{e}_0|} \times \frac{\boldsymbol{M}_1 - \boldsymbol{M}_0}{|\boldsymbol{e}_0|} + Q_0\frac{\kappa\boldsymbol{b}_0}{2} \\
&= \boldsymbol{F}_0^1 + \boldsymbol{F}_0^2 + \boldsymbol{H}_0^{-}
\end{aligned} \tag{4.36}
$$

Shear Force exercée par la poutre sur le dernier point $\boldsymbol{x}_n$:

$$
\begin{aligned}
\boldsymbol{F}_n^{\perp} &= -\big[\boldsymbol{d}_3 \times \boldsymbol{M}' + Q\kappa\boldsymbol{b}\big]_n \\
&= -\frac{\boldsymbol{e}_{n-1}}{|\boldsymbol{e}_{n-1}|} \times \frac{\boldsymbol{M}_n - \boldsymbol{M}_{n-1}}{|\boldsymbol{e}_{n-1}|} - Q_n\frac{\kappa\boldsymbol{b}_n}{2} \\
&= -(\boldsymbol{F}_n^1 + \boldsymbol{F}_n^2 + \boldsymbol{H}_n^+)
\end{aligned}
\tag{4.37}
$$

Moment of Torsion

$$
\Gamma_i = \int_{i-1/2}^{i-1/2} m(s) = Q_i - Q_{i-1} + \int_{i-1/2}^{i+1/2} \kappa_1 M_2 - \kappa_2 M_1
\tag{4.38}
$$

Note que le terme dans l'intégrale est nul pour une section isotrope. On retrouve les résultats bien connus sur les poutres axisymétriques à courbure au repos nulle. Ici, 2 possibilitées :

- soit on considère que le moment varie lentement sur l'intervalle $]i-1/2, i+1/2[$ et on considère donc le terme $\kappa\boldsymbol{b}_i \times \boldsymbol{M}_i$ constant dans l'intégrale, ce qui donne en découpant l'intervalle en $[i-1/2, i]$ et $[i, i+1/2]$:

$$
\begin{aligned}
\Gamma_i &= Q_i - Q_{i-1} + \frac{\boldsymbol{e}_{i-1}}{|\boldsymbol{e}_{i-1}|} \cdot (\kappa\boldsymbol{b}_i \times \boldsymbol{M}_i)\frac{|\boldsymbol{e}_{i-1}|}{2} + \frac{\boldsymbol{e}_i}{|\boldsymbol{e}_i|} \cdot (\kappa\boldsymbol{b}_i \times \boldsymbol{M}_i)\frac{|\boldsymbol{e}_i|}{2} \\
&= Q_i - Q_{i-1} + \frac{\boldsymbol{e}_{i-1} + \boldsymbol{e}_i}{2} \cdot (\kappa\boldsymbol{b}_i \times \boldsymbol{M}_i)
\end{aligned}
\tag{4.39}
$$

- soit on revient à l'hypothèse de continuité et de linéarité par morceaux sur le moment:

$$
\boldsymbol{M}(s) = \boldsymbol{M}_i + s\boldsymbol{M}_i' \quad \forall s \in [0, |\boldsymbol{e}_i|] \quad , \quad \boldsymbol{M}_i' = \frac{\boldsymbol{M}_{i+1} - \boldsymbol{M}_i}{|\boldsymbol{e}_i|}
\tag{4.40a}
$$

$$
\kappa\boldsymbol{b}(s) = \boldsymbol{B}_i^{-1}\boldsymbol{M}(s) + \overline{\kappa\boldsymbol{b}}(s)
\tag{4.40b}
$$

$$
\tag{4.40c}
$$

d'où :

$$
\begin{aligned}
&= \int_{i-1/2}^{i} \kappa_1 M_2 - \kappa_2 M_1 \\
&= \int_{i-1/2}^{i} \big(\tfrac{1}{[EI]_{1,i}} - \tfrac{1}{[EI]_{2,i}}\big) M_1 M_2
\end{aligned}
\tag{4.41}
$$

With

$$[EI]_i \tag{4.42a}$$

$$[GJ]_i \tag{4.42b}$$

$$\kappa\boldsymbol{b}_i = \frac{2\boldsymbol{e}_{i-1} \times \boldsymbol{e}_i}{|\boldsymbol{e}_{i-1}||\boldsymbol{e}_i||\boldsymbol{e}_{i-1} + \boldsymbol{e}_i|} \tag{4.42c}$$

$$\tau_i = \frac{\theta_{i+1} - \theta_i}{|\boldsymbol{e}_i|} \tag{4.42d}$$

$$\boldsymbol{N}_i = N_i\boldsymbol{d}_3 \quad where \quad N_i = \alpha_i\epsilon_i \quad \alpha_i = \frac{2[ES]_i[ES]_{i+1}}{[ES]_i + [ES]_{i+1}} \tag{4.42e}$$

$$\boldsymbol{M}_i = [EI]_{1,i}(\kappa_{1,i} - \bar{\kappa}_{1,i})\boldsymbol{d}_{1,i} + [EI]_{2,i}(\kappa_{2,i} - \bar{\kappa}_{2,i})\boldsymbol{d}_{2,i} \tag{4.42f}$$

$$\boldsymbol{Q}_i = Q_i\boldsymbol{d}_3 \quad where \quad Q_i = \beta_i(\tau_i - \bar{\tau}_i) \quad \beta_i = \frac{2[GJ]_i[GJ]_{i+1}}{[GJ]_i + [GJ]_{i+1}} \tag{4.42g}$$

$$\boldsymbol{F}_i^1 = -\frac{\boldsymbol{e}_i \times \boldsymbol{M}_i}{|\boldsymbol{e}_i|^2} \tag{4.42h}$$

$$\boldsymbol{F}_i^2 = +\frac{\boldsymbol{e}_i \times \boldsymbol{M}_{i+1}}{|\boldsymbol{e}_i|^2} \tag{4.42i}$$

$$\boldsymbol{H}_i^- = Q_i\kappa\boldsymbol{b}_{i+1/2}^- \tag{4.42j}$$

$$\boldsymbol{H}_i^+ = Q_i\kappa\boldsymbol{b}_{i+1/2}^+ \tag{4.42k}$$

$$\tag{4.42l}$$

Ici il y a une ambiguité sur M_i en fonction d'un éventuel changement de propriété méca EI_1 ou EI_2. En fait il faudrait préciser un moment à droite et un moment à gauche (ce qui correspond à la réalité). Le moment étant la courbure au noeud i pondérée par $2EI$ à droite ou à gauche

Toutes les discrétisations ne se valent pas ....

En fait, ça n'a pas vraiment de sens de définir EI sur le segment. Le moment est continu. Donc il est uniquement défini par la donnée de la courbure en un noeud et du EI associé à ce noeuds. Introduire un moment à gauche et un moment à droite est problématique. Ce qui ce passe, pour une poutre isostatique simple qui change de EI à mi-travée, c'est une discontinuité de courbure y'' alors que y et y' restent continues. Donc il semble plus pertinent de définir EI aux noeuds car notre modèle ne peut pas représenter des discontinuitées de courbure (ou alors il faut connecter des poutres entre-elles.

Pour la torsion, on peut s'en sortir également en définissant β aux noeuds et en supposant GJ constant entre $[i - 1/2, i + 1/2]$. Il y a donc (éventuellement) un saut de β au milieu de chaque $\boldsymbol{e}_i$.

On ne peut pas faire autrement que supposer la torsion uniforme entre 2 noeuds, c'est à dire une variation linéaire (par morceaux) de θ. Et il y a donc une discontinuité potentielle aux noeuds.

On écrit la continuité du champs de torsion entre les noeuds 1 et 2 malgré le saut de β :

A mi travée

$$Q_{12} = Q_{mid} = Q_1^+ = Q_2^- = [GJ]_1 \frac{\theta_{mid} - \theta_1}{|\boldsymbol{e}|/2} = [GJ]_2 \frac{\theta_2 - \theta_{mid}}{|\boldsymbol{e}|/2} \tag{4.43}$$

D'où :

$$\theta_{mid} = \frac{[GJ]_1}{[GJ]_1 + [GJ]_2} \theta_1 + \frac{[GJ]_2}{[GJ]_1 + [GJ]_2} \theta_2 \tag{4.44}$$

On en déduit :

$$Q_{12} = Q_{mid} = Q_1^+ = Q_2^- = \frac{2[GJ]_1[GJ]_2}{[GJ]_1 + [GJ]_2} \left(\frac{\theta_2 - \theta_1}{|\boldsymbol{e}|} \right) \tag{4.45}$$

Donc il faut plutôt définit Q_i la torsion uniforme sur le segment $\boldsymbol{e}_i$ comme :

$$Q_i = \beta_i(\tau_i - \overline{\tau}_i) \quad where \quad \beta_i = \frac{2[GJ]_i[GJ]_{i+1}}{[GJ]_i + [GJ]_{i+1}} \tag{4.46}$$

On retrouve bien le cas d'une poutre de propriété constante lorsque $[GJ]_i = [GJ]_{i+1} = GJ$ alors $\beta_i = GJ$.

De manière identique, on résonne pour l'effort axial entre deux noeuds 1 et 2 auxquels sont associés des raideurs axiales $[ES]_1$ et $[ES_2]$. On cherche la raideur équivalente connaissant uniquement l'allongement de l'ensemble du segment :

$$N_1 = [ES]_1 \cdot \epsilon_1 \tag{4.47a}$$
$$N_2 = [ES]_2 \cdot \epsilon_2 \tag{4.47b}$$
$$N = [ES]_2 \cdot \frac{\epsilon_1 + \epsilon_2}{2} \tag{4.47c}$$

Avec :

$$\epsilon_1 = \frac{l_1 - l_0/2}{l_0/2} \tag{4.48a}$$

$$\epsilon_2 = \frac{l_2 - l_0/2}{l_0/2} \tag{4.48b}$$

$$\epsilon = \frac{l}{l_0} = \frac{\epsilon_1}{2} + \frac{\epsilon_2}{2} \tag{4.48c}$$

$$\tag{4.48d}$$

Thus,

$$N_i = N_1 = N_2 \quad \Rightarrow \quad \alpha_i = \frac{2[ES]_i[ES]_{i+1}}{[ES]_i + [ES]_{i+1}} \tag{4.49}$$

Bibliography

[Ala12]   Javad Alamatian. A new formulation for fictitious mass of the Dynamic Relaxation method with kinetic damping. *Computers and Structures*, 90-91:42–54, 2012.

[Day65]   Alister Day. An Introduction to dynamic relaxation. *The Engineer*, 1965.

[MAIK14]   Masaaki Miki, Sigrid Adriaenssens, Takeo Igarashi, and Ken'ichi Kawaguchi. The geodesic dynamic relaxation method for problems of equilibrium with equality constraint conditions. *International Journal for Numerical Methods in Engineering*, 99(9):682–710, 2014.

[Ott65]   J.R.H. Otter. Computations for prestressed concrete reactor pressure vessels using dynamic relaxation. *Nuclear Structural Engineering*, 1(1):61–75, jan 1965.

[Pap81]   M Papadrakakis. A method for the automatic evaluation of the dynamic relaxation parameters. 1981.

[RPKAZ11] M Rezaiee-Pajand, M Kadkhodayan, Javad Alamatian, and L C Zhang. A new method of fictitious viscous damping determination for the dynamic relaxation method. *Computers and Structures*, 89(9-10):783–794, 2011.

5 Marsupilami

5.1 Introduction

5.1.1 Goals and contribution

5.1.2 Related work

5.1.3 Overview

Dans ce chapitre, qui pourrait constituer comme un guide, on présente le logiciel Marsupilami dans son ensemble. On détail le modèle objet (POO) retenu et on montre sa pertinence pour formuler un grand nombre de problèmes. En particulier, on détaillera la version "conceptualisée" de la relaxation dynamique, et le principe des "modifieurs".

[Dil92]

Bibliography

[Dil92] Ellis Harold Dill. Kirchhoff's theory of rods. *Archive for History of Exact Sciences*, 1992.

6 Calculus of variations

6.1 Introduction

In this appendix we drawback essential mathematical concepts for the calculus of variations. Recall how the notion of energy, gradients are extended to function spaces.

[AMR02]

6.2 Spaces

6.2.1 Normed space

A *normed space* $V(\mathbb{K})$ is a vector space V over the scalar field $\mathbb{K}$ with a norm $\|.\|$.

A *norm* is a map $\|.\| : V \times V \longmapsto \mathbb{K}$ which satisfies :

$$\forall x \in V, \qquad\qquad \|x\| = 0_{\mathbb{K}} \Rightarrow x = 0_V \tag{6.1a}$$

$$\forall x \in V, \forall \lambda \in \mathbb{K}, \qquad\qquad \|\lambda x\| = |\lambda| \, \|x\| \tag{6.1b}$$

$$\forall (x, y) \in V^2, \qquad\qquad \|x + y\| \leqslant \|x\| + \|y\| \tag{6.1c}$$

6.2.2 Inner product space

A *inner product space* or *pre-hilbert space* $E(\mathbb{K})$ is a vector space E over the scalar field $\mathbb{K}$ with an inner product.

An *inner product* is a map $\langle\,;\,\rangle : E \times E \longmapsto \mathbb{K}$ which is bilinear, symmetric, positive-definite

:

$$\forall (x, y, z) \in E^3, \forall (\lambda, \mu) \in \mathbb{K}^2, \qquad \langle \lambda x + \mu y \,;\, z \rangle = \lambda \langle x \,;\, z \rangle + \mu \langle y \,;\, z \rangle \tag{6.2a}$$

$$\langle x \,;\, \lambda y + \mu z \rangle = \lambda \langle x \,;\, y \rangle + \mu \langle x \,;\, z \rangle$$

$$\forall (x, y) \in E^2, \qquad \langle x \,;\, y \rangle = \langle y \,;\, x \rangle \tag{6.2b}$$

$$\forall x \in E, \qquad \langle x \,;\, x \rangle \geqslant 0_{\mathbb{K}} \tag{6.2c}$$

$$\forall x \in E, \qquad \langle x \,;\, x \rangle = 0_{\mathbb{K}} \Rightarrow x = 0_E \tag{6.2d}$$

Moreover, an inner product naturally induces a norm on E defined by :

$$\forall x \in E, \quad \|x\| = \sqrt{\langle x \,;\, x \rangle} \tag{6.3}$$

Thus, an inner product vector space is also naturally a normed vector space.

6.2.3   Euclidean space

An *Euclidean space* $\mathcal{E}(\mathbb{R})$ is a finite-dimensional real vector space with an inner product. Thus, distances and angles between vectors could be defined and measured regarding to the norm associated with the chosen inner product.

An Euclidean space is nothing but a finite-dimensional real pre-hilbert space.

6.2.4   Banach space

A *Banach space* $\mathcal{B}(\mathbb{K})$ is a complete normed vector space, which means that it is a normed vector space in which every Cauchy sequence of $\mathcal{B}$ converges in $\mathcal{B}$ for the given norm.

Thus, a Banach space is a vector space with a metric that allows the computation of vector length and distance between vectors and is complete in the sense that a Cauchy sequence of vectors always converges to a well defined limit in that space.

6.2.5   Hilbert space

A *Hilbert space* is an inner product vector space $\mathcal{H}(\mathbb{K})$ such that the natural norm induced by the inner product turns $\mathcal{H}$ into a complete metric space (i.e. every Cauchy sequence of $\mathcal{H}$ converges in $\mathcal{H}$).

The Hilbert space concept is a generalization of the Euclidean space concept. In physics it's common to encounter Hilbert spaces as infinite-dimensional function spaces.

Hilbert spaces are Banach spaces, but the converse does not hold generally.

For example, $\mathcal{L}^2([a, b])$ is an infinite-dimensional Hilbert space with the canonical inner product $\langle f \,;\, g \rangle = \int_a^b fg$.

Note that $\mathcal{L}^2$ is the only Hilbert space among the $\mathcal{L}^p$ spaces.

6.3 Derivative

The well known notion of function derivative in $\mathbb{R}^{\mathbb{R}}$ can be extended to maps between Banach spaces. This is useful in physics when formulating problems as variational problems, usually in terms of energy minimization. Indeed, energy is generally defined over a functional vector space and not simply over the real line.

In this case, the research of minimal values of a potential energy rests on the calculus of variations of the energy function compared to variations to other functions defining the problem (geometry, materials, boundary conditions, ...).

Mathematical concepts extended well-known notions of derivative, jacobian and hessian in Euclidean spaces (typically $\mathbb{R}^2$ or $\mathbb{R}^3$) for Banach functional spaces.

6.3.1 Fréchet derivative

Differentiability

Let $\mathcal{B}_V$ and $\mathcal{B}_W$ be two Banach spaces and $U \subset \mathcal{B}_V$ an open subset of $\mathcal{B}_V$. Let $f : u \longmapsto f(u)$ be a function of $U^{\mathcal{B}_W}$. f is said to be *Fréchet differentiable* at $u_0 \in U$ if there exists a continious linear operator $\boldsymbol{D}f(u_0) \in \mathcal{L}(\mathcal{B}_V, \mathcal{B}_W)$ such that :

$$\lim_{h \to 0} \frac{f(u_0 + h) - f(u_0) - \boldsymbol{D}f(u_0) \cdot h}{\|h\|} = 0 \tag{6.4a}$$

Or, equivalently :

$$f(u_0 + h) = f(u_0) + \boldsymbol{D}f(u_0) \cdot h + o(h) \quad , \quad \lim_{h \to 0} \frac{o(h)}{\|h\|} = 0 \tag{6.4b}$$

In the literature, it is common to found the following notations : $df = \boldsymbol{D}f(u_0) \cdot h = \boldsymbol{D}f_{u_0}(h) = \boldsymbol{D}f(u_0, h)$ for the differential of f, which means nothing but $\boldsymbol{D}f(u_0)$ is linear regarding h. The dot denotes the evaluation of $\boldsymbol{D}f(u_0)$ at h. This notation can be ambiguous as far as the linearity of $\boldsymbol{D}f(u_0)$ in h is denoted as a product which is not explicitly defined.

Derivative

If f is Fréchet differentiable at $u_0 \in U$, the continous linear operator $\boldsymbol{D}f(u_0) \in \mathcal{L}(\mathcal{B}_V, \mathcal{B}_W)$ is called the *Fréchet derivative* of f at u_0 and is also denoted :

$$f'(u_0) = \boldsymbol{D}f(u_0) \tag{6.5}$$

f is said to be $\mathcal{C}^1$ in the sens of Fréchet if f is Fréchet differentiable for all $u \in U$ and the function $\boldsymbol{D}f : u \longmapsto f'(u)$ of $U^{\mathcal{L}(\mathcal{B}_V, \mathcal{B}_W)}$ is continuous.

Differential or total derivative

$df = \boldsymbol{D}f(u_0) \cdot h$ is sometimes called the *differential* or *total derivative* of f and represents the change in the function f for a perturbation h from u_0.

Higer derivatives

Because the differential of f is a linear map from $\mathcal{B}_V$ to $\mathcal{L}(\mathcal{B}_V, \mathcal{B}_W)$ it is possible to look for the differentiability of $\boldsymbol{D}f$. If it exists, it is denoted $\boldsymbol{D}^2 f$ and maps $\mathcal{B}_V$ to $\mathcal{L}(\mathcal{B}_V, \mathcal{L}(\mathcal{B}_V, \mathcal{B}_W))$.

6.3.2   Gâteaux derivative

Directional derivative

Let $\mathcal{B}_V$ and $\mathcal{B}_W$ be two Banach spaces and $U \subset \mathcal{B}_V$ an open subset of $\mathcal{B}_V$. Let $f : u \longmapsto f(u)$ be a function of $U^{\mathcal{B}_W}$. f is said to have a *derivative in the direction $h \in \mathcal{B}_V$* at $u_0 \in U$ if :

$$\left. \frac{d}{d\lambda} f(u_0 + \lambda h) \right|_{\lambda=0} = \lim_{\lambda \to 0} \frac{f(u_0 + \lambda h) - f(u_0)}{\lambda} \tag{6.6}$$

exists. This element of $\mathcal{B}_W$ is called the *directional derivative* of f in the direction h at u_0.

Differentiability

Let $\mathcal{B}_V$ and $\mathcal{B}_W$ be two Banach spaces and $U \subset \mathcal{B}_V$ an open subset of $\mathcal{B}_V$. Let $f : u \longmapsto f(u)$ be a function of $U^{\mathcal{B}_W}$. f is said to be *Gâteaux differentiable* at $u_0 \in U$ if there exists a continious linear operator $\boldsymbol{D}f(u_0) \in \mathcal{L}(\mathcal{B}_V, \mathcal{B}_W)$ such that :

$$\forall h \in \mathcal{U}, \quad \lim_{\lambda \to 0} \frac{f(u_0 + \lambda h) - f(u_0)}{\lambda} = \left. \frac{d}{d\lambda} f(u_0 + \lambda h) \right|_{\lambda=0} = \boldsymbol{D}f(u_0) \cdot h \tag{6.7a}$$

Or, equivalently :

$$\forall h \in \mathcal{U}, \quad f(u + \lambda h) = f(u) + \lambda \boldsymbol{D}f(u_0) \cdot h + o(\lambda) \quad , \quad \lim_{\lambda \to 0} \frac{o(\lambda)}{\lambda} = 0 \tag{6.7b}$$

In other words, it means that all the directional derivatives of f exist at u_0.

Derivative

If f is Gâteaux differentiable at $u_0 \in U$, the continous linear operator $\boldsymbol{D}f(u_0) \in \mathcal{L}(\mathcal{B}_V, \mathcal{B}_W)$ is called the *Gâteaux derivative* of f at u_0 and is also denoted :

$$f'(u_0) = \boldsymbol{D}f(u_0) \tag{6.8}$$

f is said to be $\mathcal{C}^1$ in the sens of Gâteaux if f is Gâteaux differentiable for all $u \in U$ and the function $\boldsymbol{D}f : u \longmapsto f'(u)$ of $U^{\mathcal{L}(\mathcal{B}_V, \mathcal{B}_W)}$ is continuous.

The Gâteaux derivative is a weaker form of derivative than the Fréchet derivative. If f is Fréchet differentiable, then it is also Gâteaux differentiable and its Fréchet and Gâteaux derivatives agree, but the converse does not hold generally.

6.3.3   Useful properties

Let $\mathcal{B}_V$, $\mathcal{B}_W$ and $\mathcal{B}_Z$ be three Banach spaces. Let $f, g : \mathcal{B}_V \longmapsto \mathcal{B}_W$ and $h : \mathcal{B}_W \longmapsto \mathcal{B}_Z$ be three Gâteaux differentiable functions. Then, the following useful properties holds :

$$\boldsymbol{D}(f + g)(u) = \boldsymbol{D}f(u) + \boldsymbol{D}g(u) \tag{6.9}$$

$$\boldsymbol{D}(f \circ h)(u) = \boldsymbol{D}h(f(u)) \circ \boldsymbol{D}f(u) = \boldsymbol{D}h(f(u)) \cdot \boldsymbol{D}f(u) \tag{6.10}$$

Recall that the composition of $\boldsymbol{D}h(f(u))$ with $\boldsymbol{D}f(u)$ means "$\boldsymbol{D}h(f(u))$ applied to $\boldsymbol{D}f(u)$" and is also denoted by $\cdot$ as explained previously.

6.3.4   Partial derivative

Following [AMR02] the main results on partial derivatives of two-variables functions are presented here. They are generalizable to n-variables functions.

Definition

Let $\mathcal{B}_{V_1}$, $\mathcal{B}_{V_2}$ and $\mathcal{B}_W$ be three Banach spaces and $U \subset \mathcal{B}_{V_1} \oplus \mathcal{B}_{V_2}$ an open subset of $\mathcal{B}_{V_1} \oplus \mathcal{B}_{V_2}$. Let $f : u \longmapsto f(u)$ be a function of $U^{\mathcal{B}_W}$. Let $u_0 = (u_{01}, u_{02}) \in U$. If the derivatives of the following functions exist :

$$
\begin{array}{cccc}
f_1 : & \mathcal{B}_{V_1} & \longrightarrow & \mathcal{B}_W \\
& u_1 & \longmapsto & f(u_1, u_{02})
\end{array}
\quad , \quad
\begin{array}{cccc}
f_2 : & \mathcal{B}_{V_2} & \longrightarrow & \mathcal{B}_W \\
& u_2 & \longmapsto & f(u_{01}, u_2)
\end{array}
\tag{6.11}
$$

they are called *partial derivatives* of f at u_0 and are denoted $\boldsymbol{D}_1 f(u_0) \in \mathcal{L}(\mathcal{B}_{V_1}, \mathcal{B}_W)$ and $\boldsymbol{D}_2 f(u_0) \in \mathcal{L}(\mathcal{B}_{V_2}, \mathcal{B}_W)$.

Differentiability

Let $\mathcal{B}_{V_1}$, $\mathcal{B}_{V_2}$ and $\mathcal{B}_W$ be three Banach spaces and $U \subset \mathcal{B}_{V_1} \oplus \mathcal{B}_{V_2}$ an open subset of $\mathcal{B}_{V_1} \oplus \mathcal{B}_{V_2}$. Let $f : u \longmapsto f(u)$ be a function of $U^{\mathcal{B}_W}$. If f is differentiable, then the partial derivatives exist and satisfy for all $h = (h_1, h_2) \in \mathcal{B}_{V_1} \oplus \mathcal{B}_{V_2}$:

$$\boldsymbol{D}_1 f(u) \cdot h_1 = \boldsymbol{D} f(u) \cdot (h_1, 0) \tag{6.12}$$

$$\boldsymbol{D}_2 f(u) \cdot h_2 = \boldsymbol{D} f(u) \cdot (0, h_2) \tag{6.13}$$

$$\boldsymbol{D} f(u) \cdot (h_1, h_2) = \boldsymbol{D}_1 f(u) \cdot h_1 + \boldsymbol{D}_2 f(u) \cdot h_2 \tag{6.14}$$

6.4   Gradient vector

Let $\mathcal{H}$ be a Hilbert space with the inner product denoted $\langle \, ; \rangle$. Let $U \subset \mathcal{H}$ an open subset of $\mathcal{H}$. Let $F : u \longmapsto F(u)$ be a scalar function of $U^{\mathbb{R}}$. The *gradient* of F is the map $grad\, F : x \longmapsto (grad\, F)(x)$ of $U^{\mathcal{H}}$ such that :

$$\forall h \in \mathcal{H}, \quad \langle (grad\, F)(x) ; h \rangle = \boldsymbol{D} F(x) \cdot h \tag{6.15}$$

Note that the gradient vector depends on the chosen inner product. For $\mathcal{H} = \mathbb{R}^n$ with the canonical inner product, one can recall the usual definition of the gradient vector and the corresponding linear approximation of F :

$$\boldsymbol{F}_{x+h} = \boldsymbol{F}_x + (grad\, F)_x^T H + \boldsymbol{o}(H) \quad , \quad grad\, F_x = \begin{bmatrix} \frac{\partial F}{\partial x_1} \\ \vdots \\ \frac{\partial F}{\partial x_n} \end{bmatrix} \in \mathbb{R}^n \tag{6.16}$$

Recall that the canonical inner product on $\mathbb{R}^n$ is such that $\langle x ; y \rangle = X^T Y$ in a column vector representation. In this case it is common to denote $grad\, F = \nabla F$.

For function spaces the usual definition of the gradient can be extended. For instance if F is a scalar function on $\mathcal{L}^2$, the gradient of F is the unique function (if it exists) from $\mathcal{L}^2$ which satisfies :

$$\forall h \in \mathcal{L}^2, \quad \boldsymbol{D} F(x) \cdot h = \langle (grad\, F)(x) ; h \rangle = \int (grad\, F) h \tag{6.17}$$

In this case it is common to denote $grad\, F = \frac{\delta F}{\delta x}$. The gradient is also known as the *functional derivative*. The existence and unicity of $grad\, F$ is ensured by the *Riesz representation theorem*.

6.5   Jacobian matrix

Let f be a differentiable function from $\mathbb{R}^n$ to $\mathbb{R}^m$. The *differential* or *total derivative* of such a fonction is a linear application from $\mathbb{R}^n$ to $\mathbb{R}^m$ which could be represented with the

following matrix called the *jacobian matrix* :

$$\boldsymbol{D}f(x) = \boldsymbol{J}_x = \frac{df}{dx} = \begin{bmatrix} \frac{\partial f}{\partial x_1} & \cdots & \frac{\partial f}{\partial x_n} \end{bmatrix} = \begin{bmatrix} \frac{\partial f_1}{\partial x_1} & \cdots & \frac{\partial f_1}{\partial x_n} \\ \vdots & \ddots & \vdots \\ \frac{\partial f_m}{\partial x_1} & \cdots & \frac{\partial f_m}{\partial x_n} \end{bmatrix} \in \mathcal{M}_{m,n}(\mathbb{R}) \tag{6.18}$$

Thus, with the matrix notation, the Taylor expansion takes the following form :

$$\boldsymbol{F}_{x+h} = \boldsymbol{F}_x + \boldsymbol{J}_x H + \boldsymbol{o}(H) \tag{6.19}$$

In the cas $m = 1$, the jacobian matrix of the functional F is nothing but the gradient vector transpose itself :

$$\boldsymbol{D}F(x) = \boldsymbol{J}_x = \frac{dF}{dx} = \begin{bmatrix} \frac{\partial F}{\partial x_1} & \cdots & \frac{\partial F}{\partial x_n} \end{bmatrix} = \nabla F^T \tag{6.20}$$

6.6 Hessian

Let F be a differentiable scalar function from $\mathbb{R}^n$ to $\mathbb{R}$. The second order differential of such a fonction is a linear application from $\mathbb{R}^n$ to $\mathbb{R}^n$ which could be represented with the following matrix called the *hessian matrix* :

$$\boldsymbol{D}^2 F(x) = \boldsymbol{H}_x = \frac{d^2 F}{dx}(x) = \begin{bmatrix} \frac{\partial F_1^2}{\partial x_1^2} & \frac{\partial F_1^2}{\partial x_1 \partial x_2} & \cdots & \frac{\partial F_1^2}{\partial x_1 \partial x_n} \\ \frac{\partial F_1^2}{\partial x_2 \partial x_1} & \frac{\partial F_1^2}{\partial x_2^2} & \cdots & \frac{\partial F_1^2}{\partial x_2 \partial x_n} \\ \vdots & & \ddots & \vdots \\ \frac{\partial F_p^2}{\partial x_n \partial x_1} & \frac{\partial F_p^2}{\partial x_n \partial x_2} & \cdots & \frac{\partial F_p^2}{\partial x_n^2} \end{bmatrix} \in \mathcal{M}_{n,n}(\mathbb{R}) \tag{6.21}$$

Thus, with the matrix notation, the Taylor expansion takes the following form :

$$\boldsymbol{F}_{x+h} = \boldsymbol{F}_x + \boldsymbol{J}_x H + \tfrac{1}{2} H^T \boldsymbol{H}_x H + \boldsymbol{o}(H) \tag{6.22}$$

6.7 Functional

A *functional* is a map from a vector space $E(\mathbb{K})$ into its underlying scalar field $\mathbb{K}$. Here $\mathcal{E}_p[\boldsymbol{x}, \theta]$ is a functional depending over $\boldsymbol{x}$ and θ.

Bibliography

[AMR02] Ralph Abraham, Jerrold E. Marsde, and Tudor Ratiu. *Manifolds, Tensor Analysis, and Applications (Ralph Abraham, Jerrold E. Marsden and Tudor Ratiu).* 2002.

7 Bench for HPC

7.1 Introduction

In this section aims at providing basic but reliable guidlines to produce fast and mannagable code for our algorithms

Most compilers with which you are probably familiar are standalone programs which take as input some source code text and compile it into machine code (or some other target representation).

cach miss : une donnée n'est pas dans le cache

[**?**] [**?**]

L1 = 64kB L2 = 512kB L3 = 4096kB

7.2 Languages

- Csharp - Julia - C++ - Intel MKL - OpenBLAS

Parallelization vs. Vectorization (SIMD)

SIMD :

http://www.drdobbs.com/windows/64-bit-simd-code-from-c/240168851

7.3 From syntax to processor

A short story about how a code is translated to get machin instructions

7.4   Data Structure

Array of Structures (AOS) vs Structure of Arrays (SOA)

The most common and likely well-known data structure is the array, which contains a contiguous collection of data items that can be accessed by an ordinal index. This data can be organized as an Array Of Structures (AOS) or a Structure Of Arrays (SOA). While AOS organization is excellent for encapsulation it can be poor for use of vector processing. Selecting appropriate data structures can also make vectorization of the resulting code more effective. To illustrate this point, compare the traditional array-of- structures (AoS) arrangement for storing the r, g, b components of a set of three- dimensional points with the alternative structure-of-arrays (SoA) arrangement for storing this set.

http://hectorgon.blogspot.fr/2006/08/array-of-structures-vs-structure-of.html

http://arxiv.org/pdf/1402.4986.pdf

sqrt | Float64	CPU (ns/el)	Allocation (Bytes)
Allocation	4	8,112
Julia vectorized	9	8,080
Julia broadcast	13	8,352
Julia broadcast!	7	16
Julia map	100	48,000
Julia map!	92	48,000
VML (allocation)	6	8,080
VML (in-place)	4	0

Table 7.1 – Memory allocations for various methods computing sqrt(a) for $n = 10^4$

7.5 Memory allocation and garbage collection

Toutes les syntaxes ne sont pas égales en terme de gestion de la mémoire. Le problème, c'est le passage de la GC qui est couteux en temps. Donc il faut essayer de minimiser l'utilisation mémoire. Idéalement le problème peut rester dans le cache du processeur (mémoire d'accès bcp plus rapide que la RAM). Donc la meilleur stratégie consiste à pré-allouer les tableaux et à faire des opération "in-place" au maximum, c'est à dire d'écraser les donner au fur et à mesure du calcul.

Par ailleurs les accès mémoires sont lents. Plus la taille du problème reste petite, plus le problème peut être résolu en restant dans le cache. (latency).

http://stackoverflow.com/questions/4087280/approximate-cost-to-access-various-caches-and-main-memory

MOST CPU's today uses the memory on multiple level. Generally the memory at the proximity of CPU is costly and less, whereas the memory at the distance (wire distance) is bigger, slower and cheap [1]. Today getting the computer in market with 8GB DRAM is cheap, but L1/L2 cache of such computer is very small in terms of 10's of KB's and few MB's respectively. The access time of L1 (that is generally SRAM) is few cycles whereas L2 is few 10's cycles and accessing main memory is considered a bad programming if accessed too frequently. The access time is huge and in terms of 100's of cycles. So optimizing the code to run and access L1 Instruction and Data cache is the simplest way to optimizing the code.

On remarque que l'allocation mémoire est très différente d'une fonction à l'autre. Il est important de privilégier des opération "in-place" pour contenir l'allocation mémoire, sinon on risque de déclencher la GC qui est couteuse.

Les temps CPU sont indicatifs car le bench est fait sur une durée caractéristique trop courte

Ici on met en évidence la non linéarité du coût d'allocation par élément d'un tableau de taille n. On remarque que la différence entre le coût de sqrt et le coût de l'allocation est constante : c'est le coût de sqrt hors allocation. Attention, cette notion est "language dependent" car les allocations sont gérées par la GC.

Remarque, on trouverait sans doute la même chose pour MKL, à cause du marshalling : le coût d'appel à une fonction C est supérieur à celui d'une fonction managée (cf HPC .Net)
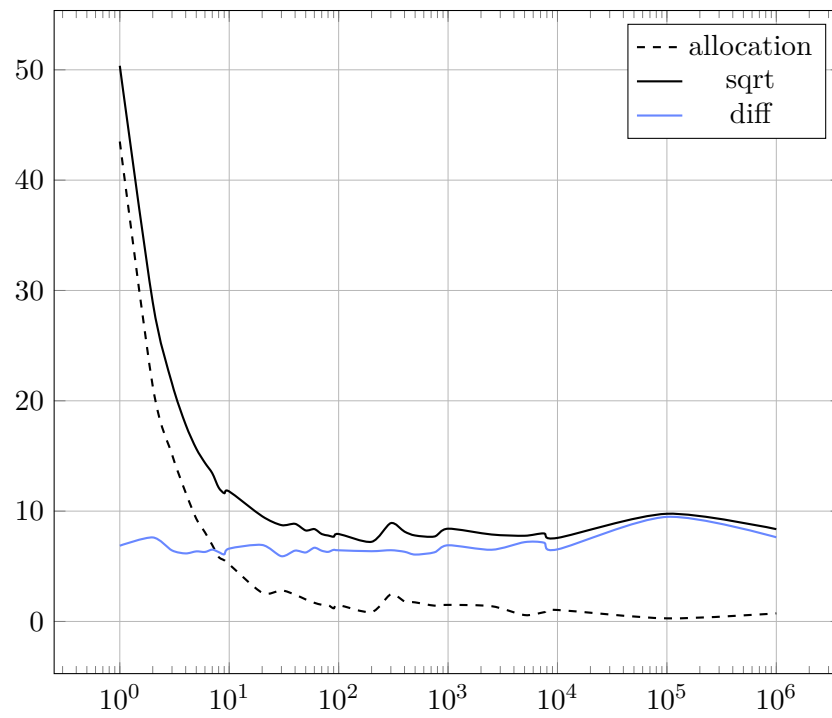
Figure 7.1 – Nonlinear cost of CPU time in ns/el of memory allocation for arrays (Float64).
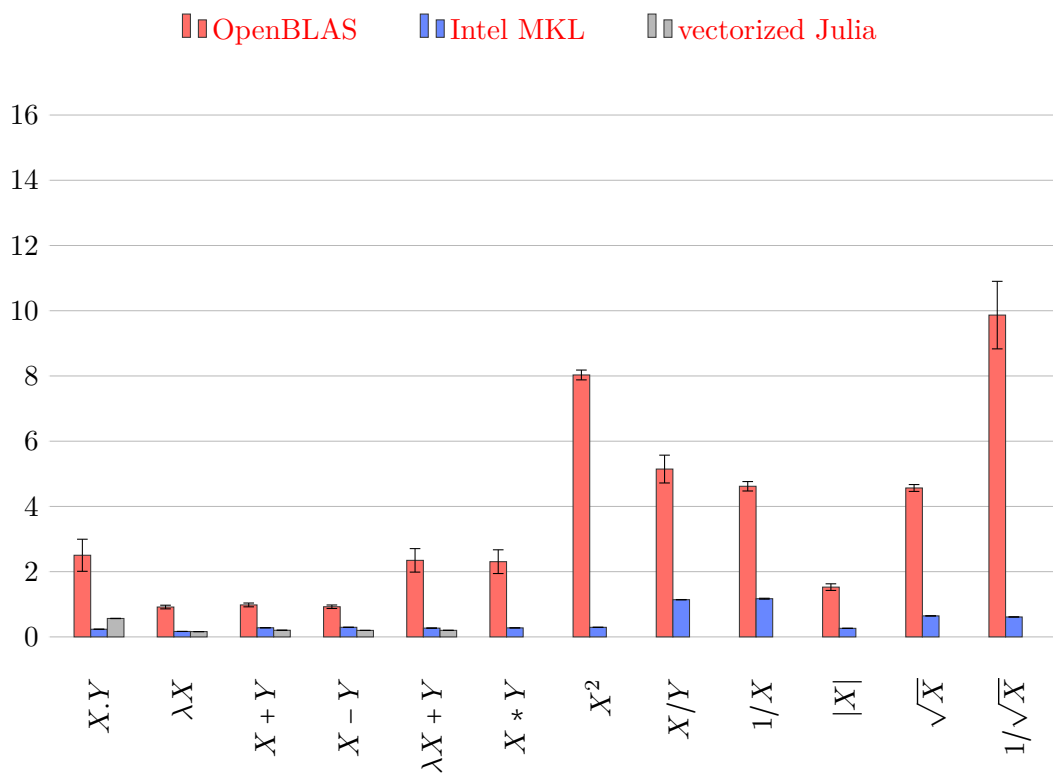
(a) Float32
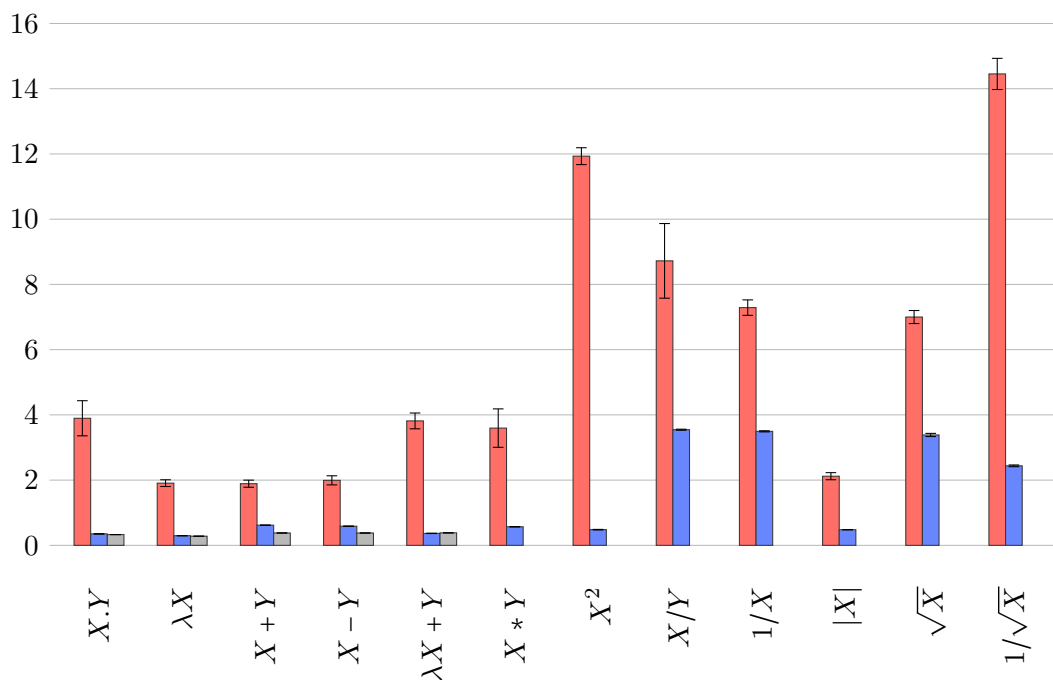
(b) Float64

Figure 7.2 – Absolute CPU time in *ns/element* for $n = 104$ elements. Error bars indicate 95% condifdence interval.
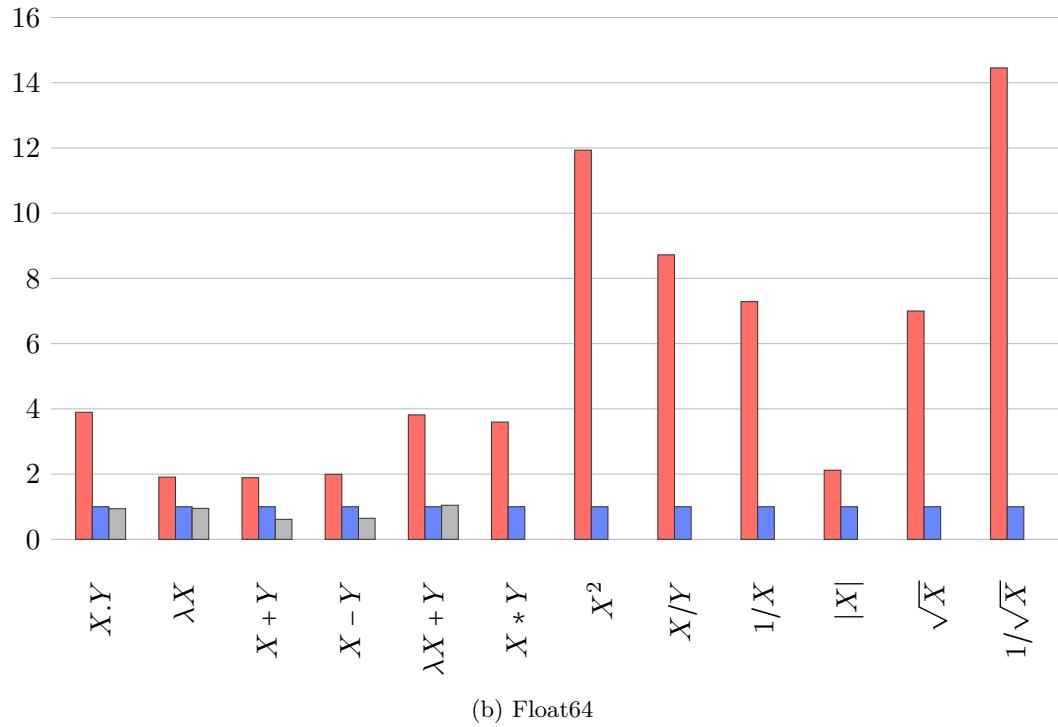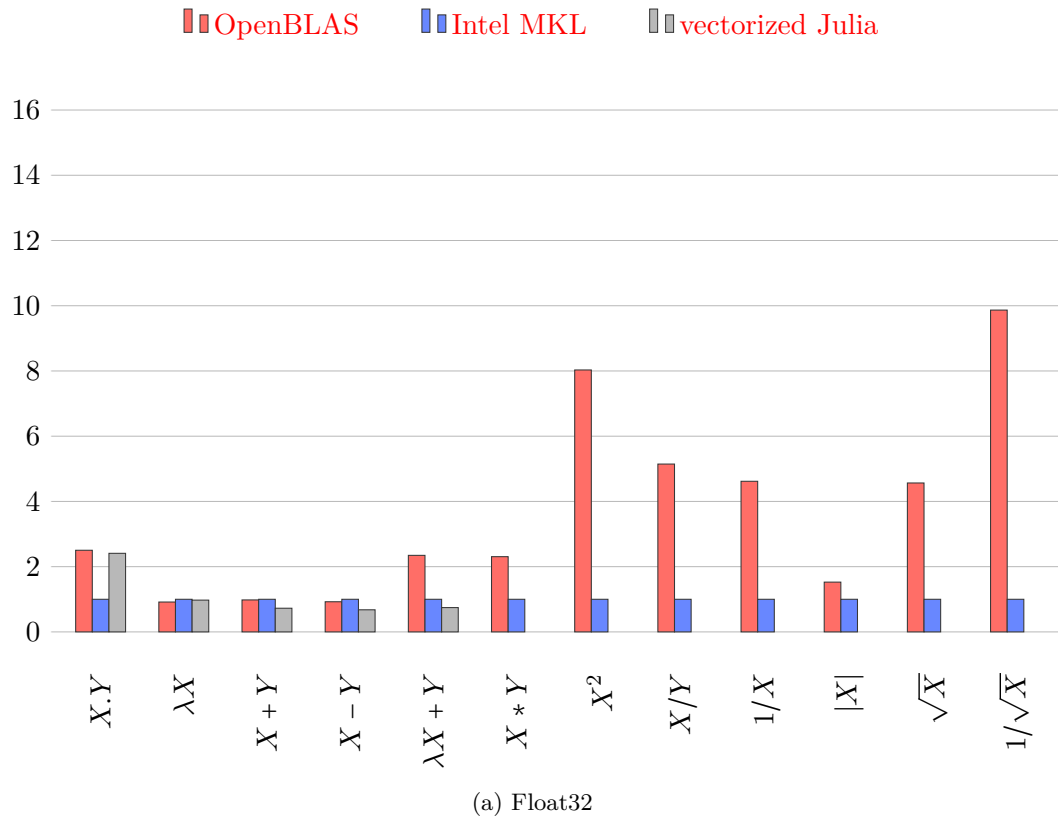
(a) Float32

(b) Float64
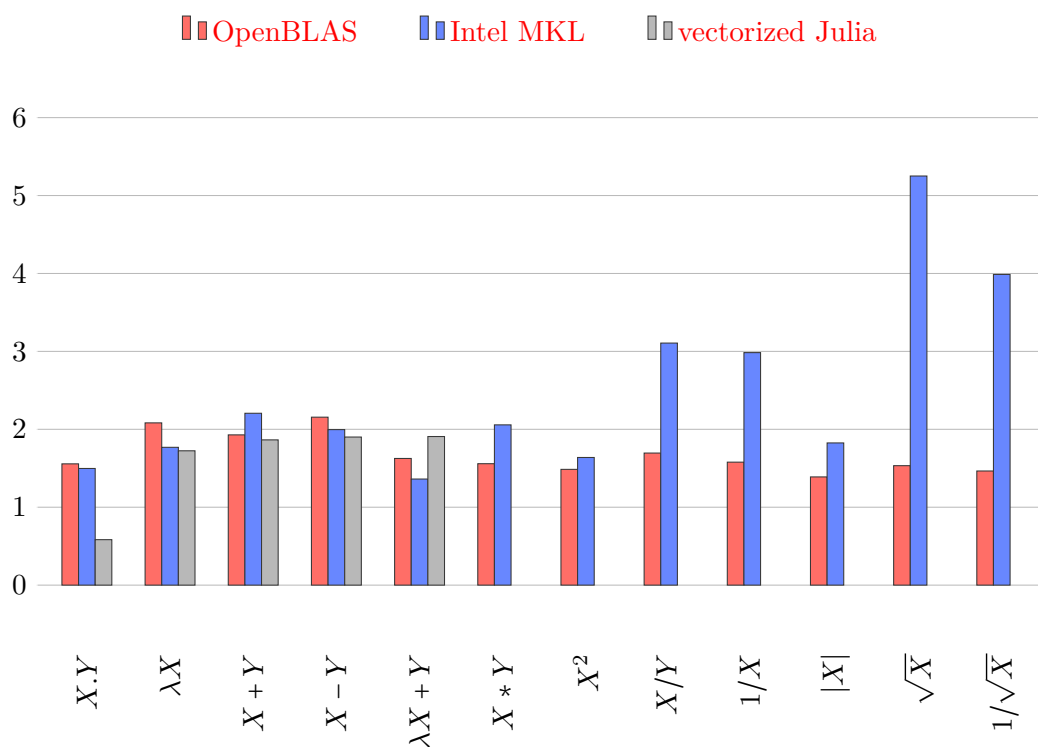
Figure 7.3 – CPU time relative to Intel MKL for $n = 104$ elements.

Figure 7.4 – relative CPU time performance for double versus single precision numbers for $n = 10^4$ elements.

profiling : https://software.intel.com/en-us/intel-vtune-amplifier-xe

SIMD : http://www.drdobbs.com/architecture-and-design/simd-enabled-vector-types-with-c/240168888

https://software.intel.com/en-us/articles/optimize-for-intel-avx-using-intel-math-kernel-librarys-basic-linear-algebra-subprograms-blas-with-dgemm-routine

- https://msdn.microsoft.com/en-us/library/ms973852.aspx

- http://www.sebastiansylvan.com/post/why-most-high-level-languages-are-slow/

- http://creamysoft.blogspot.fr/2013/05/c-vs-c-performance.html

- http://www.codeproject.com/Articles/212856/Head-to-head-benchmark-Csharp-vs-NET

- https://software.intel.com/en-us/articles/speeding-up-c-code-with-the-vtune-amplifier-xe-performance-profiler

- http://jonathankinlay.com/index.php/2015/02/comparison-programming-languages/

Bibliography

```
1   kusing nVML
2
3   c# wrap functions to avoid global scoping while testing
4   kfunctionn+nf sqrt_jvectorizedp{nTo<:nNumberp}(nap::nVectorp{nTp})
5       nsqrtp(nap)
6   kend
7   kfunctionn+nf sqrt_jbroadcastp{nTo<:nNumberp}(nap::nVectorp{nTp})
8       nbroadcastp(nsqrtp,nap)
9   kend
10  kfunctionn+nf sqrt_jbroadcasto!p{nTo<:nNumberp}(ndestp::nVectorp{nTp}, nap::nVectorp{nTp})
11      nbroadcasto!p(nsqrtp,ndestp,nap)
12  kend
13  kfunctionn+nf sqrt_jmapp{nTo<:nNumberp}(nap::nVectorp{nTp})
14      nmapo!p(nsqrtp,nap)
15  kend
16  kfunctionn+nf sqrt_jmapo!p{nTo<:nNumberp}(ndestp::nVectorp{nTp}, nap::nVectorp{nTp})
17      nmapo!p(nsqrtp,ndestp,nap)
18  kend
19  kfunctionn+nf sqrt_jloopp{nTo<:nNumberp}(ndestp::nVectorp{nTp},nap::nVectorp{nTp})
20      p@ninbounds kfor ni kin neachindexp(nap) ndestp[nip]o=nsqrtp(nap[nip]) kend
21  kend
22
23  kfunctionn+nf sqrt_benchp()
24      c# define vector size and floating precision
25      nn o= l+m+mi1_000
26      nT o= k+ktFloat64
27      c# allocate vectors
28      ndest  o= nonesp(nTp,nnp)
29      p@ntime na o= nrandp(nTp,nnp)
30      c# bench
31      ngcp()
32      ngc_enablep(nfalsep)
33      p@ntime nsqrt_jvectorizedp(nap)
34      p@ntime nsqrt_jbroadcastp(nap)
35      p@ntime nsqrt_jbroadcasto!p(ndestp,nap)
36      p@ntime nsqrt_jmapp(nap)
37      p@ntime nsqrt_jmapo!p(ndestp,nap)
38      p@ntime nVMLo.nsqrtp(nap)
39      p@ntime nVMLo.nsqrto!p(ndestp,nap)
40      ngc_enablep(ntruep)
41  kend
42
43  nsqrt_benchp()
```

Listing 1 – Example from external file

```
1   kusing nDataFramesp, nVML
2
3   kfunctionn+nf sqrt_benchp()
4
5       c# vector size
6       nN o=
    ↪  p[l+m+mi1p,l+m+mi2p,l+m+mi3p,l+m+mi4p,l+m+mi5p,l+m+mi6p,l+m+mi7p,l+m+mi8p,l+m+mi9p,
7
    ↪  l+m+mi10p,l+m+mi20p,l+m+mi30p,l+m+mi40p,l+m+mi50p,l+m+mi60p,l+m+mi70p,l+m+mi80p,l+m+mi90p,l+m+mi100p,
8
    ↪  l+m+mi1_000p,l+m+mi2_500p,l+m+mi5_000p,l+m+mi7_500p,l+m+mi10_000p,l+m+mi100_000p,l+m+mi1_000_000p]
9
10      c# dataframe for results
11      ndf o=
    ↪  nDataFramep(nNo=p[],nALLOCo=k+ktFloat64p[],nJULIAo=k+ktFloat64p[],nMKLo=k+ktFloat64p[])
12
13      p@ninbounds kfor ni kin l+m+mi1p:nlengthp(nNp)
14          nT o= k+ktFloat64
15          nn o= nNp[nip]
16          na o= nrandp(nTp,nnp)
17          ndest o= nzerosp(nTp,nnp)
18
19          c# evaluate sqrt and allocation
20          c# for small n @elapsed applies to a bunch of evaulations
21          nnrep o= l+m+mi1000
22          nncycle o= l+m+mi10_000 err÷ nn o+ l+m+mi1
23
24          c# trigger garbage collection
25          ngcp()
26          ntalloc o= l+m+mf0.0 p; ntalloc o= l+m+mf0.0 p; ntsqrt o= l+m+mf0.0
27          kfor nj kin l+m+mi1p:nnrep
28              ntalloc o+= p@nelapsed kfor nk kin l+m+mi1p:nncycle nVectorp{nTp}(nnp) kend
29              ntsqrt o+= p@nelapsed kfor nk kin l+m+mi1p:nncycle nsqrtp(nap) kend
30          kend
31
32          c# scale results (ns/element)
33          ntalloc o= ntalloc o/ nnrep o/ nncycle o/ nn o* l+m+mf1e9
34          ntsqrt  o= ntcpu o/ nnrep o/ nncycle o/ nn o* l+m+mf1e9
35
36          c# write results
37          npusho!p(ndfp,[nnp,ntallocp, ntsqrtp])
38      kend
39      ndf
40  kend
41
42  nsqrt_benchp()
```

Listing 2 – Example from external file